MECHANISMS AND DEVELOPMENT OF ETCH RESISTANCE FOR HIGHLY AROMATIC MONOMOLECULAR ETCH MASKS – TOWARDS MOLECULAR LITHOGRAPHY

A Dissertation
Presented to
The Academic Faculty

by

Erik Jonas Järvholm

In Partial Fulfillment
of the Requirements for the Degree
Doctor of Philosophy in the
School of Chemistry and Biochemistry

Georgia Institute of Technology
May 2007

MECHANISMS AND DEVELOPMENT OF ETCH RESISTANCE FOR HIGHLY AROMATIC MONOMOLECULAR ETCH MASKS – TOWARDS MOLECULAR LITHOGRAPHY

Approved by:

Dr. Laren M. Tolbert, Advisor
School of Chemistry and Biochemistry
Georgia Institute of Technology

Dr. Clifford L. Henderson
School of Chemical and Biomolecular Engineering
Georgia Institute of Technology

Dr. Andrew Lyon
School of Chemistry and Biochemistry
Georgia Institute of Technology

Dr. Dennis W. Hess
School of Chemical and Biomolecular Engineering
Georgia Institute of Technology

Dr. Lawrence A. Bottomley
School of Chemistry and Biochemistry
Georgia Institute of Technology

Dr. Mohan Srinivasarao
School of Polymer, Textile, & Fiber Engineering
Georgia Institute of Technology

Date Approved: April 6, 2007

I would like to dedicate this dissertation to my best friend and wife, Jessica. Without her I would be nothing! Thank you for carrying my child. I would also like to dedicate this to my Mother (Kerstin), late Father (Ulf), and Sister (Emma), their support and understanding have been extremely important to me. I wish could see you guys more often! Last but not least I would like to dedicate this to my Mother-In-Law (Mary) and Father-In-Law (Fred) who has taken me into their family and made me feel like home here in the USA.

ACKNOWLEDGEMENTS

First, I would like to thank my advisor, Dr. Laren M. Tolbert, for allowing me to join his research group and for giving me the opportunity to do the research presented in this dissertation. Since no research can be done alone and without guidance I also would like to thank Dr. Jürgen Rühe (for inviting me to do research in Freiburg, Germany, 2003), Dr. Janusz Kowalik, Dr. Mohan Srinivasarao, Dr. Phillip First, Dr. Klaus Müllen, Dr. Oswald Prucker, Dr. Clifford Henderson, and Dr. Dennis Hess for their invaluable advice and discussion over the past few years.

Dr. Loretta Crow's friendship and knowledge (not only scientific but also where things are located in the lab, since I cannot find anything) has been extremely helpful and she needs a special thanks. I also want to thank Dr. Christina Bauer for her interest in my project but also for her help with both surface analysis and surface modifications. I would also like to thank her for reading this thesis and helping me correct all grammatical and weird wordings. I would like to thank Janusz who has helped me on a daily basis with ideas and discussions. Of course I also want to thank the rest of the Tolbert research group who has helped tremendously.

I also would like to thank all my collaborators Dr. Simon Jones for helping me make the fullerene compounds, Nikhil Sharma for helping me with the necessary STM analysis, Dr. Müllen for kindly giving the C96 molecules to me, Dr. Paul Sheehan for trying dip-pen lithography with my compounds, Joel Pikarsky for training and helping me with the AFM and SEM instruments, and the MIRC staff for helping me with all processes in the cleanroom.

I also would like to thank all my friends Jack, Colin, JP, Caroline, Kenneth, Matt, Rahul, Henrik, Gavin, Stephen and many more, for listening about my work at Ga Tech and also for playing golf and tennis with me to keep me sane.

TABLE OF CONTENTS

LIST OF TABLES

LIST OF FIGURES

LIST OF SYMBOLS AND ABBREVIATIONS

IC	integrated circuit
PMOS	positively charged metal-oxide semiconductors
NMOS	negatively charged metal-oxide semiconductors
MOS	metal-oxide semiconductors
Si	silicon
SiO_2	silicon dioxide
V_g	gate voltage
CAR	chemically amplified resist
mm	millimeter
nm	nanometer
FET	field effect transistor
MOSFET	metal-oxide semiconductor field effect transistor
PAG	photo acid generator
RIE	reactive ion etching
ICP	inductively coupled plasma
k_1	resolution factor
λ	wavelength
NA	numerical aperture
n	index of refraction
θ	angle of incidence
DI water	distilled water
pBPES	Poly(3,4-bis(phenylethybyl)styrene
N	number of atoms in a molecule

N_C	number of carbons in a molecule
N_O	number of oxygen in a molecule
M_{CR}	molecular mass of carbons in ring structures of a molecule
M_{TOT}	total molecular mass of a molecule
DDCS	dodecyltrichlorosilane
CODS	chlorodimethyloctadecylsilane
PAHs	poly aromatic hydrocarbons
HBC	hexa-*peri*-benzocoronene
DSC	differential scanning calorimetry
XRD	X-ray diffraction
N_d	nematic-discotic
N_{Col}	nematic-columnar
Col_{ho}	columnar hexagonal ordered
C_d	columnar-disordered
AFM	atomic force microscopy
MIRC	microelectronic research center
Ga Tech	Georgia Institute of Technology
Å	ångstroms
SEM	scanning electron microscopy
EDS	energy dispersive X-ray analysis
XPS	X-ray photoelectron spectroscopy
TEM	transmission electron microscopy
Φ	quantum yield
SWNT	single-walled carbon nanotubes
APTES	3-aminopropyltriethoxysilane

APB	4-allyloxybenzophenone
M	molarity
ITRS	the International Technologies Roadmap for Semiconductors
RF	radio frequency
sccm	standard cubic centimeter per minute
TMAH	tertamethylammoniumhydroxide
MW	molecular weight
PDI	poly dispersity index
t_g	glass transition temperature
ROMP	ring-opening metathesis polymerization
ROMP-C60	ROMP polymer from 1-(3-(bicyclo[2.2.1]hept-5-en-2-yl)hexyl-2-(3,4-dibutoxyphenyl-fulleropyrrolidine
BHDF	N-(6-Bicyclo[2.2.1]hept-5-en-2-yl-hexyl)-2-(3,4-bis-dodecyloxy-phenyl)-3,4-fulleropyrrolidine
SAMs	self-assembled monolayers
MNFP	1-methyl-2-nonyl-[60]fulleropyrrolidine

SUMMARY

The road map of the semiconductor industry has followed Moore's Law over the past few decades. According to Moore's Law the number of transistors in an integrated circuit (IC) will double for a minimum component cost every two years. The features made in an IC are produced by photolithography. Industry is now producing devices at the 65 nm node, however, for every deceasing node size, both the materials and processes used are not only difficult but also expensive to develop. Ultimately, the feature size obtainable via photolithography is dependent on the wavelength used in the process. The limitations of photolithography will eventually make Moore's Law unsustainable. Therefore, new methodologies of creating features in the semiconductor substrate are desired.

Here we present a new way to make patterns in silicon (Si) and silicon dioxide (SiO_2), molecular lithography. Individual molecules and polymers, in a monolayer, serves directly as the etch mask; eliminating the photolighographic size limitation of light at a specific wavelength. The Ohnishi- and Ring parameter suggests that cyclic carbon rich molecules have a high resistance towards the plasma process, used to create the features in the substrate. Therefore highly aromatic molecules were investigated as candidates for molecular lithography.

A monolayer of poly cyclic hydrocarbons, fullerene containing polymer, and fullerene molecules were created using the versatile photochemistry of benzophenone as the linker between the substrate and the material. First, a chlorosilane benzophenone derivative was attached to the Si/SiO_2 surface. A thin film of the desired material is then

created on top of the silane benzophenone layer. Irradiation at ~350 nm excites the benzophenone and reacts with neighboring alkyl chains. After covalent attachment the non-bonded molecules are extracted from the surface using a Soxhlet apparatus. Self-assembly, molecular weight, and wetting properties of the material dictates the features shape and size. These features are then serving as an etchmask in a fluorine plasma. The organic etch resist is then removed either in an oxygen plasma or in a piranha solution. AFM analysis revealed that 3 to 4 nm wide defined structures were obtained using C96 as the etch mask. This is about ten times smaller then industry standards. Also a depth profile of 50 nm, which is the minimum feature depth used in industry, was created using a fullerene containing polymer as the etch mask. Directionality and control over the shape and sizes of the features are naturally critical for implementing this technology in device fabrication. Therefore, alignment of the materials used has also been examined.

Monolayers of highly stable molecules has successfully been used as etch masks. Further research and development could implement molecular lithography in device fabrication. Self-assembly among other forces would dictate which materials could be used successfully as a molecular resist.

CHAPTER 1

INTRODUCTION TO MOLECULAR LITHOGRAPHY

1.1 Historical Background

The world of microelectronic technology including, cell phones, computers, I-Pods, memory sticks, and many more such devices would not have been possible without the integrated circuit (IC). The breakthrough invention of the first transistor, which laid the groundwork for the IC, was done in 1947 by Shockley, Bardeen, and Brattain at Bell Laboratories and was followed by the first silicon transistor in 1954[1]. These primitive transistors only allowed for base switching and were quite large, which inhibited their use in making sophisticated devices. The production of complex, high density, and fast switching devices was not possible until both the IC (1958)[2] and later the metal-oxide-semiconductor (MOS) integrated circuit (1964) had been invented. The MOS transistors opened the door for the development in the late 1960's of calculators and many other of today's commonplace devices. The IC allows transistors to work independently from each other on a common substrate and the size of each individual transistor determines how many transistors can fit in a defined area. Much effort has been made to shrink the size of the individual transistor. Transistors are made using masks and photolithography to produce the necessary patterns in silicon (Si) and silicon dioxide (SiO_2) which are used as building blocks. Advancement and development in photolithography, mainly by the invention of chemically amplified resists (CAR) by Willson at IBM in the mid-1980's[3,4], has allowed the industry to now make devices at the 65 nm node, meaning that the features as small as 35 nm can be made. To make even smaller features in Si, using photolithography, requires of new materials and technologies which are not only difficult but also extremely expensive to develop[5]. Therefore, it is important to look for alternative methods to make features in Si. This dissertation begins by explaining the history and

future of photolithography. Then it introduces a new concept, molecular lithography, which makes patterns in a semiconductive substrate using individual molecules as etch templates allowing for molecular size structures to be produced. Finally, the bulk of the discussion is focused on the materials and processes used to create features in SiO_2 and Si as small as the diameter of individual molecules. A conclusion about the work done and the future direction of molecular lithography is also presented.

1.2 The Transistor

Before new concepts and ideas are presented it is important to understand the purpose and direction of those new ideas. Molecular lithography is geared towards the fabrication of the structures in Si to build transistors. Here is an introduction to the transistor and how it works.

Since its discovery, the MOS (Figure 1.1[6]) transistor has been the fundamental building block for today's silicon IC fabrication. There are two different types of MOS: positively charged metal-oxide semiconductors (PMOS) and negatively charged metal-oxide semiconductors (NMOS). Both PMOS and NMOS can be put on a single wafer which is then called complimentary metal-oxide semiconductors (CMOS). PMOS and NMOS work under the same principle of a p-n junction on either a positively (p)-doped

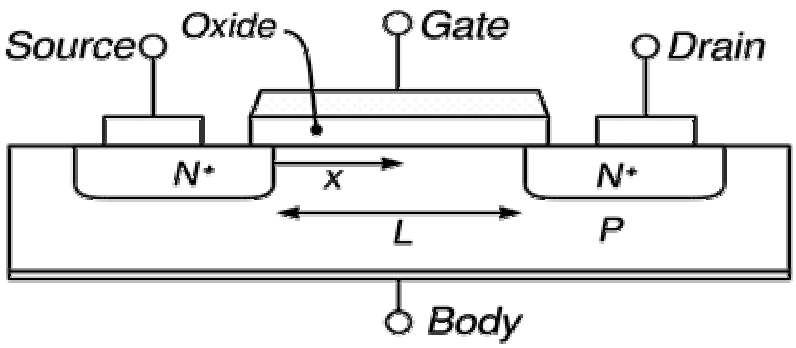

Figure 1.1. MOS in this case NMOS

silicon area (for PMOS) or a negatively (n)-doped silicon area (for NMOS). The transistor has either an off state of an on state depending on what action is required. The transistor is in the off state when the holes in the p-doped area remain and the same is also true for the electrons in the n-doped area. In the on state an electrical field is applied to the junction, thereby permitting the electrons to flow across the junction due to the lowered threshold. This allows a change of electron flow in the applied field, also known as a field-effect, and therefore the transistor is called a field-effect transistor (FET). A transistor of MOS type with an applied field is called a MOSFET. For a MOSFET to work correctly and efficiently the semiconductor material needs to prohibit the electrons from flowing freely over the p-n junction between the electrodes but at the same time respond promptly when the gate voltage (V_g) is applied and allow electrons to flow over the p-n junction. Much work has been done in optimizing the performance of the transistor, using different type of materials over the junction, etc. This dissertation does not concern the performance of the transistor but rather with the process of making the necessary structures for building a transistor. As seen in Fig. 1.1 and 1.2, structures of particular shapes in Si are needed for the transistor to work. Obviously, the smaller one can make the features in Si the more transistors can fit in a defined area. Photolithography is used to create these features and the process is described below. Later a new method, molecular lithography, is introduced were a monolayer of highly aromatic organic molecules is used as the mask to make the Si/SiO_2 structures.

1.3 Photolithography

Over the last decades the semiconductor industry has relied on photolithography to make the structures needed to make an IC. All photolithography is done in a clean-room so that the wafer during the process has no exposure to dust particles and other contaminates that will degrade the process. A thin film of photosensitive material is deposited on the Si wafer. A mask is placed over the wafer and exposed to light. The

photosensitive material undergoes a chemical reaction in the irradiated areas, a positive resist becomes more soluble and a negative resist becomes less soluble. The resist is then developed to remove the more soluble parts of the resist and leave behind the desired areas. The wafer is then placed in an etch tool that etches into the exposed Si, creating the desired features in the Si. Removal of the resist now leaves a patterned Si surface behind which is then used to build the IC[7]. The photolithography process can be seen in Figure 1.2.

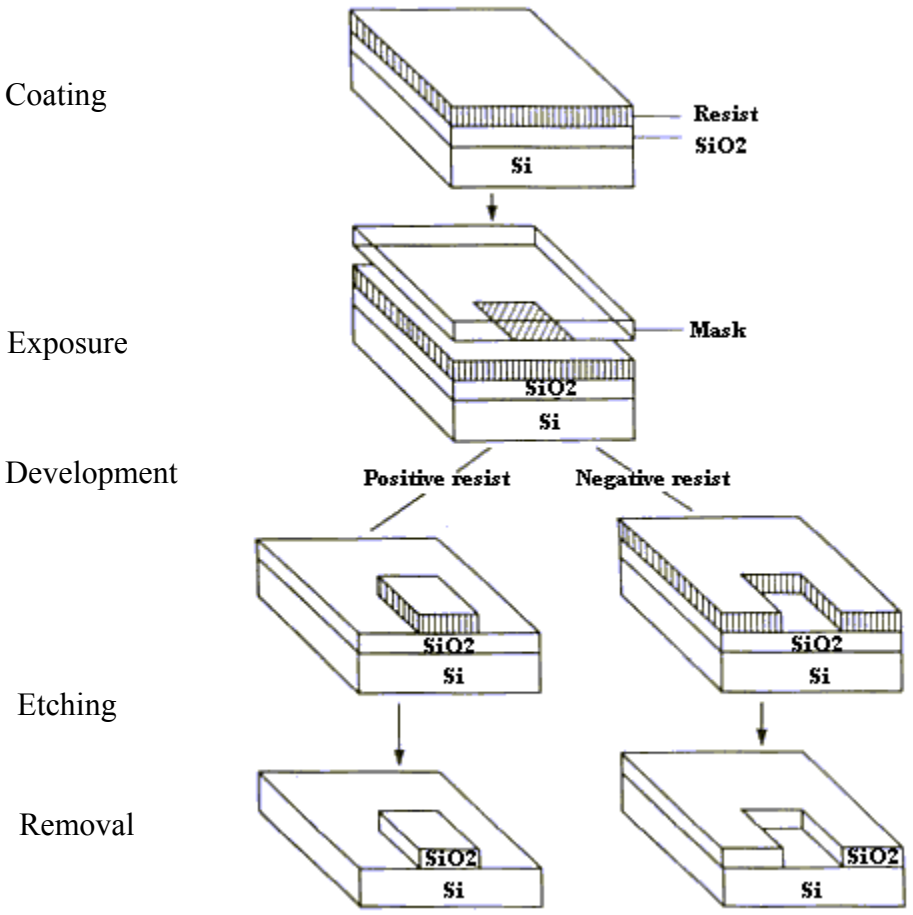

Figure 1.2 The photolithographic process

1.3.1 Materials

The substrate, or wafer, used for photolithography in the semiconducting industry is made of crystalline silicon (Si). The Si wafer is made of purified silica, usually done in a process called “zone refining”. The final product is a single-crystal ingot that must be devoid of imperfections since such imperfections would later degrade the quality of the device fabrication and ultimately the outcome of the final product[8]. The substrate is finally sliced and polished to an almost perfectly flat surface, also called silicon mirror. Today most leaders in industry, IBM, Intel, Micron, Samsung, Texas Instrument, etc, are using Si wafers that are either 200 mm or 300 mm in diameter. Of course a larger diameter wafer can fit more ICs that are then used to make microprocessors. By increasing the diameter of the wafer less wafer are needed to make a certain number of microprocessors and therefore the company saves time and money. The primary chemical substance used for photolithography is called a photoresist or just resist. The photoresist, usually a polymeric material, undergoes a photochemical reaction which is triggered by light of a specific wavelength. The reaction causes changes in the solubility properties of the resist which one can then take advantage of. Usually a photo acid generator (PAG) is used as the light absorbing species in what is termed a “chemically amplified resist”. The

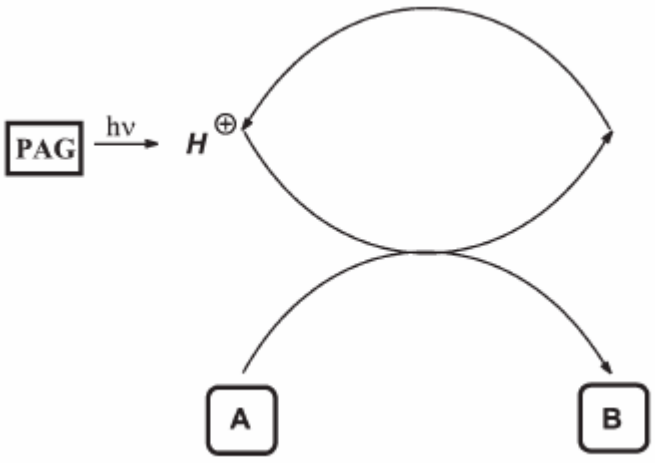

Figure 1.3 Illustration of the mechanism for a PAG

PAG creates a proton (H^+) upon irradiation which then catalyzes a reaction in the polymeric material[9], See Figure 1.3. A positive resist becomes soluble upon irradiation and can then subsequently be washed away upon development, leaving the areas that were not exposed to the light unchanged. A negative resist works in the opposite fashion; the exposed areas now become insoluble and the non-exposed areas can be washed away upon development. Most resists used in industry are positive resists. It is extremely important to remove all resist which were meant to be removed during development; otherwise residues will prevent proper outcome of the etching process.

1.3.2 Coating

The first step in creating features in the substrate is to coat the Si with photoresist using a spin-coating technique. The resist is dispensed onto the surface which is then accelerated to make a smooth and flat surface; the thickness of the resist can be controlled by varying the spin speed of the coating process and is usually in the range of 1000-3000 rpm. The wafer is then put onto a hotplate that removes any residue solvent.

1.3.3 Exposure

The goal of exposure is to transmit an image of a desired pattern onto the resist film. A photomask (or reticle) is placed above the resist and a light source is then turned on which causes a chemical change in the resist in the areas that are exposed to the light. The chemical change in the resist causes the material to change solubility properties in certain solvents. Washing off exposed resist is known as development.

1.3.4 Development

Developing the resist means that wafer is immersed in a developer. After exposure a portion (the irradiated resist if positive and the non-irradiated resist if negative) of the resist is soluble in the developer. After development the wafer is ready for the etch process where the features are transferred onto the substrate.

1.3.5 Etching

After pattern has been made in the photoresist, it is time to transfer that pattern into the Si wafer. This is done with dry-etch techniques, using a reactive ion etcher (RIE) or an inductively coupled plasma (ICP) plasma reactor, which uses fluorine or chlorine as the etchant of the substrate. The resist pattern protects specific areas of the substrate while the non-protected areas are exposed to the plasma. The rate, at which the plasma removes or etches the Si over time, is discussed in more detail in Chapter 2.

1.3.6 Removal or Stripping

The last step in photolithography is to remove the remaining resist, leaving behind only the structured Si. The resist can be stripped by either immersing the wafer in a heated resist-stripping solution or placing it in a batch plasma-stripping chamber, where oxygen plasma removes the resist. After removal the wafer is inspected for defects and also measurements are taken to make sure that the features has the right size and shape.

1.3.7 Summary and Perspectives

Photolithography as described above is a complex process to create the necessary structures in Si. It is normal for the wafer to go through the photolithographic process about 50 times using different photomasks and also depositing new materials to create all features necessary to make an IC. Each new cycle and its photomask have to be perfectly aligned to the previous features to make a working device. For the process to become successful, meaning that the final outcome of structures does not have any defects that would interfere with the performance of the device, all processes have to work within very narrow tolerances. Also, as the structures made get smaller and smaller the more likely is the incorporation of defects. Therefore it is important to investigate and develop alternative technologies (which could work independently or in conjunction with photolithography) that could improve the whole process of making features in Si or SiO_2. Here we introduce an alternative approach to photolithography, for which the size and shape of the features created are not dependent on photolithography but rather of size upon the individual molecules and their self-assembled aggregates.

1.4 Moore's Law

The road map of the semiconductor industry has followed Moore's Law[10] over the last four decades, see Figure 1.4[9]. Moore's law, named after Gordon E. Moore (co-founder of Intel), was first introduced in 1970 by Carver Mead[11], which was about five years after the observation was made. According to Moore's Law the number of transistors in an IC will double for a minimum component cost every two years[12,13]. This means that not only will the size of every transistor shrink but also the cost per transistor will decrease. When making smaller transistors the risk is higher that defects are introduced and therefore some chips will have to be discarded. The cost of discarded chips is balanced by the decrease in cost per transistor and a "minimum cost" is achieved. At some point Moore's Law will not longer be relevant since there is a physical limit of how small one can make a transistor, for example; a transistor cannot be smaller then an individual molecule which would have to be the case if Moore's Law remained true many

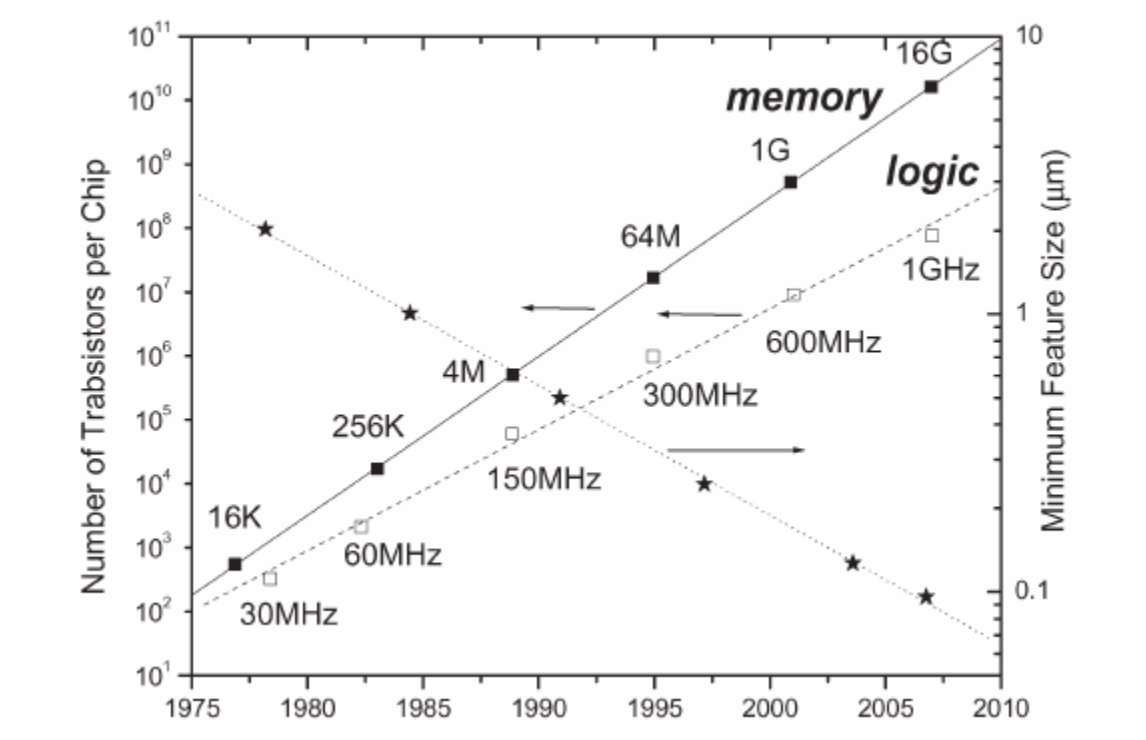

Figure 1.4 Moore's Law

decades from now. However, this observation has been true for decades and has become the norm and driving force for the industry, which has allowed for tremendous improvements in photolithography.

1.5 The Rayleigh Equation

As discussed in the previous paragraph the size of transistors decreases rapidly with time. Advancements in photolithography have overcome many hurdles over the course of the last four decades to keep up with the pace in Moore's Law. However, for each new generation of chips, 90 nm, 65 nm (today), 45 nm, 32 nm, 22nm, and 16 nm, the processes and materials become more and more not only difficult to make but also expensive. A state-of-the-art lithography tool costs around 40-50 million dollars, and the cost for each new instrument increases with decreasing node sizes[14]. The feature size which one can print in the resist at a particular wavelength is described in the Rayleigh Equation[15], where k_1 is the resolution factor, λ is the wavelength of irradiation, and NA is

$$\text{Feature size} = k_1\lambda/\text{NA} \qquad \textbf{Equation 1.1}$$

the numerical aperture (NA = $n \sin\theta$), see Equation 1.1. According to this observation there are only two way to decrease the feature size that can be printed in the photoresist: (1) decrease the wavelength of light used to irradiate the resist (2) increase the refractive index (n) of the medium between the lens and the resist and also increase n of the resist itself. Today ArF (193 nm) excimer laser exposure tools are used to provide the necessary photons that are used for the irradiation of the photoresist. Much research has been done in trying to decrease the wavelength of light and use the F_2 (157 nm) excimer laser as the light source for coming node generations. It turns out that the materials and tools needed for this process have not been developed successfully due to the difficultly in making the materials perform satisfactory using the 157 nm F_2 excimer laser[16]. Instead the focus has turned to increasing n with immersion lithography, in which a high n fluid layer is placed between the lens and the resist to increase the refractive index, See Figure

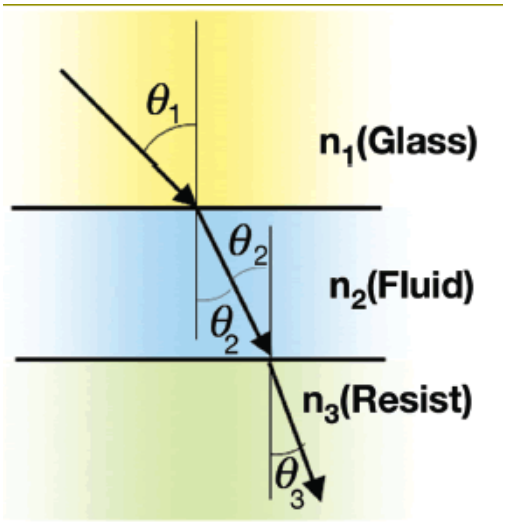

Figure 1.5 Schematic of immersion lithography

1.5. This technology has evolved over the past few years and is now the leading technology. It will eventually work at the 32 nm node. Deionized (DI) water (n=1.42 at 193 nm) is an ideal immersion fluid in many aspects due to its transparency and n and is used as the immersion fluid. To take immersion lithography to the next level new immersion fluids with $n > 1.60$ must be developed. This will most likely be some sort of saturated hydrocarbon. Since photolithography has many barriers to overcome before reaching the 32 nm node, alternative methods of patterning Si/SiO_2 are of great interest. One approach is to use block co-polymers to make patterns, and these have evolved as an attractive alternative to photolithography[17]. The work presented here uses a monolayer of organic molecules as the mask for plasma etching. This means that no irradiation is needed to determine the feature size of what can be etched into the substrate; therefore, the Rayleigh equation would be irrelevant for this approach. Such a system would allow for the ultimate limit of all types of lithography; the imaging of an individual molecule into a substrate. Molecular design and self-organization, through self-assembly, would be the limiting factors of what features can be achieved through molecular lithography. Of course it would be extremely optimistic, frankly unrealistic, to think that this approach

would evolve so that it by itself would make all sophisticated patterns necessary for a device. However, a realistic goal would be to use this technology for the creation of the critical dimension in various devices, such as interconnects.

1.6 Molecular Lithography

The large-downward (or top-down) approach creates devices by manipulating materials and processes from above, such as in photolithography. As discussed above this technology will meet its physical limitations within the next decades and new methods need to be explored. As a response to eventual limitations with the top-down approach Richard P. Feynman said in his famous speech to the American Physical Society "there is plenty of room on the bottom"[18]. The small-upward (or bottom-up) is an alternative approach towards technology at the nanometer scale. It starts with atoms and molecules to build up nanostructures. As chemists we have an outstanding opportunity to develop the bottom-up approach since we already have experience with manipulating atoms or molecules. The concept of molecular lithography is not truly the bottom-up but it combines it with the top-down approach to make nanometer structures. This can be seen as a bridge between the two methodologies and have potential to work in device fabrication. The idea of molecular lithography arose a few years before, Xiaohua Chen, working in the Tolbert research group,[19] investigated the etch resistance of several highly aromatic compounds towards a fluorine (SF_6) plasma. Poly(3,4-bis(phenylethynyl)styrene) (pBPES) was synthesized and examined for its fluorine plasma etch resistance before and after Bergmann cyclization to a polynaphthalene derivative. The plasma etch resistance before and after the curing process was measured with both SF_6 and O_2 plasmas. The etch resistance of pBPES was higher than that of the standard Novolac photoresist by a factor of nearly 2. After curing, the relative etch rate of the polymer decreased to a factor of 3, indicating an improved response for the more aromatic polymer. The selectivity of the cured pBPES to the silicon substrate was 1 to 58 using SF_6 gas in a RIE tool[20]. The idea was then; due to the excellent etch resistance, to

use these types of systems directly as an etchmask. The research described here has been focused on developing this idea into a working system where highly aromatic molecules themselves would act as the resist and therefore no photochemical reaction is necessary to produce the patterns, as in photolithography. The whole process resembles photolithography in a sense that many steps of the process are in the same order, but the key difference is that the resist is created not by a photoresist, but rather by a monolayer of highly stable self-organizing molecules. By using this monolayer as an etch-mask (a "molecular mask") we essentially bypass the photolithographic process while maintaining the advantages of the silicon infrastructure, See Figure 1.6. Self-organization creates the shape of the features of the etch mask which are transferred to the underlying

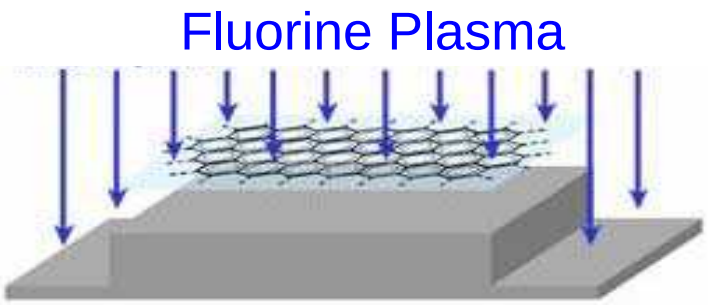

Figure 1.6 Schematic of molecular lithography

silicon. This will allow us to approach the ultimate limit for all types of lithography, the imaging of a single molecule in Si/SiO_2. There are at least seven requirements for the materials and processes used for molecular lithography to become successful: (1) the material has be soluble in solvent so thin films can be created using various coating techniques, (2) the material used has to in a monolayer on the surface to provide boundaries for the etch process, (3) the material has to either self-assemble or have the ability to be manipulated into usable patterns, (4) the monolayer has to be stable on the surface during the etch process and not move around, (5) the material has to be stable in the plasma so deep enough structures, usable for device fabrication, are achieved in the silicon upon etching, (6) the etch process has to be anisotropic; otherwise the small Si

structures would be destroyed by undercutting, (7) after etching the material has to be removable from the surface, leaving the Si structures standing. The monolayers of different molecules created here are covalently attached to the surface through a silane benzophenone derivative. The covalent attachment to the surface provides both the opportunity to create monolayer, since all non-bonded molecules can be extracted from the surface, and the necessary stability of the molecules on the surface to work as molecular resists. The chemistry behind this methodology is both reliable and straightforward, which makes this system easy to implement. The versatility of the benzophenone photochemistry[21,22,23,24,25,26,27,28] allows for many organic molecules to become attractive candidates for use as etchmasks. The only requirement for the benzophenone probe is that the organic molecules have an alkyl chain for the photochemical reaction attachment. This dissertation is focused on the proof of concept of molecular lithography. The work done here will provide the necessary tool to further develop this technology. Most structures seen here are random in a sense that we cannot control either the shape or direction of the features. The next step in developing molecular lithography will be to organize molecules into usable patterns and then transfer that pattern into a Si substrate.

1.7 The Ohnishi and Ring Parameter

Since a monolayer of molecules is used as the etch barrier special properties of the molecule are required. Not only is it necessary for the molecule to have high solubility and the required alkyl chain for covalent attachment to the surface. One of the most important properties is for the molecule to be stable in the plasma, since removal of only one layer of molecules would result in total loss of patterns. The Ohnishi and Ring parameters predict the etch resistance of material due to its chemical and structural composition. The Ohnishi parameter[29] states that the etch resistance of a resist is

$$\text{Ohsnishi Parameter} = N / (N_C - N_O) \qquad \textbf{Equation 1.2}$$

dependent on the number of carbon atoms in the monomer unit, see Equation 1.2, where N, N_C, and N_O are the total number of atoms, number of carbons, and number of oxygen. The ring parameter[30] also takes into account the molecular structure of the resist rather than only on the molecular composition, like the Ohnishi parameter, see Equation 1.3,

$$\text{Ring parameter} = M_{CR}/M_{TOT} \qquad \textbf{Equation 1.3}$$

where M_{CR} and M_{TOT} are the mass of the resist existing as carbons in a ring structure and the total resists mass. All materials discussed have an excellent etch resistance towards fluorine plasma. Both the Ohnishi and Ring parameter are calculated for the materials and the results are presented in the appropriate chapter.

1.8 Impact

The development of photolithography is not only approaching its physical limitations, due to the wavelengths and materials needed, but is also becoming extremely expensive, rendering Moore's Law unsustainable. Molecular lithography is a new alternative technology to photolithography and has the potential upon further development be incorporated in the production of ICs. The feature size achievable using this technique is that of the diameter of an individual molecule which is also the ultimate limit for all types of lithography. It is certainly optimistic to believe that molecular lithography could be used to produce a whole device by itself since it relies on self-assembly or mechanical stimuli to create the shape of the features used as the etchmask. However, in conjunction with photolithography one could develop a methodology where the critical dimensions in the device was produced with molecular lithography while the rest of the structures are made using photolithography. Since this technology depends on self-assemble of molecules into usable patterns either straight lines or pillars would be the easiest structures to create. The result of this would not only be a cheaper methodology but also by using individual molecules as the mask synthetic organic chemistry would the limiting factor in what sizes the features can obtain. However, it is

important to realize that the molecule used for this application must meet some requirements described earlier in this chapter. Finally, we cannot discount the immense power of synthetic organic chemistry in achieving the structures needed for long-range self-assembly, given the outstanding achievements in the field of medicinal chemistry. This thesis merely presents the opening salvos in that effort.

1.9 REFERENCES

[1] Bardeen, J.; Shokley, W.; Brattian, W. *Bell Syst. Techn. J.* **1949,** *28*, 435.

[2] Kelby, J US Patent #US3138747.

[3] Ito, H.; Wilson, G.; *Polym. Eng. Sci.* **1983,** *23,* 1012.

[4] Frechet, J.; Bouchard, F.; Houlihan, F.; Kryczka, B.; Eichler, E.; Clecak, N.; Wilson, G. *J. Imag. Sci.* **1986,** *30,* 59.

[5] Oizumi, H.; Tanaka, Y.; Shiono, D.; Hirayama, T.; Taku, H.; Onodera, J.; Yamaguchi, A.; Nishiyama. I. *J. Photopolym. Sci. & Techn.* **2006,** *19,* 507.

[6] http://en.wikipedia.org/wiki/MOSFET, Feb/2007

[7] Elliot, D. *Integrated Circuit Fabrication Technology;* McGraw-Hill Book Company: Newton, Massachusetts, 1982.

[8] "Basic Technology Course manual," *Integrated Circuit Engineering,* Phoenix, Arizona, **1978**.

[9] Hiroshi, I. *Adv. Polym. Sci* .**2005,** *172,* 37.

[10] Resnick, D.J.; Mancini, D.; Dauksher, W.J.; Nordquist, K.; Bailey, T.C.; Johnson, S.; Sreenivasan, S.V.; Wilson, C.G. *Microelectronic Engineering* **2003**, *69,* 412.

[11] IEEE *Solid-State Circuits Society Newsletter*, **2006.**

[12] Moore, G. *Electronics*, **1965,** *38(8),* 1.

[13] Excerpts from a conversation with Gordon Moore: Moore's Law, **May 2 2006,** Intel Corp.

[14] http://www.eetasia.com/ART_8800425484_480200_712e9bf8200607.HTM Feb/2007

[15] Gil, D.; Brunner, T.; Fonseca, C.; Seong, N.; Streefkerk, B.; Wagner, C.; Stavenga, M. *J. Vac. Sci. Technol. B.: Microelectronics and Nanometer Structures.* **2004**, 3431.

[16] Honda, T.; Kishikawa, Y.; Iwasaki, Y.; Ohkubo, A.; Kawashiam, M.; Yoshii, M. *Proceedings of SPIE – The International Society for Optical Engineering,* **2006,** *6145(Pt. 2 Optical Microlithography XIX),* 615422/1-615422/9.

[17] Bendejacq, D.; Ponsinet, V.; Joanicot, M.; Loo, Y.-L.; Register, R. *Macromolecules,* **2002**, *35*, 6645.

[18] Feynman, R. *Lecture at the Annual Meeting of the American Physical Society,* California Institute of Technology, **1959.**

[19] Chen, X., Ph.D. Thesis, Georgia Institute of Technology, 2000.

[20] Chen, X.; Tolbert, L.; Hess, D.; Henderson, C. *Macromolecules*, **2001,** *34,* 4104.

[21] Turro, N. *Modern Molecular Photochemistry;* University Science Books: Mill Valley, **1991**.

[22] Prucker, O.; Naumann, C.A.; Rühe, J.; Knoll, W.; Frank, C.W. *J. Am. Chem. Soc.* **1999,** *121*, 8766.

[23] Dormán, G.; Prestwich, G. *Biochemistry,* **1994,** *33,* 5661.

[24] Horie, K.; Ando, H.; Mita, I. *Macromolecules,* **1987,** *20,* 54.

[25] Mets, G.; Hamouly, S.; Oh, T. *Pure Appli. Chem.* **1984**, *56,* 439.

[26] Horie, K.; Morishita, K.; Mita, I. *Macromolecules,* **1984,** *17,* 1746.

[27] Horie, K.; Mita, I. *Eur. Polym. J.* **1984,** *20,* 1037.

[28] Bräuchle, C.; Burland, D.; BjorklundG. *J. Phys. Chem.* **1981,** *85,* 123.

[29] Gokan, H.; Esho, S.; Ohnishi, Y *J. Electrochem. Soc.* **1983,** *130(1),* 143.

[30] Kunz, R.; Palmateer , S.; Forte, A.; Allen, R.; Wallraff, G.; DiPetro, A.; Hofer, D. *SPIE*, **Vol. 2724,** 365.

CHAPTER 2

C96 - DISCOTIC MOLEULES AS MOLECULAR RESISTS

2.1 Introduction

C96-C_{12}[1,2] is member of a class of molecules called polycyclic aromatic hydrocarbons (PAHs). PAHs were discovered in tar coal during the middle of the 20th century and quickly became an important class of molecules for industry. Since then, PAHs has been studied by both chemist and theoreticians to a vast extent[3]. More specifically, C96-C_{12} is a larger brother of hexa-*peri*-benzocoronene[4] (HBC), as shown in Figure 2.1. The nomenclature for these types of compounds is not trivial and C96 denotes to the number of carbons present in the core of the molecule (96 carbon atoms equals 16 benzene rings) and -C_{12} refers to the number of carbons present in each of the six side chains. There are several different derivatives of molecules based of C96 but since C96-

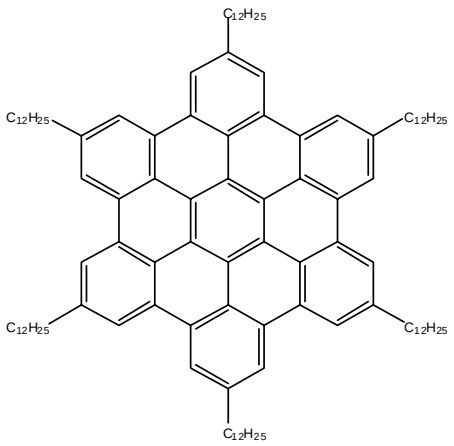

HBC

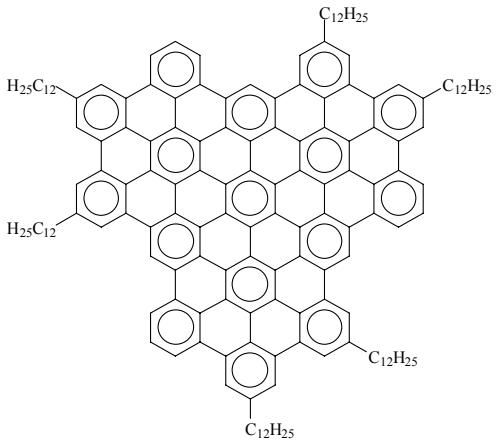

C96

Figure 2.1 Structures of HBC and C96

C_{12} is the only molecules of this kind discussed in this chapter, it will be from here on known as only C96. Extensive work has been done on these types of molecules, in Mainz, Germany, by Prof. Klaus Müllen, who also developed a beautiful synthetic route for making different derivatives of PAHs[5]. More specifically, the properties of C96 and its many derivatives have been thoroughly investigated and analyzed with differential scanning calorimetry (DSC), X-ray diffraction (XRD), and solid-state NMR to determine the properties, dynamics, and arrangements of these discotic materials[6,7,8,9,10,11]. C96 and its relatives are not only attractive candidates for molecular lithography but are also interesting for other functions in microelectronics due to their fascinating electronic and opto-electronic properties[12]. The highly aromatic cores of PAHs π-π stack into one-dimensional columnar supramolecular structures[13,14,15,16,17,18]. The overlap of the delocalized π-orbitals in the supramolecular structures allows for efficient charge carrier mobility along the axis of orientation. The charge carrier mobility is an important electronic property in the performance of devices such as field effect transistors (FETs)[19]. Since structural control and uniaxial directionality is also necessary for PAHs to perform with its highest carrier mobility in field effect transistors, much work has been devoted to aligning and controling the one dimensional supramolecular columnar organization. PAHs are known to organize in into highly ordered layers using Langmuir-Blodgett deposition[20], zone-casting[21], zone-crystallization[22], or solution casting onto pre-aligned polytetrafluoroethylene[23]. The π-π stacking also arises from alkyl substitution which enables them to form discotic mesophases. C96 is ~2 nm in diameter and is a liquid crystal at room temperature with a phase transition at 38º C. The phase transition is thought to involve the alkyl chains and has no impact on the structure and orientation of

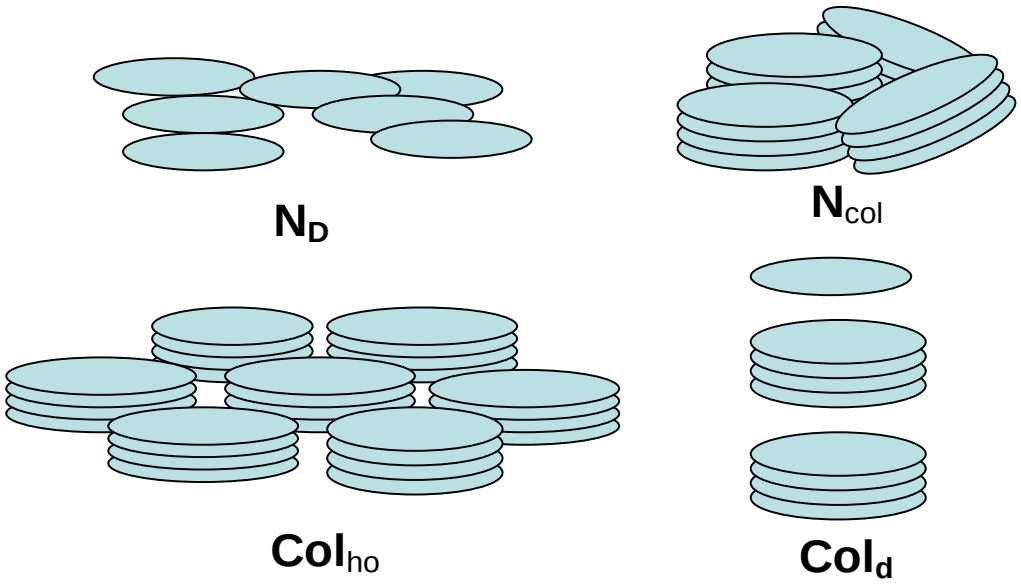

Figure 2.2 Schematic of discotic mesophases

the molecule[2]. In 1977, Chandrasekar discovered a new class of liquid crystal phases or mesophases[24], which are called discotic mesogens. These consist of disk-like molecules with planar rigid cores to which flexible side chains are attached, and include, C96. These types of mesogens can order in four ways including, nematic-discotic (N_d), nematic-columnar (N_{col}), columnar hexagonal ordered (Col_{ho}), and columnar-disordered (Col_d) are the three ways that these types of mesogens can be ordered[25], see Figure 2.2. Thus, the molecular orientation that can result from the liquid crystalline behavior of C96 can be utilized for preparing molecular masks. The discotic molecules can assemble into lines or pattern on the surface which can then be patterned into the substrate. The process and order we investigated C96 and other materials for the use of molecular lithography are: (1) covalent attachment of the molecules to a Si or SiO_2 surface, (2) removal of non-bonded molecules on the surface, (3) plasma etching, (4) and removal of the molecular resist. All surfaces are analyzed after each step to provide the necessary information for a

thorough understanding and further development and optimization of this technology. This chapter will include reasoning, descriptions of analysis of surfaces, and processes that are common for all materials throughout the dissertation. The following three chapters will include results regarding the specific materials used with these surfaces and processes.

2.2 Experimental

Since molecular lithography builds on the principle of using individual molecules as the etch resist, one must first create a monolayer of the desired material. Monolayers are needed as multilayers of molecules would not provide the defined molecular boundaries necessary for molecular lithography to become successful. Several analytical tools were used to image the surfaces to be sure that a monolayer was used as an etch barrier in the etch process. This section describes surface preparation and analysis for molecular lithography.

2.2.1 Methods of Surface Analysis

Atomic force microscopy (AFM) has been used vastly to analyze a variety of surfaces during the process of molecular lithography. The Veeco AFM system used is located at the Microelectronic Research Center (MIRC) at Georgia Institute of Ttechnology (Ga Tech). AFM was performed on all samples in tapping mode; the tips used were NSC 18 produced by μmasch. The C96 fibers are excellent candidates for AFM analysis, as they were dense and have nicely defined edges. It was easy to monitor the progress of the sample during the course of the process since AFM had vertical resolution on the order of Ångströms (Å). This provided accurate data to observe surface

changes before and after the etch process. SEM and other imaging techniques can not provide the same resolution required to identify changes of only a few nm vertically. The only setback with using the AFM was that the vertical resolution was not matched by the lateral resolution, since the AFM tip influences the lateral resolution. The radius of the AFM tip (~10 nm) was larger then the width of the fibers and due to the methodology of the AFM, the fibers appear wider in the analysis then in reality, see Figure 2.3[26].

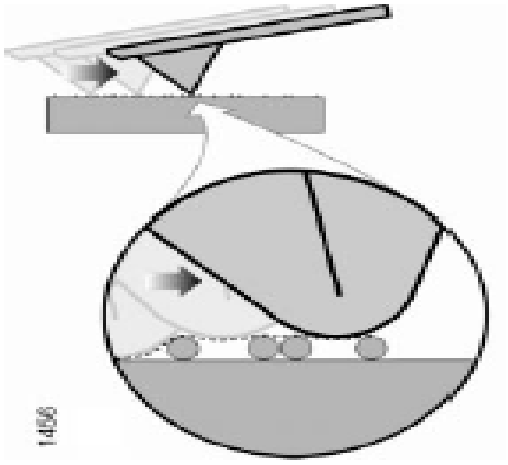

Figure 2.3 Schematic of resolution limitations using AFM

Static water contact angle measurements have also been used to monitor the surface. The goniometer, Video Contact Angle System 2500XE AST, is located in Prof. Henderson's lab at Ga Tech. All contact angle results discussed in this dissertation were static contact angles. Although the droplet used for contact angle (2 μl) was enormous compared to the nano-structures produced on the surface, it could still provide important information about the material on the surface. Each step of the process had a particular associated contact angle, which was easily recognizable after gaining experience with the process.

Energy dispersive X-ray analysis (EDS or EDX), located on the SEM at the MIRC, and X-ray Photoelectron Spectroscopy (XPS), located in Prof. Hess' lab at Ga Tech, have been used to provide the elemental analysis on the surface for each step of the process. This gave information about what elements were present on the sample at a given point during the process. This information was extremely important for the final analysis of the structured SiO_2 surface, and it was necessary to determine that the final structures are solely made of SiO_2 and not another residual material.

Scanning electron microscope (SEM), Zeiss SEM ultra 60, has been used to analyze the surface morphology of the sample. This instrument is located in MIRC at Ga Tech. This technique was quite difficult to master when dealing with features as small as 3-4 nm. Therefore, only the initial surface, which was patterned with C96 or fullerene polymer, was analyzed with this technique, as discussed later in the chapter. MNFP (individual C_{60}) could not be observed in the SEM due to their small size (0.7 nm in diameter, as shown with transmission electron microscopy (TEM))[27].

Scanning tunneling microscopy (STM) has been used to analyze the MNFP monolayer. All STM images have been done in collaboration with Prof. First in the Physics department at Ga Tech; Nikhil Sharma performed all STM images. This technique was ideal for this purpose since it relied on tunneling electrons from a fine tip versus AFM which touched the surface or SEM, which relied on back scattered electrons. Therefore, STM allowed for observations of individual molecules on the surface, as described in chapter 4.

A Woollam ellipsometer was used to measure thicknesses of SiO_2 before and after etching to determine etch rates of various fluorine plasmas. The Woollam ellipsometer was located in the cleanroom at MIRC.

2.2.2 Thermal Growth of SiO_2

The surfaces used for molecular lithography with a C96 mask were mainly SiO_2. The SiO_2 was thermally grown in a Lindberg Oxidation tube. Wet oxidation conditions were utilized, meaning that H_2O vapor was transported into the chamber during the process. Wet oxidation was used because it was quicker than dry oxidation. A n-doped Si (100) wafer was placed in the oxidation tube and the temperature was set to 1000° C at a ramp speed of 25° C/minute (min). The wafer was left in the tube at the desired temperature for 3-4 hours depending on the availability of the furnace. The thickness of the SiO_2 was not of significant importance for this application since only the first 10 nm was actively used during the process. However, normal thicknesses of the oxide layer were 4200 - 5200 Å, as determined by ellipsometry.

2.2.3 The Benzophenone Photoprobe

The C96 monolayer was created by first covalently binding a chlorosilane benzophenone derivative to the semiconductor substrate, and then using the photochemically reactive benzophenone moiety to covalently bind the desired molecule to the surface. The prerequisite for molecule to be covalently attached with benzophenone upon irradiation was that the molecule must have an alkyl chain. Therefore, all materials used in this section contain alkyl chains as the source for covalent attachment to the benzophenone. A benzophenone derivative was chosen over other

photophores such as diazo esters, aryl azides, and diazirines, as the linker between the surface and C96 due to the chemical stability, ease of activation with light at 340-360 nm, and its preferential reactivity, sometimes with high specificity, with otherwise unreactive C-H bonds. Even in the presence of solvent (water) and nucleophiles, the reactivity towards unreactive C-H bonds was sustained. This methodology of photochemical attachment to the surface also allowed any non-bonded C96 molecules to be washed away in a Soxhlet extraction apparatus. Upon irradiation at ~ 350 nm, the benzophenone undergoes a transition where one electron from a non-bonding sp^2 like n-orbital on the oxygen moves to an antibonding π^*-orbital on the carbonyl carbon[28]. The triplet state is a diradicaloid by nature and one radical abstracts a hydrogen atom from the alkyl chain and the other radical recombines with the radical which was located at the point where hydrogen was abstracted, see Figure 2.4[27]. The triplet state has a lifetime of 80-120 μs

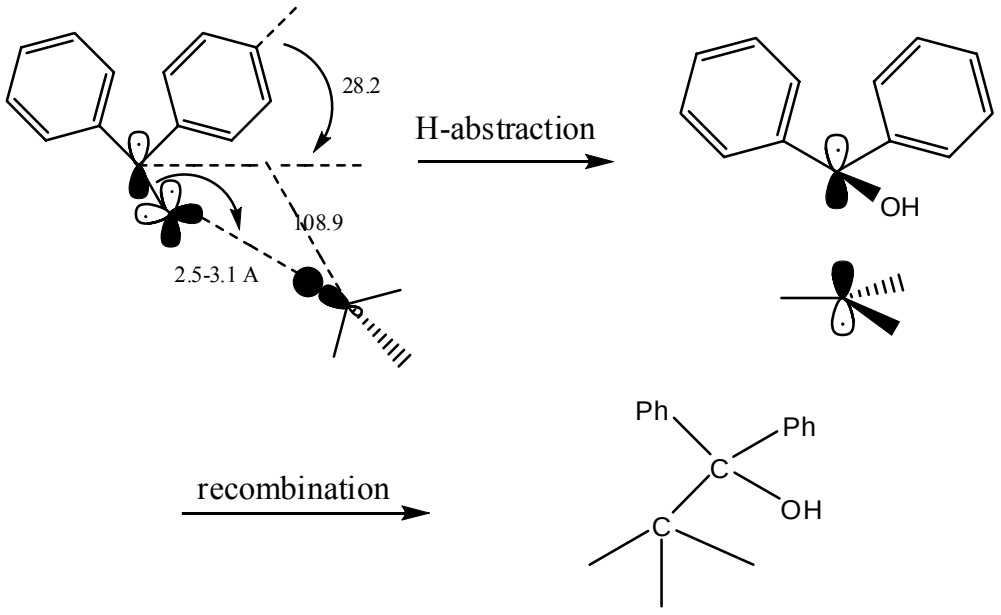

Figure 2.4 Schematic of benzophenone photochemistry

if no C-H bonds were in the appropriate vicinity, however if the transition occurred in the presence of a C-H, the life time is considerably shorter. If no reaction occurs, the triplet state relaxed back to the ground state and can again form a triplet state if irradiation continues. Since the $n \rightarrow \pi^*$ transition was reversible the sample can be irradiated over a long period of time to ensure that the attachment of almost all available C96 molecules occur. The substituent on the benzophenone, in this case chlorodimethylpropyloxy silane, in the *para* position, could have an effect on the overall quantum yield (Φ). Generally, an electron donating group would decrease Φ, while electron withdrawing groups would increase Φ. This was because the electron donating group and electron delocalization into the aromatic system causes a shift in the excited state triplet electron transition from $n \rightarrow \pi^*$ to $\pi \rightarrow \pi^*$, and therefore become less reactive toward the C-H moiety. Also the susbtituent could influence the Φ by steric hindrance; *ortho* and *metha* substituted benzophenones have lower quantum yields than *para* substituted derivatives. Not only does the structure of the benzophenone derivative determine the Φ, but also the accessibility to the binding molecule. The maximum distance for the photochemical attachment to take place is 3.1 Å. Apart from geometrical factors, the efficiency of the covalent attachment heavily depends on the chemical and electronic environment of the benxophenone and the C-H moiety. The strength of the bond being broken (normally C-H) and the stability of the resulting radical plays a large role in the determining factors if the reaction will proceed or not. The C_{12} alkyl chains on C96 are an excellent attachment site since the alkyl chains are flexible and can adjust to the right distance and geometry for the photochemical reaction to proceed efficiently. Normally, the overall Φ is 0.05 – 0.4, with the higher values occurring when the transition is a simple $n \rightarrow \pi^*$ transition[29].

2.2.4 Preparation of the Silane Benzophenone Monolayer

This easy to use and straight forward methodology of creating a silane benzophenone monolayer on Si or SiO_2, followed by covalent attachment of other molecules on a surface was developed by Curtis Frank, Wolfgang Knoll, and Jürgen Rühe in 1999[30]. The formation of a dense silane benzophenone monolayer was vital for the rest of the molecular lithographic process. Not only did it allow for the C96 monolayer formation, but it also provided the necessary stability of the C96 monolayer to withstand the plasma process. Therefore, great care was taken during both the synthesis and immobilization on the surface of the chlorosilane benzophenone derivative. Both the dimethyl chlorosilane and 4-(3'-Chlorodimethylsilyl)propyloxybenzophenone were hydroscopic and would degrade if exposed to air or moisture.

2.2.5 Materials

All materials used in this section were purchased from Fisher except triethylamine (Et_3N), which was purchased from Acros. Toluene was distilled from molten sodium hydroxide using benzophenone as an indicator, dark blue color indicates dry toluene. The distillation took place under inert atmosphere using N_2 gas. Et_3N was stored using NaOH (s) pellets as drying agent. Dimethyl chlorosilane was stored in the fridge and was under inert atmosphere when syringed. All reactions involving a chlorosilane derivative was done under inert atmosphere using standard Schlenk glassware and technique. All other chemicals were used as received.

2.2.6 Syntheis of 4-Allyloxybenzophenone (ABP)

This compound was made in large quantities using standard Williamson ether synthesis procedures[31]. In a standard synthesis 19.8 g (0.1 mol) 4-hydroxybenzophenone and 13.3 (0.11 mol) allyl bromide was dissolved in 60 ml of acetone. 14 g of potassium carbonate was added to the solution and refluxed for 8 hrs, and then cooled to room temperature. Distilled water (80ml) was added to the mixture and thereafter extracted twice with diethyl ether. The organic phase was washed with NaOH (aq) 10% twice and dried over Na_2SO_4 until the solvent evaporated. The product (slight yellowish) was purified via recystallization from MeOH and gave about 17 g (80%) of the desired compound. ^{1}H NMR ($CDCl_3$, δ in ppm) 4.6 (m, 2H, OCH_2), 5.3-5.5 (m, 2H, CH_2=), 6.1, (m, 1H, =CH-), 6.9-7.9 (various m, 9H, C-$H_{aromatic}$).

2.2.7 Synthesis of 4-(3'-Chlorodimethylsilyl)propyloxybenzophenone (CSBP)

This compound was synthesized using standard hydrosilation methods[32,33]. 2g of ABP was dissolved in 20 ml (excess) of dimethyl chlorosilane under inert atmosphere. The catalyst, Pt-C 10% 10 mg, was added to the mixture and was stirred and refluxed for 5 hrs. The unreacted dimethyl chlorosilane was removed *in vacuo* leaving the product, CDMSPBP, in high yield (~90%) as an oil. ^{1}H NMR ($CDCl_3$, δ in ppm), 0.3 (s, 6H, $SiCH_3$), 0.9 (m, 2H, $SiCH_2$), 1.9 (m, 2H, CH_2, CH_2, CH_2), 3.9 (t, 2H, OCH_2), 6.9-7.9 (various m, 9H, C-$H_{aromatic}$), note that this reaction can go either Markovikov or anti-Markonikov, meaning that the hydrosilantion could occur at either carbon on the double bond. For its intended purpose here either way would work. The oil was dissolved in freshly distilled toluene (about 30 ml) and the catalyst was filtered off using a schlenk type frit. This solution was stored under inert atmosphere in a freezer until usage. The complete synthesis of CSBP can be seen in Figure 2.5[29].

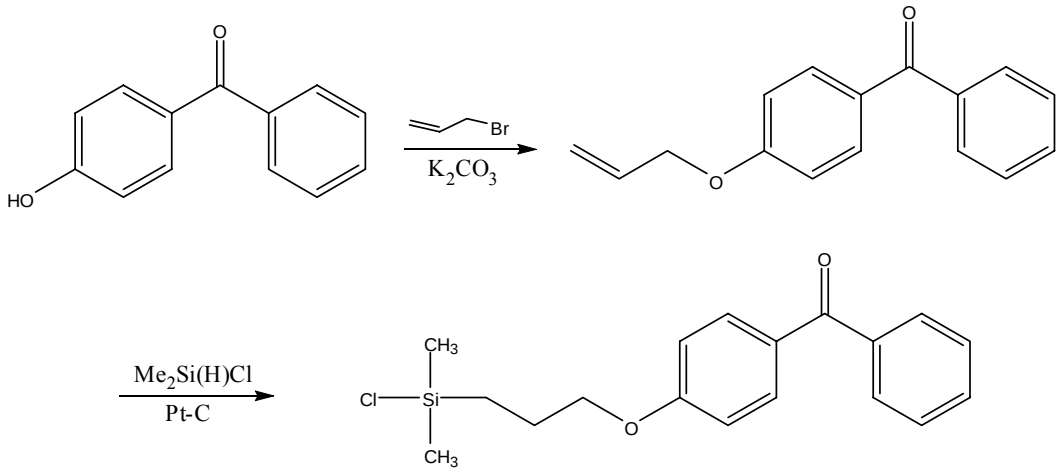

Figure 2.5 Synthesis of CDMSPBP

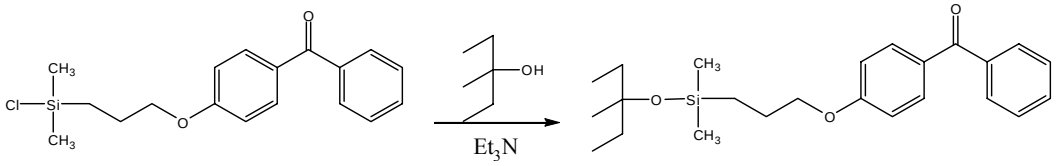

Figure 2.6 Schematic of the immobilization of CDMSPBP to SiO_2

2.2.8 Immobilization of CSBP to a SiO_2 Surface

CSBP could easily be attached to Si/SiO_2; the only requirement was that the Si has a native oxide (pure SiO_2 surfaces also works well for this reaction). Pieces of a SiO_2 wafer were cleaned in piranha (H_2SO_4 70%, H_2O_2 30%) and rinsed thoroughly with distilled water and then dried with N_2 before use. 5 ml of the solution containing CSBP was diluted with about 50 ml of dry toluene (enough so the pieces of wafer are immersed) in a Schlenk type beaker and a few drops of dry Et_3N were added. The Et_3N binds to the

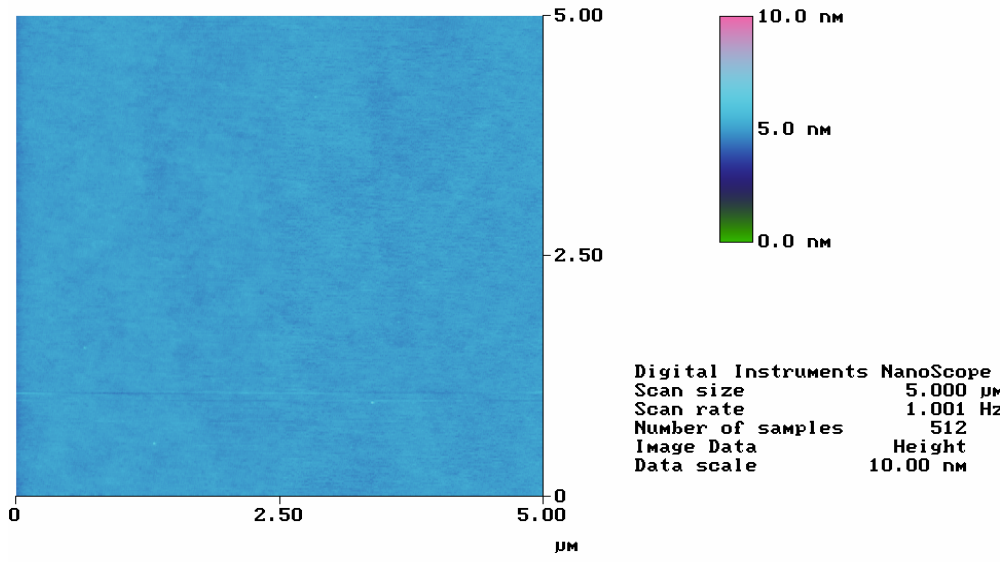

Figure 2.7 AFM of silane benzophenone on SiO_2

resulting HCl and also worked as a catalyst in this reaction. The solution was left standing over night and a cloudy solution was a good indication that the immobilization was successful. See Figure 2.6 for a schematic of the immobilization. The wafer pieces were the cleaned by rinsing extensively with chloroform and then dried with N_2. The monolayer of the benzophenone derivative was analyzed via contact angle and ellipsometry. The static water contact angle was 69 ± 2 and ellipsometry values indicate that the thickness was 1.0 ± 0.2 nm, assuming a refractive index of 1.5. AFM images indicated a very smooth surface, 0.2 ± 0.1 nm of roughness, which also means that there was a high density of CSBP on the surface, see Figure 2.7. These surfaces are then immediately used for irradiation and photochemical attachment of C96.

2.2.9 Synthesis of C96

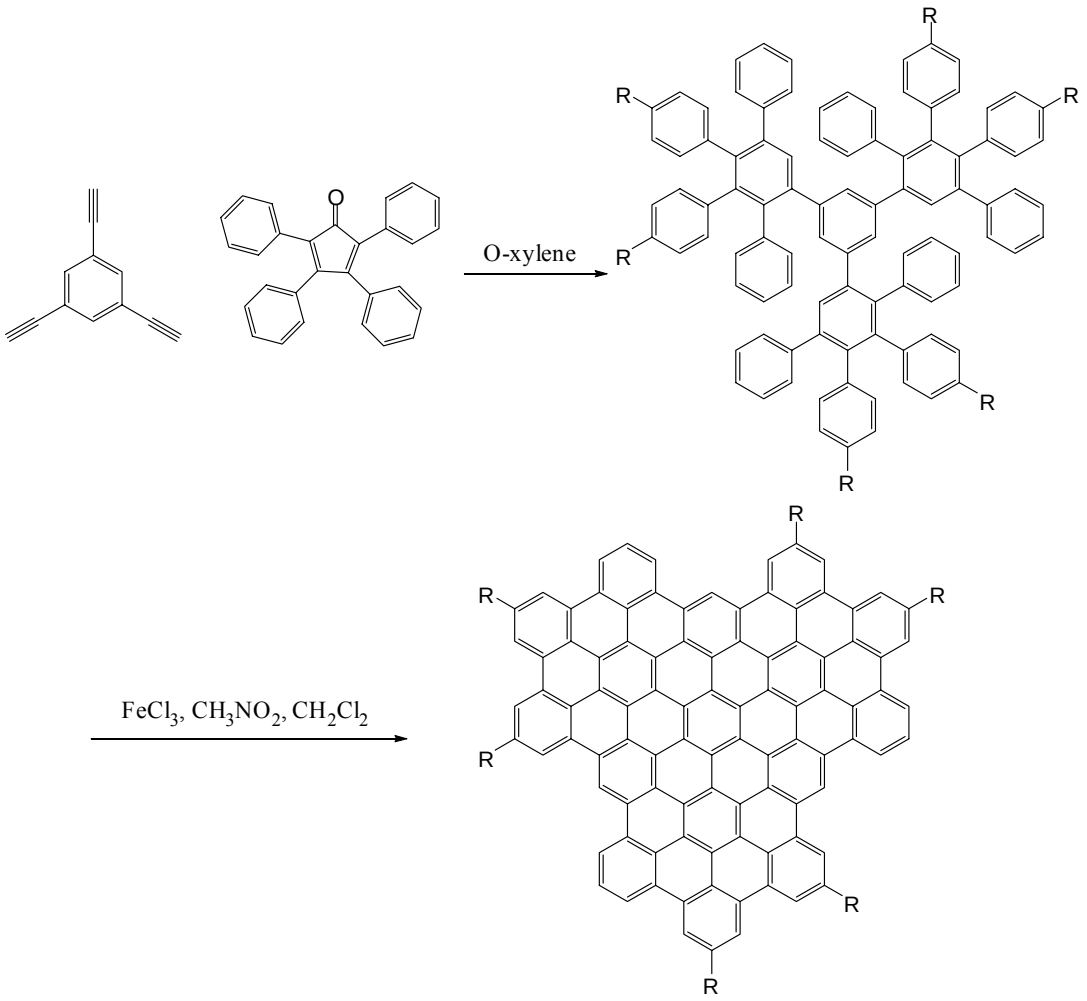

Figure 2.8 Synthesis of C96

C96 was synthesized in Klaus Müllen's laboratories in Mainz, Germany, who kindly supplied us with this molecule and is also one of our collaborators on this project. The synthesis can be seen in Figure 2.8. A Diels-Alder cylcoaddition was the first step of the reaction, followed by a cylcodehydrogenation of the C96 precursor formed from the first reaction. First, 1,3,5-triethylbenzene (76 mg, 0.51 mmol) and 3,4-bis(4-dodecylphenyl)-2,5diphenylcylcopentadienone (1.31 g, 1.82 mmol) were dissolved in o-xylene (4 ml) and heated for 18 hrs at 170º C under inert atmosphere. The solvent was

removed *in vacuo* and the residue was purified by column chromatography on silica gel (petrol ether/dichloromethane) to yield the C96 precursor at (1.10g, 97%). ^{1}H-NMR (500 MHz, $C_2D_2Cl_4$, 60º C): δ = 7.10-7.02 (m, 15H, Ar-H), 6.75-6.49 (m, 45H, Ar-H), 2.32 (t, ^{3}J(H,H)=7.3 Hz, 6H α=CH_2), 2.27 (t. ^{3}J(H,H)=7.3 Hz, 6H, α=CH_2), 1.44-1.02 (m, 120H, CH_2), 0.83 (t, ^{3}J(H,H)=6.9 Hz, 18 H, CH_3). The C96 precursor (0.35 g, 0.16 mmol is then dissolved in dichloromethane (150 ml) in a two-necked round bottom flask. A solution of $FeCl_3$ (2.29 g, 14.1 mmol) in CH_3NO_2 (15 ml) was added drop wise into the flask. Argon was bubbled through the solution to remove the HCl formed. Dichloromethane was added to replace the evaporated solvent. After 15 hrs methanol (MeOH) was added (200 ml) and the precipitate was filtered and washed with MeOH (300 ml). The finished product, C96 (~70 %), was red in color and was purified by column chromatography on silica gel (first column, H_2O/THF 30%/70%, second column, toluene) [34].

2.2.10 Covalent Attachment of C96 to the Silane Benzophenone Modified Si/SiO_2 Surface

Solutions of various concentrations of C96 were prepared in chloroform or dodecane. A thin layer of C96 was created either via spin-casting the solution onto a benzophenone modified surface at various rpms for 1 min, dip-coating at various speeds, or drop-casting and letting the solvent evaporate. The samples were then placed onto a hotplate at 100º C for 30 sec to remove any solvent residue. The sample was placed into a Stratalinker 2400 for 120 min. The lamps used only irradiates at ~ 356 nm which gave rise to a $n \rightarrow \pi^*$ transition in the benzophenone which allowed for a reaction with the alkyl chain at C96. The $n \rightarrow \pi^*$ transition is reversible, we irradiated for this long of a period to ensure that almost all attachments between the benzophenone and C96 that were possible

have taken place, see Figure 2.9 for mechanism of the covalent attachment. After irradiation, the excess molecules that had not been covalently attached to the surface were extracted with chloroform in a Soxhlet extraction apparatus.

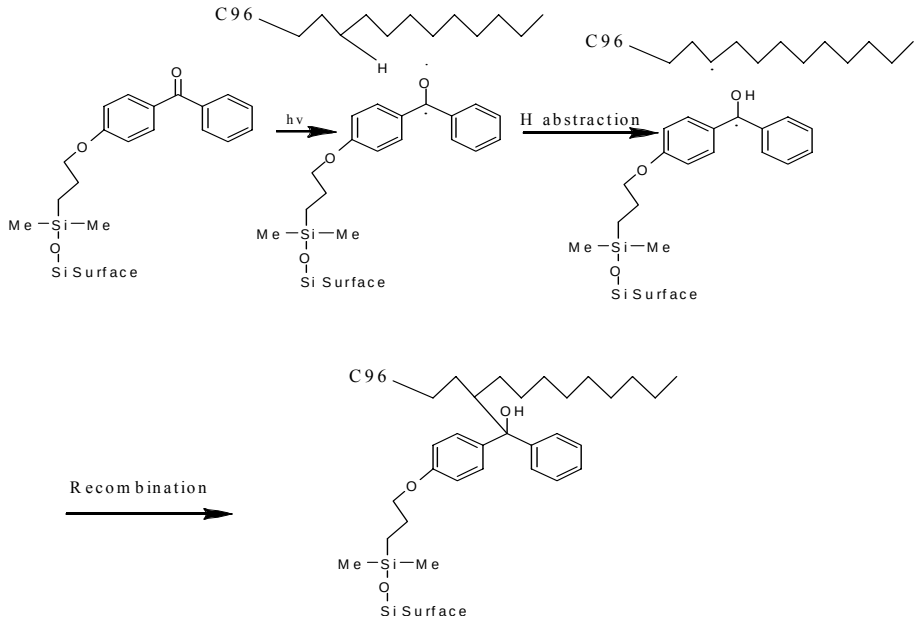

Figure 2.9. Covalent attachment of benzophenone to alkyl C96

2.2.11 Surface Morphology Study Depending on the C96 Concentration

C96 solutions in chloroform or dodecane of 10^{-3}, 10^{-5}, and 10^{-7} M concentration were prepared. Thin films of each solution were prepared using various coating techniques described in the previous paragraph. The samples were then irradiated at 356 nm with the Stratalinker 2400 for 120 min. After irradiation, the samples were rinsed thoroughly in the Soxhlet apparatus to remove the unattached molecules. The water contact angle increased from 69 ± 2 (benzophenone surface) to 83 ± 1 when a monolayer of C96 attached for 10^{-3} and 10^{-5} M solutions using either spin- or dipcoating. For 10^{-7} M

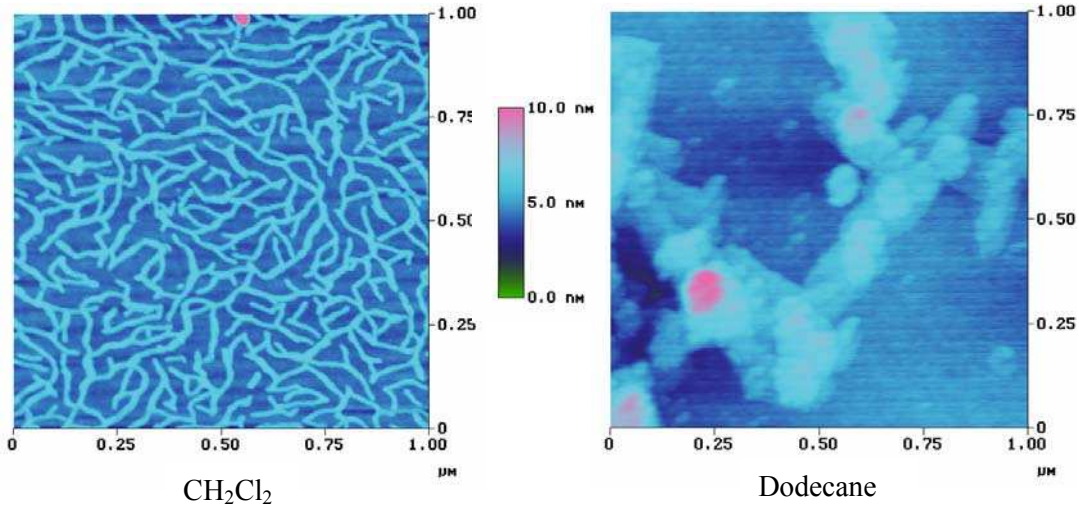

CH_2Cl_2 Dodecane

Figure 2.10 AFM of C96 spincoated from CH_2Cl_2 and dodecane at 10^{-3} M.

solutions the contact angle was considerably lower, 72 ± 3, which indicates that less material was on the surface, this was also confirmed with AFM. AFM analysis of the different samples shows that there were differences in the surface morphology depending on both the solvent and the coating technique. The structures on the surface were dictated by three different sources: (1) the π-π interaction between the C96 molecules, (2) the difference in hydrophobicity between the surface and the molecules, (3) the solvent used for thin film fabrication. For all samples prepared with chloroform the molecules stood perpendicular to the surface and formed strands or fibers on the surface due to the π-π stacking. These fibers gave excellent boundaries in the etching processes, which are described later. On the other hand films prepared with dodecane as solvent showed a different morphology. The structures seen in the AFM are islands of molecules rather then fibers. The molecules were also laying down flat onto the surface rather then standing up. This was due to interaction of the solvent and the molecules, as the long alkyl chains of the solvent disturbs the π-π interaction of the C96 molecules and forces

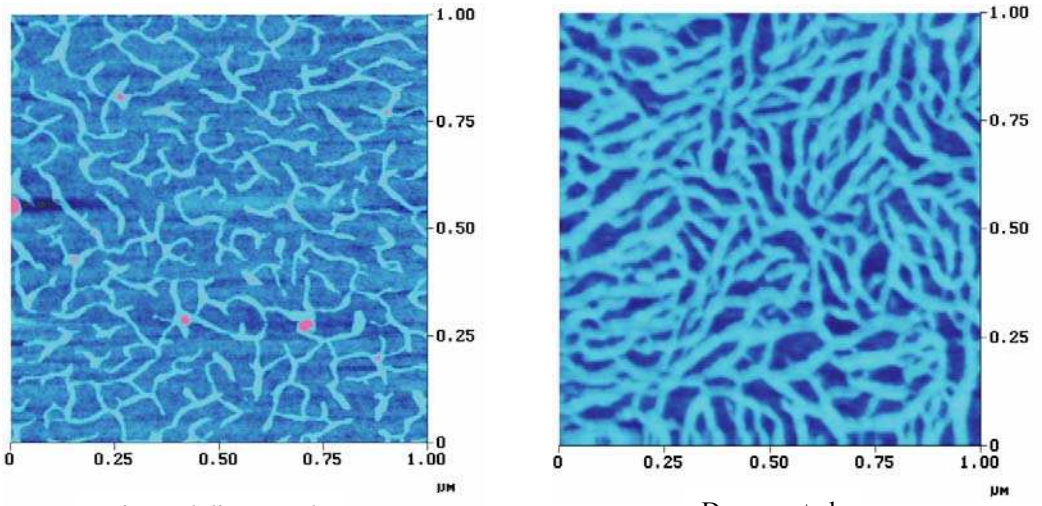

Figure 2.11 Spin- and dip-coated vs. Drop-coated from 10^{-5} M.

them to lie down on the surface, see Figure 2.10. Another reason for this was that dodecane wets the silicon surface better then chloroform and therefore makes the C96 molecules less prone to stand perpendicular on the surface. Dip and spin coated surfaces had similar morphologies at the same concentration due to the similar film thicknesses and because of the motion of the substrate during film formation. Drop coated surfaces on the other hand differed from the other coating technique in that the when the solvent evaporated the concentration of the molecules increased drastically and the molecules had time to organize themselves into long fibers, see Figure 2.11. All fibrous structures had the same width and height. The width of the fibers in the AFM images were 10-18 nm, however SEM images showed that the width of the fibers were about 3-4 nm, see Figure 2.12. The height of the perpendicular standing C96 fibers is 2.3 ± 0.2 nm which corresponds well with the diameter of C96. There was no difference in the fibrous structures using 10^{-3} and 10^{-5} M solutions using spin-coating or dip-coating techniques. The 10^{-7} M solution on the other hand was below the threshold concentration for the

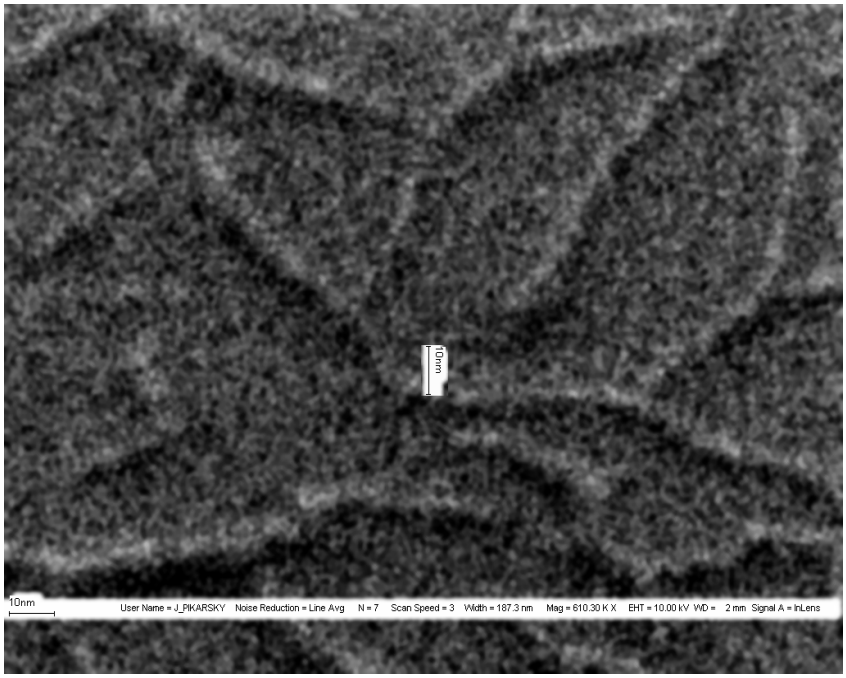

Figure 2.12 SEM of C96 fibers

formation of π-π stacked C96 fibers as no visible features were seen using spin-coating or dip-coating techniques. Drop-coated surfaces showed the same structures as for the other concentration, which was expected since the molecules had time to organize and concentrate for thick layer formation even from very dilute concentrations. The structures on the surface were identical using either Si or SiO_2 as the substrate. XPS results showed a 22% increase in the concentration of carbon on the surface before and after C96 monolayer formation. There have been no previous reports of XPS results using a C96 monolayer, but the increase in carbon was similar to other high carbon containing monolayers, such as fullerenes[35].

2.2.12 The Ohnishi and Ring Parameter for C96

As described in the first chapter, the Ohnishi[36] and Ring[37] parameter are indicators on how resistant a material is towards a fluorine or oxygen plasma process. Here we present the parameter values for C96 as the whole molecule and also for the core of the molecule. Since C96 does not have any oxygen atoms the Ohnishi parameter can be simplified to $V=N/N_c$. See Equation 1.1 and 1.2 in Chapter 1. The Ohnishi parameter was calculated to be 1.89 for the whole molecule. Since the molecular structure of C96 is quite unique in the sense that all aromatic rings are localized to the core of the molecule, it was interesting to calculate the Ohnishi parameter of only the core since it potentially could withstand the plasma more so than the alkyl chains. The Ohnishi parameter for the core only was 1.31 and 3.08 for the alkyl chains. The calculation of the parameters for only the core itself became important not only for the chemical structure of C96, but also for the π-π stacked molecules which results in that all the cores for the molecules are localized. Therefore the core of the molecule could still act as an effective resist after the alkyl chains had been burned off. For optimal etch resistance the parameter would be 1, but the parameter values of C96 still indicated that it had high etch resistance which was also confirmed though experimental data. The Ohnishi parameter for many commercial photoresists is around 2.5-5. The Ring parameter goes beyond the Ohnishi parameter and put weight on not only the molecular composition of the molecule, but also the molecular structure. Another difference is that the ring parameter is calculated by the mass of the molecule and not just the number of molecules as for the Ohnishi parameter. For the entire C96 molecule, the ring parameter is 0.53 and for the core, 0.97. Of course the ring parameter cannot be calculated for the alkyl chains since they have no ring structure. The maximum etch resistance for a molecule of a particular molecular weight is 1 and the

lowest etch resistance is 0. Both parameters indicated that C96 would perform exceptionally well in a plasma process. Separate from the two parameters discussed above, C96 assemblies also gained stability from the fact that it was π-π stacked. Pisula et al. suggest that the distance between the cores of C96 is 0.34 – 0.36 nm which resembles the distance of interlayer graphite (0.34 nm) and it has been predicted that the columns have nearly the same density as graphite, ρ_c = 2.25 g/cm. The high density of C96 assemblies combined with its exceptional Ohnishi- and Ring parameters provided support that extraordinary stability of the self-assembled structures against the fluorine plasma could be possible.

2.2.13 Etching Using C96 as a Molecular Mask

All experiments involving plasma processes have been performed in the claenroom at the MIRC at Georgia Institute of Technology. The semiconductor industry is moving towards using thinner and thinner films of photoresist to use for etch processes. The International Technologies Roadmap for Semiconductors (ITRS) roadmap lists no manufacturable resist that has a thickness of less then 120 nm or line width roughness (LWR) less then 3 nm[38]. Here we used the thinnest layer possible as the etch barrier, a monolayer of individual molecules. Theoretically, that would mean that limiting edge resolution would could be much smaller then the ITRS roadmap. The thickness of this monolayer was 2.3 ± 0.2 nm according to AFM data. One of the most difficult steps to overcome in this was to identify appropriate etching conditions. All Si/SiO_2 etching was done with fluorine as etchant, more specifically CF_4. Many etch processes towards Si or SiO_2 etching is done either via inductively coupled plasma (ICP) or reactive ion etching (RIE) processes, here experiments were done in both etch tools but only the RIE was able

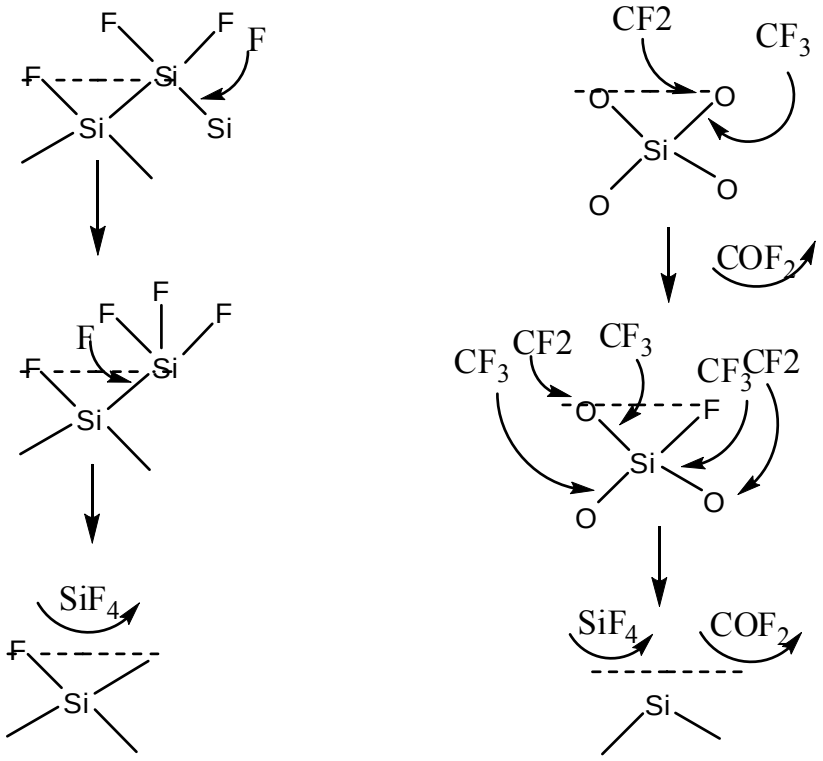

Figure 2.13 Schematic of a fluorine plasma etching Si and SiO_2

to provide conditions to where C96 could both withstand the plasma and work as an etchmask. Conditions achieved in the ICP proved to be too harsh towards the monolayer. Many fluorine plasma processes have a common goal of a high etch rate and anisotropic etching. The conditions strived for here differed in a sense that we would like to have a rather slow etch rate of Si or SiO_2, which would result in less harsh conditions for the C96 monolayer. Typical etching of SiO_2 is done under conditions where the etch rate is fast (1500-8000 Å/min). Here a slow etch rate (~90 Å/min) was used as a "soft" plasma was desired. Not only does the plasma have to be soft, but it also needs to provide an anisotropic etch. If the etching was isotropic, the undercutting of the plasma would result in a loss of etch-mask almost immediately since the C96 fibers were only 3-4 nm wide. All parts of the recipe (etchant gas, additive gas, flowrates, RF power, pressure, and etch

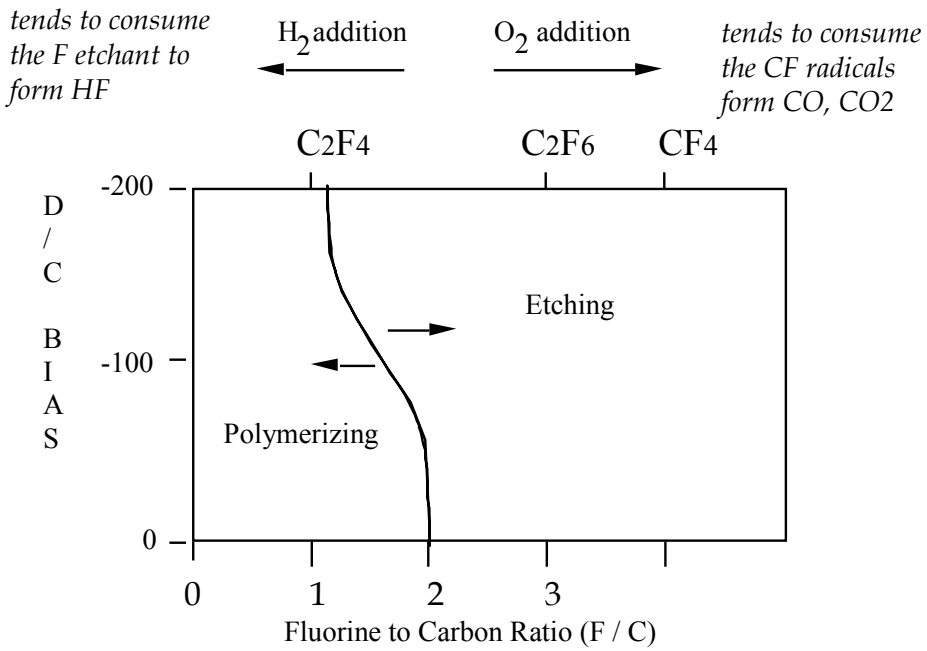

Figure 2.14 Schematic of the resulting plasma using different recipes

time) have to be optimized to achieve the desired conditions of the plasma. The plasma created here has been developed for SiO_2 etching rather then Si. Even though the same plasma would perform satisfactory for both SiO_2 and Si, the etch rate will differ and for the plasma described below the etch rate is higher for SiO_2. This is because the mechanism is different for each substrate. Upon etching Si, a thin Si-F layer is produced and this drives the etching downward with the formation of the volatile species SiF_4. For SiO_2, the etch mechanism is a little bit different and the etchant species is different which means the etch rate will differ[39], see Figure 2.13. Fluorine plasmas can either be etching or polymerizing towards the surface depending on the gases (ratio F/C), additive gas (oxygen or hydrogen), and DC bias used to create the plasma[40], see Figure 2.14. Here we aimed to create conditions to where the plasma was etching but at the same time being close to polymerizing conditions to decrease the force of the plasma on the C96

monolayer. Instead of using O_2 as the additive gas here, H_2 gas was used. The H_2 gas tends to consume the F etchants and produce HF, while O_2 tends to consume polymerizing fluorocarbon radicals and produce CO_2 and CO. The RF power used was also set to promote the generation of a "soft" plasma, 75 W was used in these experiments (normal RF power for Si etching is 150-300 W). It was necessary for the RF power to be high enough to ignite the plasma; experiments using extremely low RF powers showed no ignition and therefore no plasma was created. The pressure used in the process was also vital to the outcome. Lower pressures allowed the mean free path to become too long, and the species in the plasma were accelerated quickly towards the surface and the physical bombardment was too violent for the monolayer to withstand. At the same time, if the pressure was too high, the plasma does not hit the surface with any directionality which results in poor anisotropy. The pressure was set to 50 mTorr for all etching experiments. Experiments showed that if the pressure was lowered to 5 mTorr, the ion bombardment became too violent towards the monolayer and no features could be seen upon surface analysis.

2.2.14 Etch Rates for Various Plasmas

All etching described here was done on a Vision 320 RIE in the MIRC cleanroom. Referring back to Figure 2.14, where the correlation of recipes between polymerizing and etching plasmas was described, here a plasma just on the etching side was desired. The experimental data that confirms we were close to polymerizing conditions is described below. All plasmas created have the same pressure (50 mTorr), RF power (75 W), and etchant gas CF_4 (31 sccm). The additive gas on the other hand changes from O_2 to H_2. Also, the flow rate of the gases were changed to see the

Table 2.1 Etch rates of Plasma 1, 2, 3, and 4

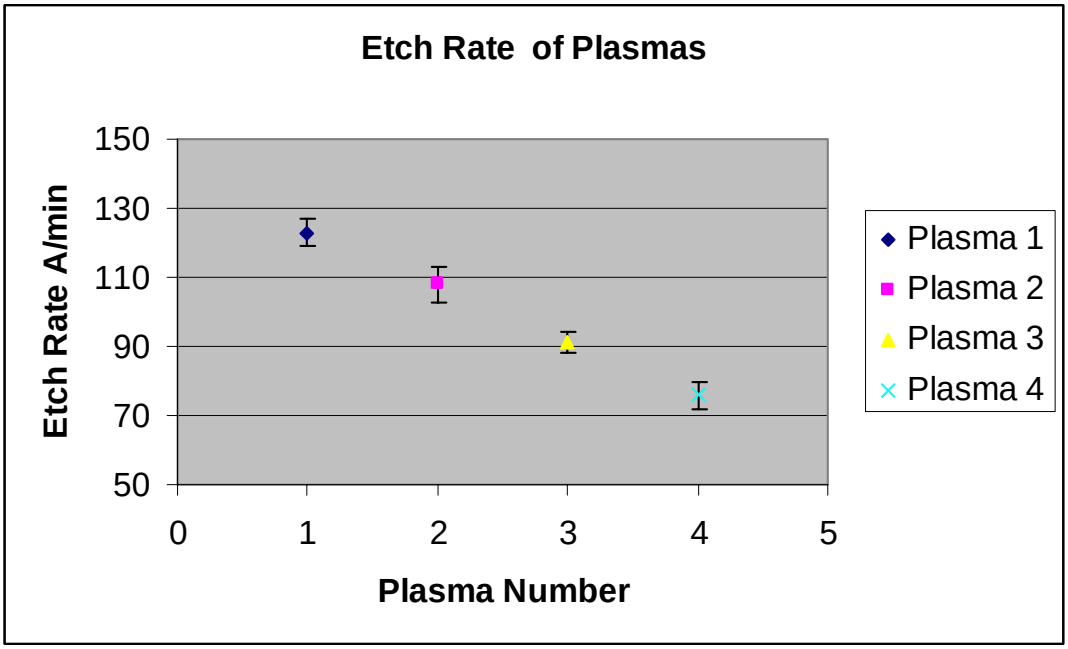

relationship between the etch rate and the additive gas. The instrument wuold not allow (due to control issues) for a flow rate below 2 sccm. The etch rate in SiO_2 was determined by using a Woollam Ellipsometer at the MIRC cleanroom. Plasma 1 (CF_4 31 sccm, O_2 2 sccm, 50 mTorr, RF power 75 W), gave an etch rate of 123 ± 8 Å/min. Plasma 2 (CF_4 31 sccm, 50 mTorr, RF power 75 W), gave an etch rate of 108 ± 8 Å/min. Plasma 3 (CF_4 (31 sccm, H_2 2 sccm, 50 mTorr, RF power 75 W), gave an etch rate of 91 ± 5 Å/min. Plasma 4 (CF_4 31 sccm, H_2 3 sccm, 50 mTorr, RF power 75 W) – gave an etch rate of 76 ± 5 Å/min. Plasma 5 (CF_4 31 sccm, H_2 4 sccm, 50 mTorr, RF power 75 W), created polymerizing conditions and deposits material on the surface and therefore has no etch rate. All etch rates are shown in Table 2.1. As expected, the etch rate of SiO_2 was the highest for the plasma having O_2 as the additive gas. The etch rate also increased with decreasing flow rates of H_2. When a SiO_2 substrate was placed in Plasma 5, no etching was observed but rather a build up of fluorocarbon polymer on the surface. By increasing

the flow rate of H_2 from 3 sccm to 4 sccm, which was equal to about a 2.5% increase of H species in the plasma, the plasma becomes polymerizing rather than etching. Therefore, the plasmas 3 and 4 were ideal for the purpose intended.

2.2.15 Polymer Buildup on C96 Structures

Upon placing the C96 monolayer in Plasma 5 (CF_4 31 sccm, H_2 4 sccm, 50 mTorr, RF power 75 W), resulted in a buildup of polymer on to the C96 fibers. Rather than depositing the polymer evenly onto the surface, the polymer prefered to build on the fibers versus the SiO_2. The AFM analysis showed the buildup as it increased with time, See Figure 2.15. This step was intended to bridge the top-down with the down-up approach in a sense that we built up the C96 structures from the bottom and then intend to etch the exposed substrate from the top. In this case that was not entirely true since we are again building up polymers onto the C96 fibers. The fibers are not only getting taller, but also wider during this process which was expected since the polymer builds on all sides of the C96 fibers. The fibers are initially 2.3 ± 0.2 nm and after 1 min of polymer deposition the fibers are ~12 nm tall, which gave a deposition rate ~10 nm/min. After 1 min a smooth surface was observed, where the material had grown in all spaces. The contact angle for all these surfaces was 94 ± 3. The high contact angle was an indication that the material on the surface was a fluorocarbon which is expected since the gas used was CF_4. This phenomenon could be advantageous if the purpose of the process is to specifically coat a carbon containing compound on a Si surface. Although this is not desired as a direct process for molecular lithography, future work could involve this process combined with the etching plasmas. This would be a cyclic process were a short

etch is followed by a buildup of polymer to reinforce the C96 structures followed by another etch to ultimately achieve taller structures then with C96 fibers alone.

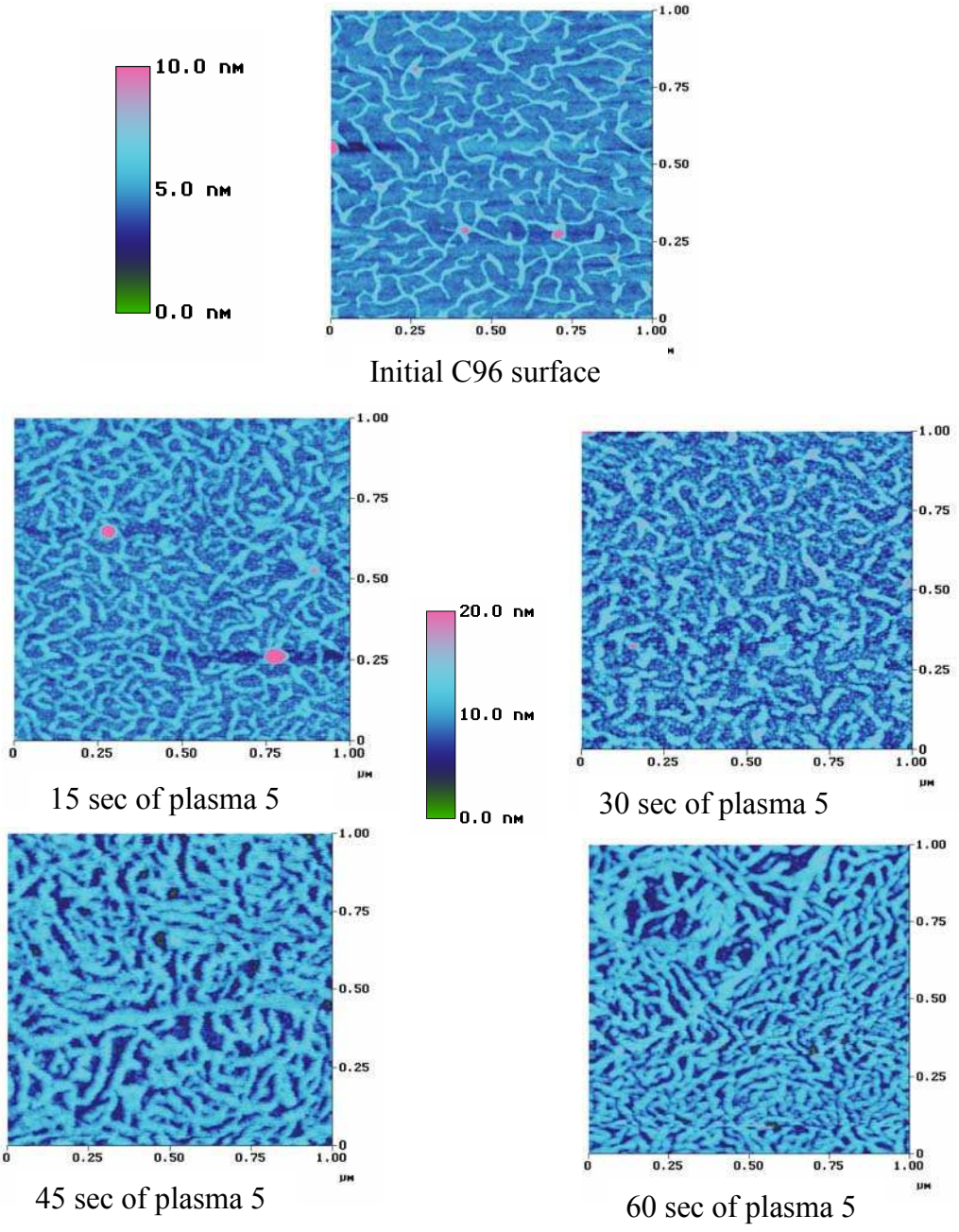

Figure 2.15 AFM of samples in plasma 5

2.2.16 C96 as an Etchmask Using Different Plasmas

As described earlier different plasma recipes should have a different impact on the effectiveness of C96 fibers as molecular resists. The final etching outcomes for each recipe were compared here. As discussed above, Plasma 5 gave rise to polymerization. Plasmas 1, 2, 3, and 4 on the other hand were etching and have different influences on C96 as a molecular mask. Plasma 1, which has O_2 as the additive gas, created a harsh environment for the C96 monolayer. O_2 gas in known to have a high reactivity towards organics and would therefore promote the degradation of the C96 molecules. Also, as mentioned before, it consumes CF radicals and enhance the production of F enchants.

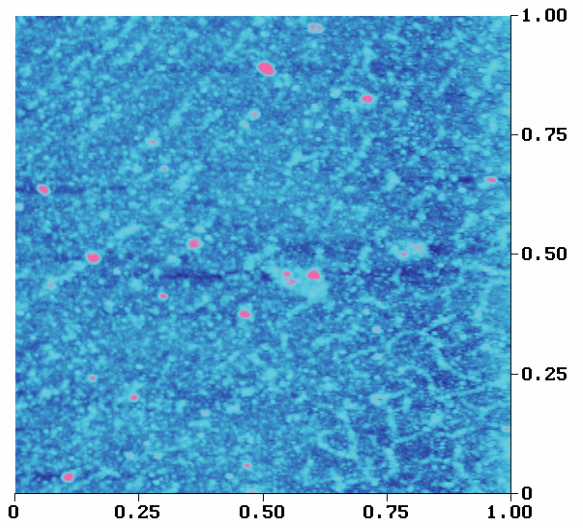

Figure 2.16 Typical etch result of C96 in plasma 1 or 2.

AFM analysis of samples exposed to this plasma show poor etch resistance and no features were seen even after only 15 seconds (sec) of processing. Plasma 2, which had no additive gas, showed similar results. However some features were seen on the surface after 15 sec of etching, see Figure 2.16 for both plasma 1 and 2. Although features were seen they are not very tall (1.8 ± 0.2 nm), indicating that the C96 fibers only were stable

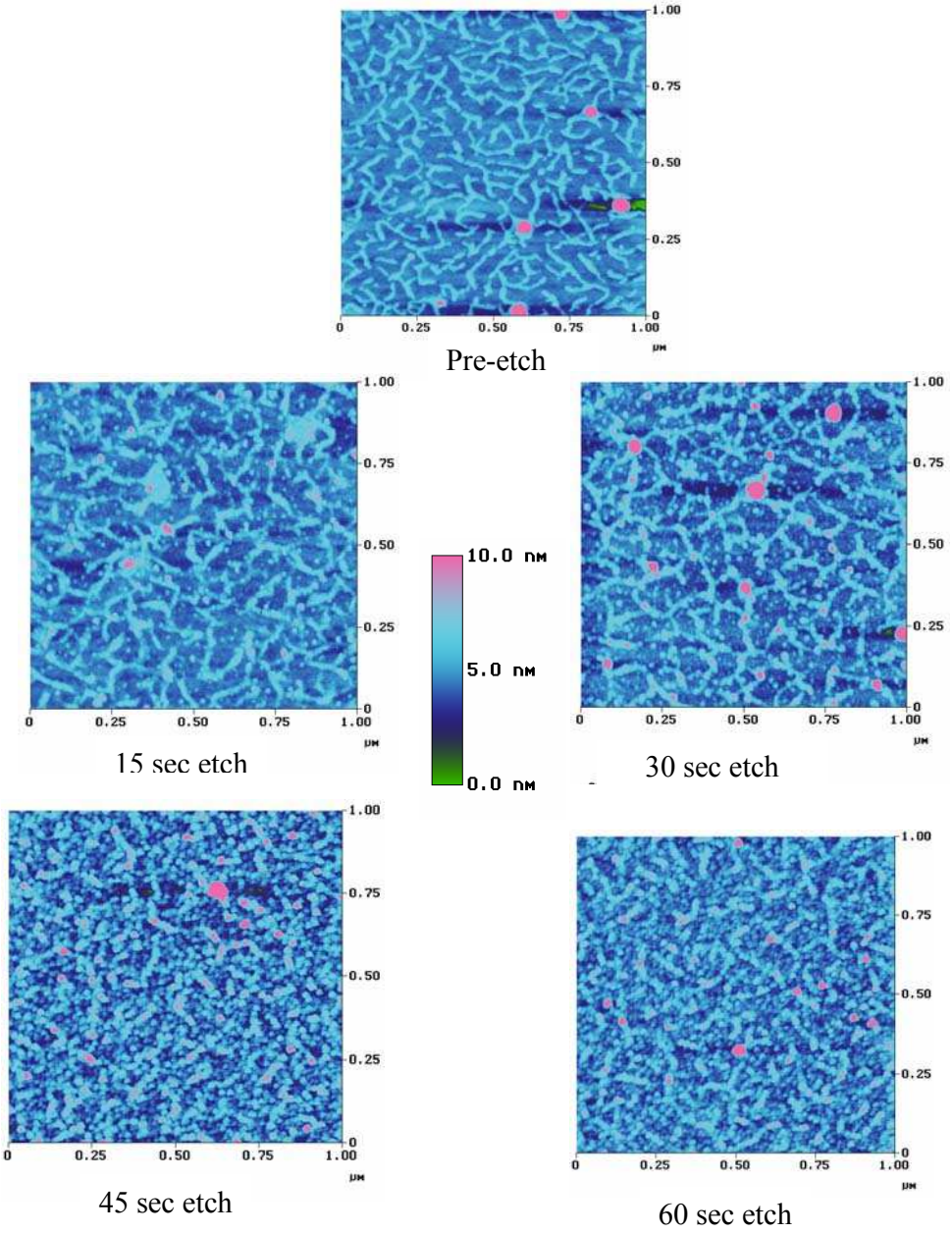

Figure 2.17 Etch results for plasma 3

for a short period of time in the plasma. The structures were also poorly defined due to the poor etch resistance. The contact angle for both plasma 1 and 2 processes decreased from 83 ± 2 with no etching to 25 ± 4 after 15 sec of process time. Plasma 3 on the other hand showed extremely good results and was the plasma mostly used for etching

throughout this research. When using H_2 as the additive gas, some F etchants were consumed and the C96 fibers were stable in the plasma. When a sample was placed in the plasma for 15 sec, the AFM analysis shows identical structures with the initial, non-plasma etched surface, the difference between the images being that the features were now taller. See Figure 2.17 for the whole etching process using Plasma 3. This was expected due to that the plasma etched around the fibers and into the substrate. The height had increased from 2.3 ± 0.2 nm to 4.7 ± 0.3 nm. Assuming that the etch mask was intact, the plasma would have etched about 2.6 nm into the SiO_2 which was consistent relative to the etch rate for plasma 3 (93 ± 9 Å/min). If the etch time was increased to 30 sec, the expected result would be that the features would have the same shape, but increased in height. At 30 sec, the features were intact and the height has increased from the original 2.3 ± 0.2 nm to 5.9 ± 0.6 nm. This showed that the C96 fibers are still stable in the plasma and acted successfully as molecular etch resists. The width of these features were 10-16 nm via AFM analysis, but as discussed earlier, had a much smaller "true" width due to the AFM tip diameter. Upon increasing the etch time another 15 sec to 45 sec, the AFM analysis revealed the same structures but now at a height of 9.5 ± 1.2 nm. These results showed that the C96 molecule had excellent etch resistance towards fluorine plasma, as expected based on the Ohnishi and Ring parameter. However, when exposing the C96 fibers to a fluorine plasma for 60 sec, features were still seen but the height have decreased from about 9.5 ± 1.2 nm nm, in the 45 sec plasma etch, to 5.0 ± 0.9 nm. The fibers were no longer intact and therefore can not work properly as an etch mask. The static water contact angle and the C96 monolayer surface was 83 ± 2. After 15 sec of etching in plasma 3, the contact angle was nearly the same at 81 ± 2. With

Table 2.2 Contact angle results for plasma 3.

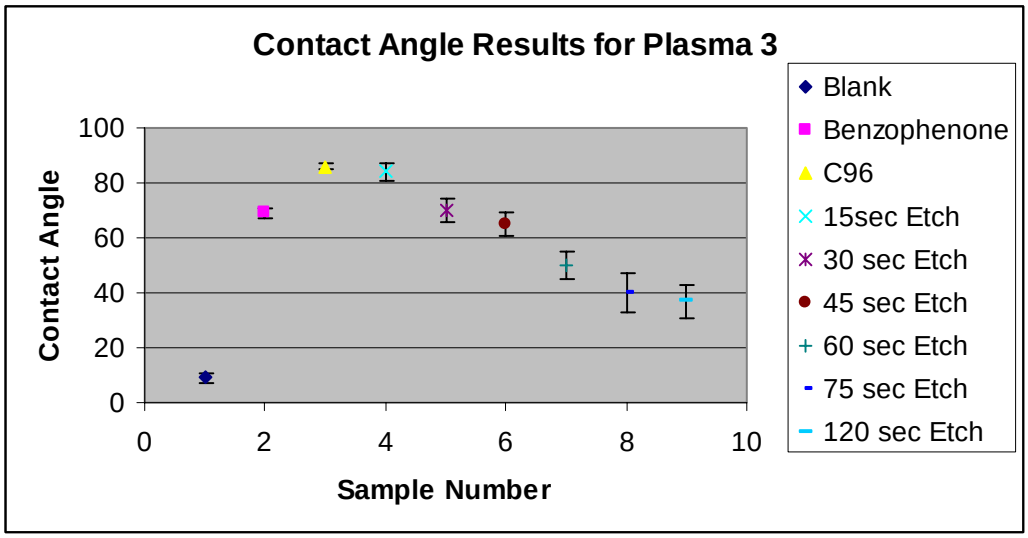

increasing process times, the contact angle decreased and the monolayer was damaged and removed. After 120 sec of etching, the contact angle was 32 ± 7 and no features were seen on the surface. See Table 2.2 for all contact angles involving plasma 3. After 45 sec of plasma etching there was a decrease of carbon on the surface according to XPS results. The concentration went from 33% to 11%, which was the concentration of adventitious carbon on a blank SiO_2 substrate. There was also 25% fluorine present on the surface which could be expected knowing the mechanism for SiO_2 etching. The concentration of oxygen was constant throughout the experiment which was also expected since there was a thick SiO_2 layer underneath removed substrate. All these results together with AFM images and contact angle results indicated that the C96 has been removed by the plasma. When exposing the sample to plasma 4, very similar results were observed as for plasma 3. The fibers were again stable for an extensive period of time in the plasma. Since plasma 4 has a higher content of H_2, the etch rate was slower but at the same time, the plasma was less damaging towards the etch resist. After 15 sec of etching the height of

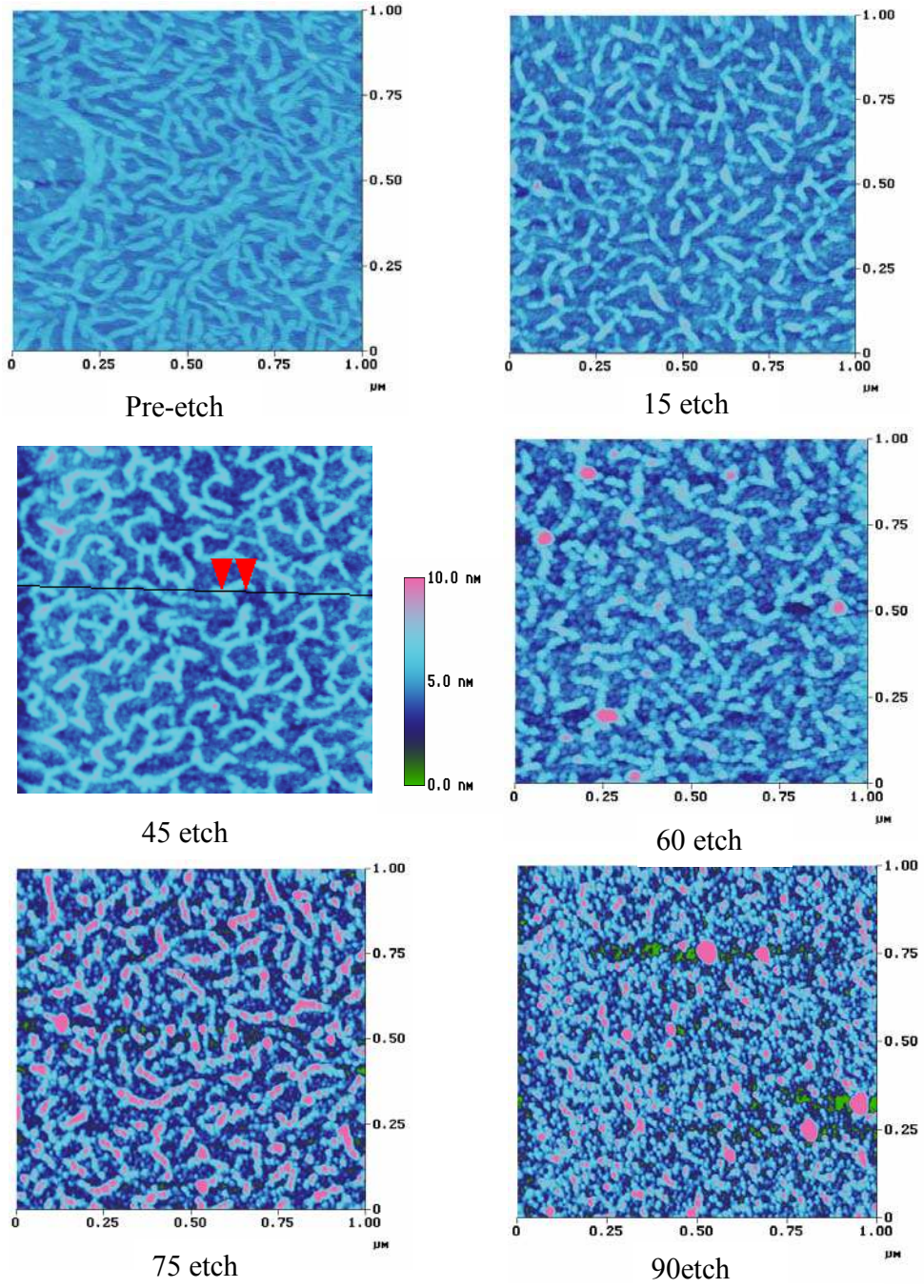

Figure 2.18 AFM of etch results for C96 in plasma 4

the features are 3.5 ± 0.3 nm which means that an etch of about 1.2 nm has occurred. After 30, sec the height has reached 4.7 ± 0.3 nm, which was also consistent with the etch rate for plasma 4. Etching for 45 sec gave rise to feature heights of 5.2 ± 0.4 nm. After 60

sec, the feature height had reached 8.6 ± 0.5 nm and the structures were still nicely defined. Still after 75 sec, the feature were intact but the height of the structures had not increased significantly from the 60 sec etch, the height of the features were 9.2 ± 0.5 nm. This may be due to the fact that the fibers now had been damaged or removed and cannot longer protect the features from the plasma and therefore no increase in height was observed. 90 sec into the process, the surface looses its defined features and the molecular etch mask had been eliminated. See Figure 2.18 for all AFM results involving plasma 4. The samples were also monitored by contact angle and showed a progressive decrease in contact angle suggesting the removal of the etch barrier during the process; See Table 2.3 for a summary of all contact angle results involving plasma 4. The contact

Table 2.3 Contact angle results from plasma 4

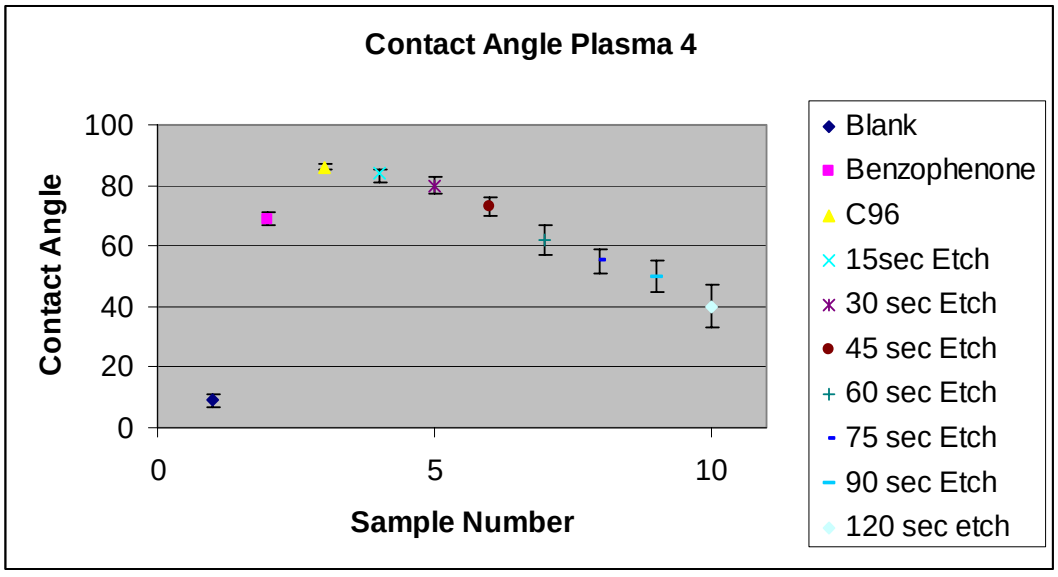

angles also slowly decreased, from the original 83 ± 2, with longer process times as for plasma 3. However, the contact angle was slightly higher for a longer period of time indicating that the C96 monolayer was more resistant to plasma 4 than plasma 3. For plasma 1 and 2, both AFM analysis and contact angle indicated a removal of the resist

after only 15 sec of processing. For plasmas 3 and 4 the contact angle indicate that the etch barrier is stable up to a certain point in the process until the monolayer is removed. In summary, for the etching process one can conclude that the assemblies of C96 molecules standing perpendicular to the SiO_2 surface with a height of 2.3 ± 0.2 nm (this height matches the diameter of molecule) can act as molecular masks. These allowed for features as tall as ~9 nm, which gives this molecule an excellent etch ratio of about 4/1 (SiO_2:C96) under these specific conditions.

2.2.17 Removal of the C96 Monolayer Using Piranha Solution

Here as well as in a photolithographic process stripping of the etch-resist off the surface after etching, leaving the standing SiO_2 behind, is necessary. The removal processes used for this step in photolithography is either performed by rinsing the substrate with a good solvent or by placing the wafer in an oxygen plasma. The oxygen plasma is highly reactive towards the organics on the surface and are subsequently removed in the process. Since C9 was covalently bound to the surface in molecular lithography, mild rinses would not remove the molecules. Therefore, our initial approach was to place the samples in the RIE, same as used for the fluorine plasma etching, now using recipe for an oxygen plasma. The recipe for the oxygen plasma was standard: O_2 50 sccm, RF power 200W, 30 mTorr, 10 min etch time. However, upon surface analysis after the plasma treatment, no features were seen in the AFM. The contact angle was 10 ± 2, indicating a pure SiO_2 surface, which was confirmed by EDS. No features were seen even after modifications of the oxygen plasma recipe to produce a less aggressive plasma. In an experiment to remove the C96 monolayer using an alternative method, the sample was placed in a piranha solution (H_2SO_4 70%, H_2O_2 30%) for 1.5 hours (hrs), after which

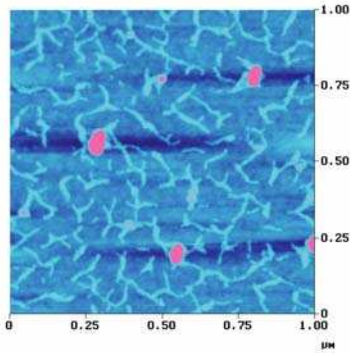

Pre-etch and pre-piranha treatment

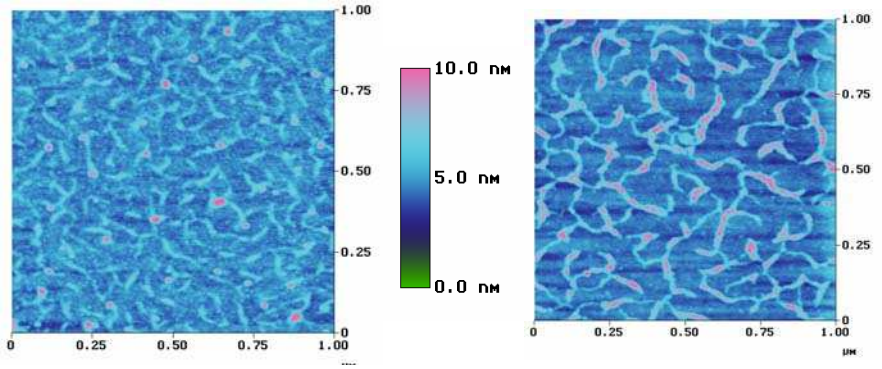

15 sec etch and piranha treatment

30 sec etch and piranha treatment

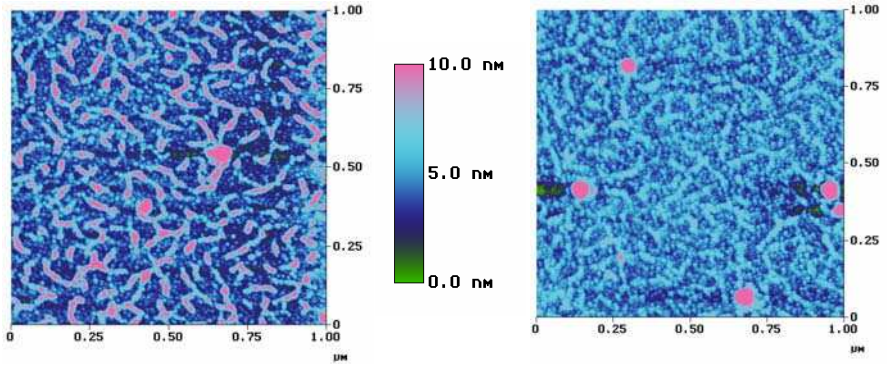

45 sec etch and piranha treatment

60sec etch and piranha treatment

Figure 2.19 AFM results from etching in plasma 3 followed by piranha

the organic layer was removed and the SiO_2 features were left standing. The results for the oxygen plasma were explained previously in the literature, where it has been observed that small and thin SiO_2 and Si structures could be damaged in an oxygen plasma[41,42]. The piranha on the other hand, which is a pure chemical process, will leave the structures

untouched. Even though the oxygen plasma and piranha both uses oxygen radicals to remove the organics on the surface, the end results was very different. Piranha would not damage the SiO_2 structures as there was no physical bombardment towards the surface. The oxygen plasma, however, also created stress on the small SiO_2 structures and would therefore result in damage. Samples exposed to plasmas 1 and 2 were not affected by the piranha treatment since no features were observed even after the fluorine etching step. All features disappeared on the samples exposed to plasma 5; this is expected since they are built up with fluorocarbon polymer, and no structures were ever created in the substrate. The removal of the polymer and C96 fibers just left a feature less surface behind. On the samples exposed to plasma 3 nicely defined features were seen even after piranha treatment, further confirming the success of molecular lithography. After 15 sec of etching the samples showed a height of 4.7 ± 0.3 nm, the initial height of the monolayer was 2.3 ± 0.2 nm, meaning that if the monolayer was intact after etching, the SiO_2 features should be around 2.5 nm tall. The AFM analysis after the piranha treatment showed features of 2.5 ± 0.2 nm standing on the surface. See Figure 2.19 to see a summary of all piranha treated surfaces using plasma 3 as the etch process. The contact angle was 9 ± 2 which indicated a clean SiO_2 surface. EDS analysis showed only Si and O on the surface confirming all results. After the 30 sec etch period and piranha treatment, the features left standing were 4.8 ± 0.3 nm, meaning that the etch continued and the C96 resist was stable. 45 sec of etching followed by piranha treatment resulted in features 8.1 ± 0.4 nm tall, which was less decrease in height than the original C96 monolayer, indicating that the degradation of the monolayer had started. 60 sec of etch followed by piranha treatment shows a decrease of feature height of about 4 nm. The

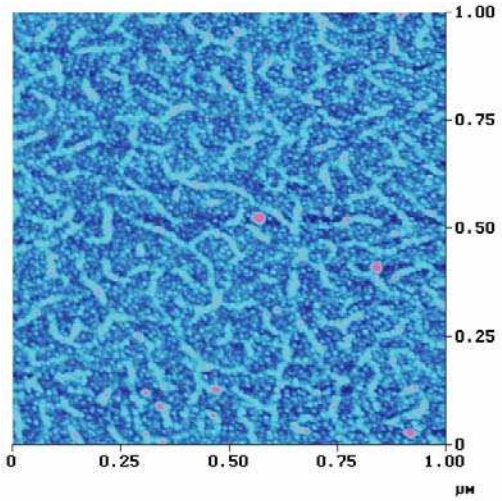

Figure 2.20 AFM of C96 etched for 60 sec in plasma 4 followed by piranha treatment

resist was gone and evidently there was nothing to protect the features from being damaged by the plasma. Plasma 4 showed again similar results to plasma 3 with one variation. The width of the features decreases when they are treated with piranha. This indicates some polymer formation onto the C96 fibers while the SiO_2 is being etched. The increase in H_2 promoted the polymer formation and the results from plasma 5 in which the polymer selectively builds up on the fibers rather then the surface is also witnessed here. As expected the etch rate of the SiO_2 was slower in plasma 4 than in plasma 3. After 15 sec of etching, the height of the features has increased from 2.3 ± 0.2 nm to 3.4 ± 0.3 nm. 30 sec of etching produces 4.2 ± 0.3 nm tall features and was consistent with the etch rate observed in the samples exposed to the plasma for 15 sec. After 45 sec, the height of the features was 5.8 ± 0.5 nm. Since plasma 4 was less harsh towards the C96 molecules the monolayer was stable for a longer time then in plasma 3. The features were stable even after 60 sec of etching and the height of the structures are 8.3 ± 0.6 nm. Even after 75 sec, of the monolayer was stable but the there is only a slight increase in height of the features to 9.1 ± 0.4 nm. After 90 sec of plasma etching the

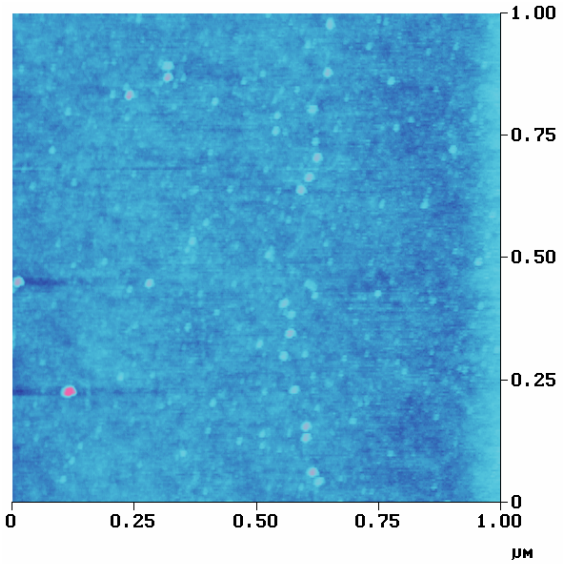

Figure 2.21 AFM of control experiment for C96

features were no longer defined and the monolayer has lost it's etch resistance. When placing the samples in the piranha solution to remove the organic layer somewhat unexpected results are observed. The height and width of the features decrease drastically, indicating that a polymer buildup on the C96 monolayer occurred during the etch process. The shapes of the features were intact after piranha treatment and both contact angle results (10 ± 2) and EDS supports the results discussed. The features are 4.3 ± 0.5 nm tall after 60 sec of etching followed by piranha treatment, see Figure 2.20. This was about 2 nm shorter then expected. The same was true for all plasma process for longer then 60 sec, the maximum height of features seen after piranha treatment using plasma 4 is 4.3 ± 0.3 nm. Therefore this plasma was a little bit harder to control than plasma 3 and therefore not used extensively. The control experiment for the whole experiment was also successful. A C96 monolayer was placed in a piranha (70 % H_2SO_4, 30 % H_2O_2) solution for 1 hr. Since the sample had not been etched with a fluorine plasma before the piranha treatment, there should be no features on the surface upon

AFM analysis, See figure 2.21. AFM analysis showed a feature less surface with a contact angle of 9 ± 2. EDS analysis also confirmed that all organic materials had been removed.

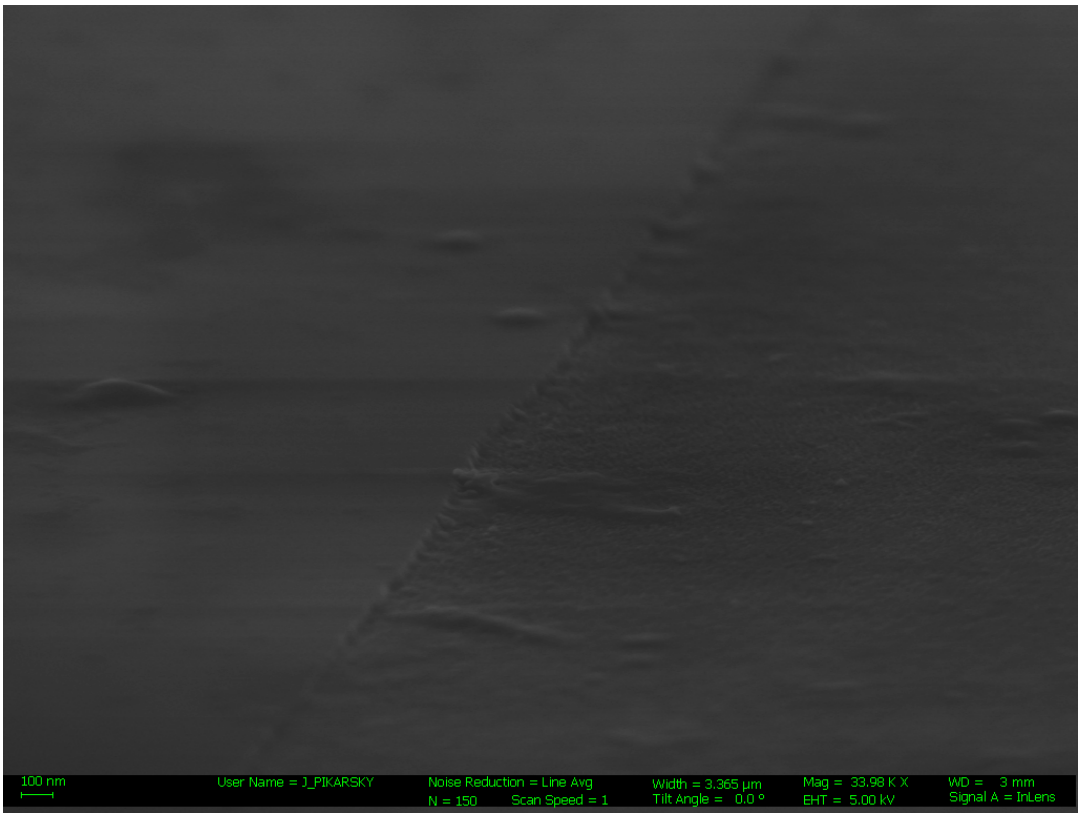

Figure 2.22 Edge of photolithographically made line etching with plasma 3 for 5 min followed by TMAH development

2.2.18 Photolithography Using Plasma 3

Since the structures shown in the previous paragraph are very thin and short, it is nearly impossible for detailed SEM analysis. Group members in Prof. Henderson's group created box patterns using conventional photolithography followed by etching using plasma 3. It will be easier to see how the plasma performs if deeper and larger features

are created in the substrate. A 6.5 μm wide pattern was made using a Novolak positive resist, SC1813, which was irradiated in the Carl Suss MA-6 instrument in the cleanroom at the MIRC. The substrate was then placed, upon development, in the Vision 320-RIE and exposed to plasma in plasma 3. The etch time used were somewhat longer the etch times used for the plasma etching when C96 was the etch mask, so that the structures could be analyzed for anisotropy. After 5 min of etching followed by removal of the remaining resist with a 0.25 M solution of tetramethylammoniumhydroxide (TMAH) in water, the sample were analyzed by SEM, See Figure 2.22. The SEM showed anisotropy which is vital for creating small features in a substrate. This can also be rationalized by the results shown earlier using C96 as the etch mask. If the etch was isotropic, the features would be destroyed after only 1-1.5 nm of undercutting which would not allow for the 9 nm tall features seen earlier.

2.3 Summary

By using molecular lithography and C96 as the etch resist structures as small as 3-4 nm were created in SiO_2. A monolayer of C96 was covalently bound to the surface through a chlorosilane benzophenone derivative using conventional photo- and surface chemistry. The hydrophilic/hydrophobic interactions with the surface allowed for the formation of self-assembled fibers consisting of perpendicular oriented C96. These fibers serves directly as the molecular mask during the fluorine etch process. The length and shape of the C96 monolayer could be altered by using solutions of varying concentration and different deposition techniques and solvents. C96 was an ideal candidate for molecular lithography due to its high aromaticity. Both the Ohnishi and Ring parameter indicated that C96 had an exceptional etch resistance towards a fluorine plasma. A soft

plasma was needed for the etch process, otherwise the monolayer would not be stable enough to act as the etch barrier. CF_4 was used at the etchant with H_2 as the additive gas, replacing H_2 for O_2 resulted in consumption of etchants in the plasma and therefore created a friendly environment for C96. Also the pressure and RF power played a big role in how harsh the plasma conditions were for the monolayer. After much trial and error conditions were achieved wherein the monolayer (2.3 ± 0.2 nm) effectively worked as a molecular mask and features as tall as 8.1 ± 0.4 nm were etched into the SiO_2, with an excellent etch ratio of molecule/SiO_2 of ~1/4. All results were confirmed with contact angle, EDS, or XPS. The aspect ratio (width/height) of the features created is ~1/2. This also indicated that the plasma etches the substrate anisotropically, since any isotropic etch would etch through the thin structures. The removal of the organic layer was conducted with a piranha solution rather than an oxygen plasma since the plasma damaged the small structures. All results showed a proof of principle that molecular lithography is feasible. Although the structures were random in a sense that the fibers were in various directions on the surface the, π-π stacking dictates how the molecules behave on the surface. Much effort has been made organizing this class of discotic molecules onto semi-conducting surfaces into lines using zone-casting. The same approach, with some modifications, could be used here to organize C96. Alignment and organization of C96 are discussed in Chapter 5.

2.4 REFERENCES

[1] Tomovic, Z.; Watson, M. D.; Müllen, K *Angew. Chem., Int. Ed.* **2004,** *43,* 755.

[2] Pisula, W.; Tomović, Z.; Simpson, C.; Kastler, M.; Pakula, T,; Müllen, K *Chem. Mater.* **2005,** *17,*4296.

[3] Clar, E. *The Aromatic Sextet*, 1st Ed., John Wiley and Sons, London, **1972.**

[4] Ito, M.; Wehnmeier, J.; Brand, C.; Kübel, R.; Epsch, J.; Rabe, K.; Müllen, K. *Chen.-Eur. J.* **2000,** *6*, 4327.

[5] Iyer, S.; Wehmeier, M.; Brand. J.; Keegstra, M.; Müllen, K. *Angew. Chem. Int. Ed. Engl.,* **1997,** *36,* 1604.

[6] Fischbach, I.; Pakula, T.; Minkin, P.; Fechtenkötter, A.; Müllen, K.; Speiss, H. W.; Saalwachter, K. J. *J. Phys. Chem. B* **2002,** *106,* 6408.

[7] Tchebotareva, N.; Yin, X. M.; Watson, M. D.; Samori, P.; Rabe, J.; Müllen, K. *J. Am. Chem. Soc.* **2003,** *125,* 9734.

[8] Fischbach, I.; Ebert, F.; Speiss, H. W.; Schnell, I. *Chemphyschem* **2004,** *5,* 895.

[9] Wu, J. S.; Watson, M. D.; Zhang, L.; Wang, Z. H.; Müllen, K. *J. Am. Chem. Soc.* **2004,** *126,* 177.

[10] Fechtenkötter, A.; Saalwachter, K. J.; Habison, M. A.; Müllen, K.; Speiss, H. W. . *Angew. Chem., Int. Ed. Engl.* **1999,** *38,* 3039.

[11] Herwig, P.; Kayser, C. W.; Müllen, K.; Speiss, H. W. *Adv. Mater.***1996,** *8,* 510.

[12] Stein, S.; Brown, R. *J. AM. Schem. Soc.* **1987,** *109,* 3721.

[13] Hatsusaka, K.; Ohta, K.; Yamamoto, I.; Shirai, H. *J. Chem Mater.* **2003,** *11,* 423.

[14] Engelkamp, H.; Middelbeek, S.; Nolte, R. *Science,* **1999,** *284,* 785.

[15] Bushby, R.; Boden, N.; Kilner, C.; Lozman, O.; Lu, Z.; Liu, Q.; Thornton-Pett, M. *J. Mater. Chem.* **2003,** *13,* 470.

[16] Yatabe, T.; Harbison, M.; Brand, J.; Wagner, M.; Müllen, K.; Samori, P.; Rabe, *J. Mater. Chem.* **2000,** *10,* 1519.

[17] Bushby, M.; Nguyen, T.; Nuckolls, C. *J. Am. Chem. Soc.* **2003,** *125,* 8264.

[18] Wu, J.; Watson, M.; Müllen, K. *Angew. Chem. Int. Ed.* **2003,** *42,* 5329

[19] Dimitrakopoulos, C.; Malenfant P. *Adv. Mater.* **2002,** *14,* 99.

[20] Reizel, N.; Hassenkam, T.; Balashev, K.; Jensen, T. R.; Howes, P. B.; Fechtenkötter, A.; Tchebotareva,

[21] Tracz, A.; Jeszka, J. K.; Watson, M. D.; Pisula, W.; Müllen, K.; Pakula, T. *J. Am. Chem. Soc.* **2003,** *125,* 1682.

[22] Liu, C. Y.; bard, A. J. *Chem. Mater.* **2000,** *12,* 2353.

[23] Bunk, O.; Nielsen, M. M;. Solling, T. I.; van de Craats A. M.; Stutzmann. *J. Am. Chem. Soc.* **2003,** *125,* 2252.

[24] Chandrasekhar, S. *Liq. Cryst.* **1993,** *14,* 3.

[25] Herwig, P.; Kayser, C.; Müllen, K.; Spiess, H. *Adv. Mater.* **1996,** *8,* 510.

[26] http://spm.phy.bris.ac.uk/techniques/AFM/ - accessed 03-2007

[27] Goel, A.; Howard, J.; Vander Sande, J. *Carbon 42,* **2004,** 1907

[28] Turro, N. *Modern Molecular Photochemistry;* University Science Books: Mill Valley, **1991**.

[29] Dormán, G.; Prestwich, G. *Biochemistry,* **1994,** *33,* 5661.

[30] Prucker, O.; Naumann, C.A.; Rühe, J.; Knoll, W.; Frank, C.W. *J. Am. Chem. Soc.* **1999,** *121*, 8766.

[31] Claisen, L.; Eisleb, O. *Liebigs Ann. Chem.* **1913,** *401*, 21.

[32] Marciniec, B. *Comprehensive Handbook of Hydrosilation;* Pergamon Press, Oxford, **1992.**

[33] Speier, J *Adv. Organomet. Chem,* **1979,** *17,* 407.

[34] Tomović, Z.; Watson, M.; Müllen, K. *Angew. Chem. Int. Ed.,* **2004,** *43,* 755.

[35] Goel, A.; Howard, J.; Vander Sande, J. *Carbon 42*, **2004,** 1907

[36] Gokan, H.; Esho, S.; Ohnishi, Y *J. Electrochem. Soc.* **1983,** *130(1),* 143.

[37] Kunz, R.; Palmateer , S.; Forte, A.; Allen, R.; Wallraff, G.; DiPetro, A.; Hofer, D. *SPIE*, **Vol. 2724,** 365.

[38] http://www.itrs.net/ accessed March/2007

[39] Flamm, D.; Manos, D. *Plasma Etching – An Introduction;* Academic Press, Inc.: San Diego, 1989.

[40] Chapman, M. *J. Appl, Phys.* **1980,** *51(7),* 3608

[41] Wiegand, M.; Reiche, M.; Gösele, U. *J. Electrochem. Soc.* **2000,** *7,* 2734.

[42] Paskaleva, A.; Atanassova, E. *Solid-State Electronics,* **1998,** *42*, 777.

CHAPTER 3

FULLERENE CONTAINING POLYMER MONOLAYERS AS MOLECULAR RESISTS

3.1 Introduction

The results presented in this chapter represents the first successful experiments using a monolayer of a material as the etch resist. When thinking about what type of molecules could be suitable for molecular lithography fullerenes comes to mind, since as an allotrope of carbon it is 100% carbon and has an Ohnishi parameter of 1. The fullerene molecule is extremely stable due to its aromatic structure and molecular composition and therefore is an attractive candidate for molecular lithography. However, fullerene alone would be kinetically stable on a silicon surface and must be incorporated into another material, i.e., a polymer, or otherwise attached to the surface (See Chapter 4). A polymer containing fullerenes should also be stable in the fluorine plasma and function as a molecular resist. Although a polymer can be viewed as an individual molecule, it possesses properties that differ from the individual monomer unit, such as melting point and solubility. In comparing the results in this chapter with the results from chapter 2 it will seen that the etch resistance of the polymer exceeds that of C96. One explanation is that the structures created on the surface by C96 is dictated by secondary interaction, π-π stacking, and will not be as robust as the covalent bonds of the polymer. A drawback of using polymers instead of individual molecules is the consistency of size and manipulability of the polymer chain. The size of the features seen on the surface is ultimately determined by the molecular weight (MW) of the polymer and by the phase

diagram of the polymer, rather then self-assembly as is the case with individual molecules. To create homogeneous features, the polymer must have a low polydispersity index (PDI), meaning that the sizes of the polymer chains are consistent compared with each other. Another concern with fullerene containing polymers is poor solubility which could lead to difficulty in the thin film fabrication. Good plasma resistance is gained by incorporating fullerenes to a polymer; however this often creates a highly insoluble compound. Obviously the polymer must be somewhat soluble so that a thin film can be created on the surface. The main differences between the results using polymer and those using individual molecules were in the height and size of the features created. Larger features in the x and z direction were accessible using a polymer but also the height of the features created was larger since the polymer outperforms an individual molecule during a plasma process. That might not be a negative aspect since the desired size of the features might be larger then individual molecules depending on the application. The melting point and glass transition temperature (t_g) of the polymer are important if dip-pen lithography is to be used for patterning.

3.2 Experimental

The methodology used to create the polymer monolayer was the same as with C96. Therefore all data concerning the creation of chlorosilane benzophenone derivative monolayer can be viewed in Chapter 2. The order of the experiments were the same as for C96: (1) creation of benzophenone monolayer, (2) thin film fabrication of fullerene polymer on the surface, (3) covalent attachment of polymer to the benzophenone derivative through photoirradiation, (4) extraction of unattached molecules in a Soxhlet extraction apparatus, (5) plasma etching, (6) stripping of the remaining organic layer

through piranha solution or oxygen plasma treatment. The samples were appropriately analyzed after each step of the process. All chemicals were used as received and purchased from Fisher unless specified.

3.2.1 Thermal Growth of SiO_2

The Lindberg oxidation furnace was used here for the growth of the SiO_2. A n-doped Si (100) wafer was placed in the oxidation tube and the temperature was set to 1000° C at a ramp speed of 25° C/minute (min). The wafer was left in the tube for 3-6 hours. The thickness of the SiO_2 is not significant, as long as the SiO_2 is thicker than the intended etching depth, which was here at maximum 50 nm. Normal thicknesses used were 4200-5200 Å determined via ellipsometry.

3.2.2 Preparation and Synthesis of the Silane Benzophenone Monolayer

The silane benzophenone monolayer was prepared as described previously in Chapter 2. The formation of a dense monolayer was critical for successful results during the process and special care was taken to keep the chlorosilane derivatives from air and moisture. Therefore, all reactions involving a chlorosilane derivative were done under inert atmosphere using standard Schlenk glassware and technique. All specific reactions and results involving the monolayer were described in Chapter 2.

3.2.3 Synthesis of ROMP polymer from 1-(3-(bicyclo[2.2.1]hept-5-en-2-yl)hexyl-2-(3,4-dibutoxyphenyl-fulleropyrrolidine (ROMP-C60)

The polymer was synthesized by Dr. Jian-Yang Cho in the Seth Marder group at Georgia Institute of Technology. The polymerization was conducted with ring-opening

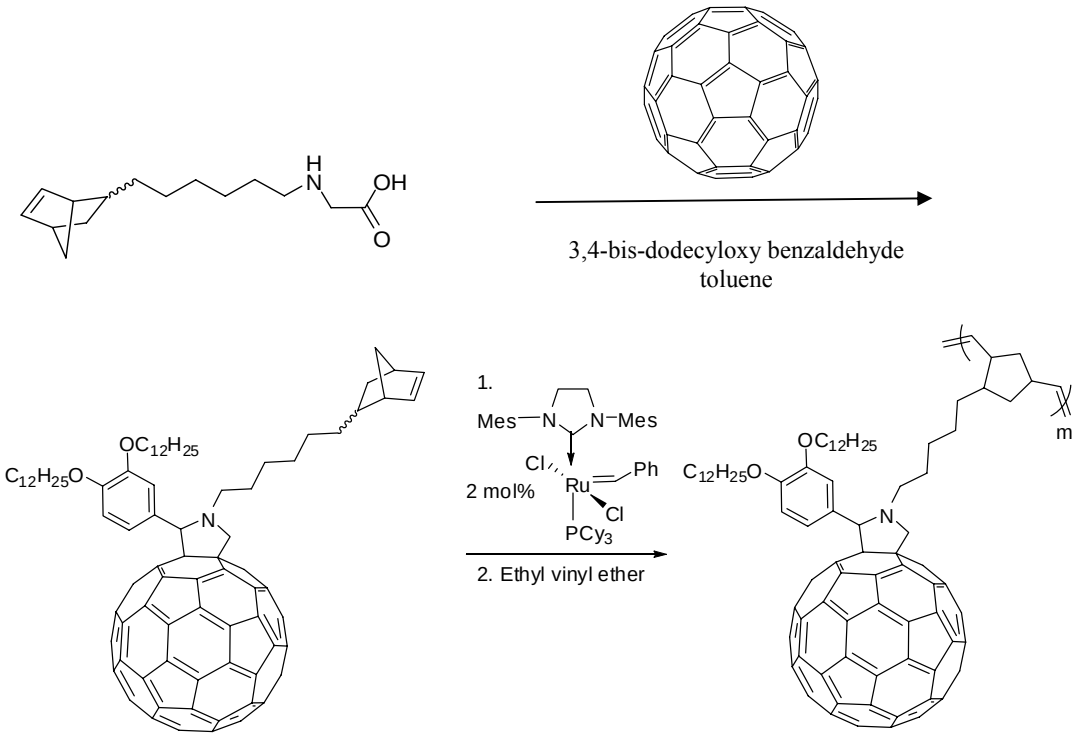

Figure 3.1 Synthesis of ROMP-C60

metathesis polymerization (ROMP)[1], of 1-(3-(Bicyclo[2.2.1]hept-5-en-2-yl)hexyl-2-(3,4-dibutoxyphenyl-fulleropyrrolidine[2] (BHDF). The polymer is referred to as ROMP-C60 throughout the thesis. First (6-Bicyclo[2.2.1]hept-5-en-2-yl-hexylamino) acetic acid was prepared to be used as a starting material for the monomer synthesis, see Figure 3.1. All chemicals were purchased from Aldrich Chemical Company except C_{60}, which was purchased from Bucky USA. Iodoacetic acid (0.7 g, 3.76 mmol) was added drop wise to a solution of 6-bicyclo[2.2.1]hept-5-en-2-yl-hexylamine[3] (5.14 g, 26.59 mmol) in H_2O (15 mL) which was stirred at 0 °C. A mixture of acetone (40 mL) and absolute ethanol (5 mL was added slowly after 24 hrs and a white precipitate was collected by filtration and dried under vacuum to give a solid (58.2%)**.** ^{1}H NMR (300 MHz, $CDCl_3$, δ): 7.80 (br s, 2H), 6.07 (dd, *J* = 5.9 Hz, 2.9 Hz, 1H), 5.85 (dd, *J* = 5.4 Hz, 2.4 Hz, 1H), 3.42 (s, 2H),

2.90 (t, J = 7.3 Hz, 2H), 2.70 (s, 2H), 0.90-2.00 (m, 14H), 0.43 (m, 1H). $^{13}C\{^{1}H\}$ NMR (75 MHz, $CDCl_3$, δ): 170.67, 136.84, 132.13, 49.56, 49.44, 47.72, 45.38, 42.51, 38.70, 34.71, 32.45, 29.61, 28.66, 27.02, 26.29. HRMS-EI (m/z): $[M]^+$ calcd for $C_{15}H_{25}NO_2$, 251.18853; found, 251.18738.

N-(6-Bicyclo[2.2.1]hept-5-en-2-yl-hexyl)-2-(3,4-bis-dodecyloxy-phenyl)-3,4-fulleropyrrolidine (BHDF) was synthesized by a route developed by Prato[4]. C_{60} (0.36 g, 0.5 mmol), (6-bicyclo[2.2.1]hept-5-en-2-yl-hexylamino)-acetic acid (0.251 g, 1 mmol), and 3,4-bis-dodecyloxy-benzaldehyde (0.237 g, 0.5 mmol) to dry toluene (200 mL) and was refluxed at 120 °C for 15 h under N_2. The solvent was removed *in vacuo*. The crude product was purified by column chromatography (silica gel, toluene:hexanes = 1:4) to give a black semi-solid (0.322 g, 46.6%) along with unreacted C_{60} (50 mg, 14%). The product was further triturated with MeOH and collected by filtration to give a black solid. Endo isomer: ^{1}H NMR (300 MHz, $CDCl_3$, δ, 25 °C): 7.00-7.40 (br m, 2H), 6.85 (d, J = 6.9 Hz, 1H), 6.10 (dd, J = 5.5 Hz, 2.7 Hz, 1H), 5.90 (dd, J = 5.5 Hz, 2.7 Hz, 1H), 5.05 (d, J = 9.1 Hz, 1H), 4.95 (s, 1H), 4.08 (d, J = 9.3 Hz, 1H), 3.90-4.04 (m, 4H), 3.14-3.31 (m, 1H), 2.75 (d, J = 9.1 Hz, 2H), 2.46-2.60 (m, 1H), 1.00-2.05 (m, 54H), 0.85 (t, J = 6.0 Hz, 6H), 0.46-0.54 (m, 1H). ^{1}H NMR (300 MHz, toluene-d_8, δ, 365.7 K): 7.61 (d, J = 1.8 Hz, 1H), 7.33 (dd, J = 1.8 Hz, 8.1 Hz, 1H), 6.85 (d, J = 8.1 Hz, 1H), 6.09 (dd, J = 6.0 Hz, 3.0 Hz, 1H), 5.93 (dd, J = 6.0 Hz, 3.0 Hz, 1H), 4.95 (s, 1H), 4.93 (d, J = 9.0 Hz, 1H), 4.05 (t, J = 6.6 Hz, 2H), 3.95 (d, J = 9.3 Hz, 1H), 3.82 (t, J = 6.3 Hz, 2H), 3.35 (t, J = 8.4 Hz, 1H), 3.31 (t, J = 8.4 Hz, 1H), 2.76 (br s, 1H), 2.68 (br s, 1H), 1.00-2.05 (m, 55H), 0.89 (t, J = 6.6 Hz, 6H), 0.53-0.61 (m, 1H). $^{13}C\{^{1}H\}$ NMR (75 MHz, $CDCl_3$, δ, 25 °C): 156.49, 154.26, 153.96, 153.64, 149.00, 148.79 (br), 147.13, 146.84, 146.38, 146.20, 146.14,

146.05, 145.97, 145.91, 145.78, 145.61, 145.44, 145.38, 145.29, 145.12, 145.06, 144.97, 144.53, 144.26, 143.54, 143.00, 142.83, 142.51, 142.41, 142.16, 142.13, 142.00, 141.97, 141.89, 141.86, 141.77, 141.65, 141.51, 141.39, 140.01, 139.92, 139.66, 139.46, 136.81, 136.44, 136.33, 136.06, 135.62, 135.59, 132.33, 129.55, 122.20 (br), 114.74 (br), 112.78 (br), 82.24, 69.27, 68.97, 68.85, 66.83, 53.14, 49.63, 45.50, 42.59, 38.84, 34.91, 32.56, 32.01, 30.07, 29.78, 29.73, 29.70, 29.60, 29.57, 29.45, 29.40, 29.22, 28.79, 28.43, 27.79, 26.14, 22.80, 14.27. HRMS-MALDI (m/z): $[M]^+$ calcd for $C_{105}H_{77}NO_2$, 1383.5954; found, 1383.5968. Anal. Calcd for $C_{105}H_{77}NO_2$: C, 91.07; H, 5.60; N, 1.01. Found: C, 90.88; H, 5.72; N, 0.98.

The ROMP-C60 was made by adding BHDF (0.3 g, 0.22 mmol) and a second-generation Grubbs catalyst (3.7 mg, 0.004 mmol) in $CHCl_3$ (2 mL) in $CHCl_3$ (16 mL). After 35 min of stirring the polymerization was quenched by adding ethyl vinyl ether. The mixture was added to MeOH and a brown solid precipitated, the solvent was removed *in vac*uo (93%) . ^{1}H NMR (300 MHz, $CDCl_3$, δ): 6.60-7.70 (br, 3H), 4.60-5.60 (br, 4H), 3.60-4.20 (br, 5H), 2.20-3.40 (br, 4H), 0.90-2.20 (55H), 0.85 (t, J = 6.3 Hz, 6H). Anal. Calcd for $(C_{105}H_{77}NO_2)_m$: C, 91.07; H, 5.60; N, 1.01. Found: C, 90.80; H, 5.66; N, 0.96.

3.2.4 The Ohnishi and Ring Parameter for BHDF

As described in the first chapter, the Ohnishi[5] and Ring[6] parameters are indicators as to how resistant a material is towards a fluorine plasma process. The Ohnishi parameter, which takes into account the molecular composition, was calculated to be 1.48 for the monomer unit, BHDF. The Ring parameter which also considers the molecular composition, but also the molecular structure was calculated to 0.68. In this case it would

not make sense to calculate the different parameter values for various separate parts of the molecule, as was done for C96, since the organization of the structures seen on the surface was not dependent or aligned to the aromatic parts of the molecule. Both parameters indicated that ROMP-C60 should have excellent etch resistance towards a fluorine plasma which will be verified below.

3.2.5 Morphology of ROMP-C60 at Different Concentrations and Coating Techniques

ROMP-60 was slightly soluble in chloroform, so the solutions necessitated sonication to ensure complete dissolution. ROMP-60 solutions in chloroform of 10^{-4}, 10^{-5}, and 10^{-7} M concentration were prepared. Thin films of each solution were prepared using either spin-casting or dip-coating techniques. Spin-coated samples were spun at 1000 rpm for 1 min, followed by baking at 100º C for 30 sec. Dip-coated samples were lifted out of solution at various speeds varying from 160 mm/min to 16 mm/min. AFM analysis showed that the speed of dip-coating had no affect outcome of the surface morphology. As for all samples used for molecular lithography, the samples were irradiated at 356 nm with the Stratalinker 2400 for 120 min. Upon irradiation, the samples were rinsed thoroughly in the Soxhlet extraction apparatus to remove any unattached polymer. ROMP-60 did not wet the surface well and the polymer clumped on the surface into various shaped patterns with defined edges. These features were then used as the etch mask in the etching experiments described later in this chapter. These ROMP-60 features are much larger than the features seen when using C96. Typically the features were around 100-200 nm in diameter. The range of size of the features was large with the smallest being ~17 nm in diameter while the largest ones were as big as 500 nm. Even though this research was aimed towards making molecular sized patterns in SiO_2, it

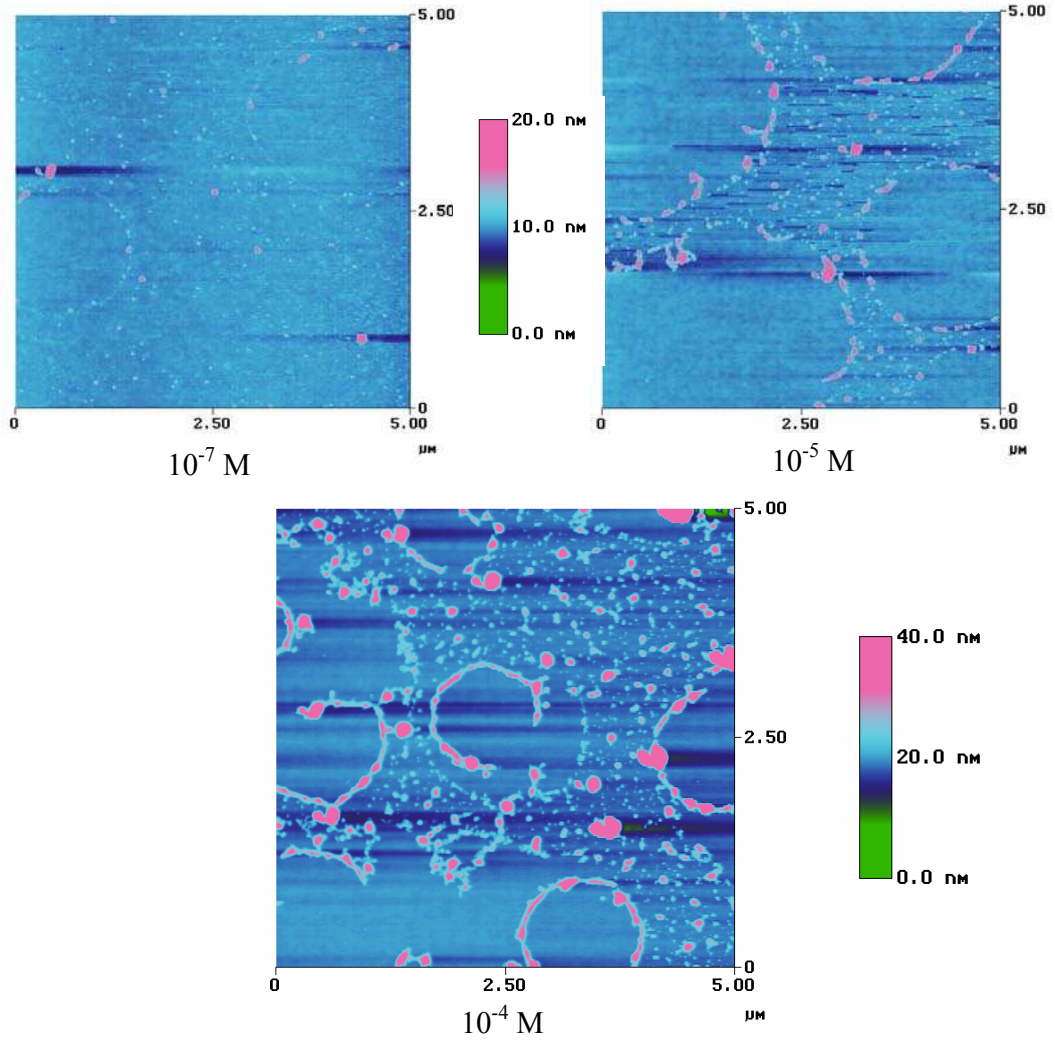

Figure 3.2 Spin-coated samples at 10^{-4}, 10^{-5}, and 10^{-7} M.

was also important to show that a monolayer spanning over large areas also could act as molecular masks. Many features necessary in IC fabrication are much larger than would be feasible to create using individual molecules in a self-assembly. Therefore, polymers could be used due to their size and stability. There are also many ways to manipulate polymers into desired patterns using various techniques such as dip-pen lithography among others; these will be discussed in more detail in Chapter 5. The coverage of the surface depended on both coating technique and concentration. The height of the features

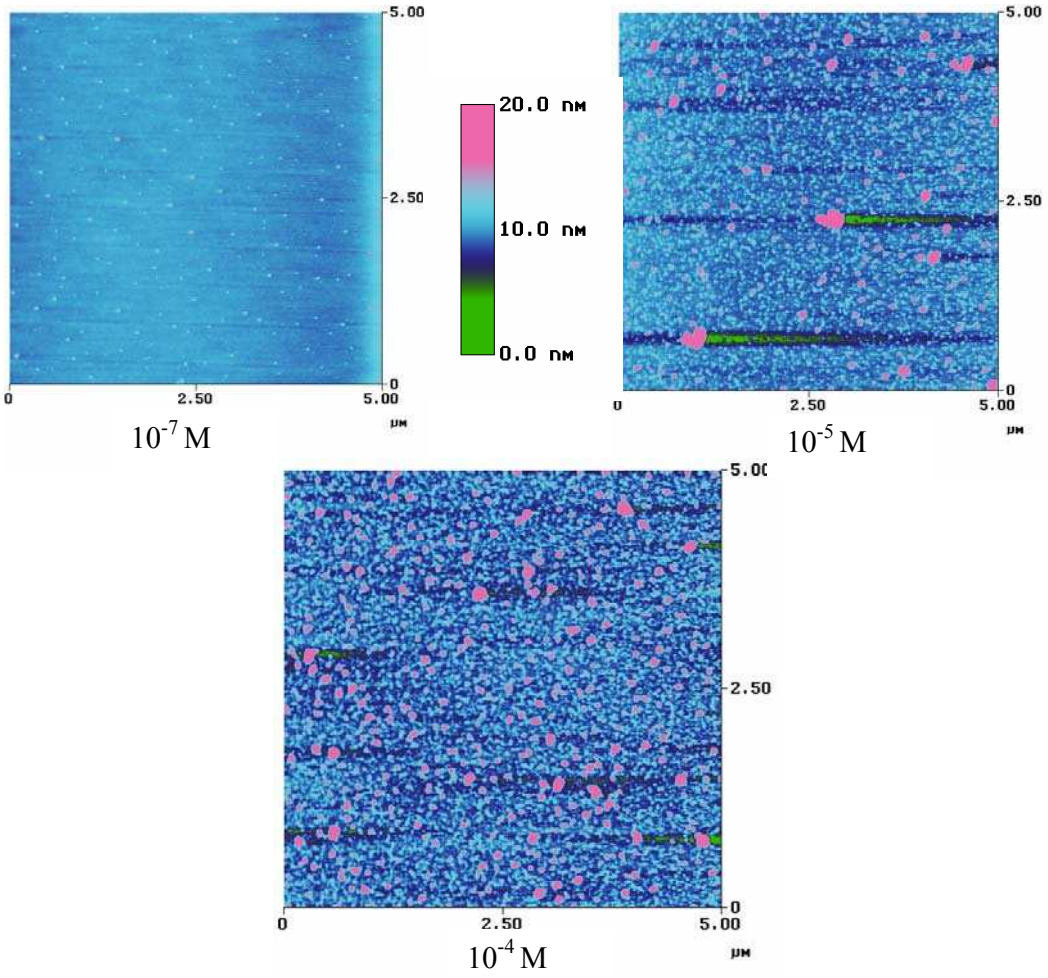

Figure 3.3 Dip-coated samples at 10^{-4}, 10^{-5}, at 10^{-7} M

also depended on the concentration of the solution used. The higher the concentration of the polymer the thicker the structures became. This might be due to the fact that polymer chains can entangle with each other and due to its fairly low solubility in the chloroform, which may prevent full the Soxhlet extraction of the non-bonded polymer. The smallest height of the features seen was ~7 nm and could reach a high as ~25 nm. For the 10^{-7} M solutions the features seen were smaller and thinner (3-10 nm) compared to the other higher concentration solutions. See Figure 3.2 for spin-coated AFM results and Figure 3.3 for dip-coated AFM results. Using either spin- or dip-coating here gave similar results

of surface morphology. The surface was also monitored by static water contact angle and for a surface with polymer increased from 69 ± 2 (benzophenone monolayer) to 76 ± 2 (for the polymer). For the 10^{-5} M solution the features increased in size and also the surface was covered with more polymers. The contact angle for film created using this solution was 80 ± 3. For the highest concentration, 10^{-4} M, the features became even larger and thicker; the thickness approached 20-25 nm. Also, the coating technique matters, the dip-coated samples had a higher polymer density than the spin-coated. When dip-coating the polymer had a longer time to stick on the surface and also will not be exposed to the same force trying to remove the molecules from the surface as the spin-coating technique does. The water contact angle for the spin-coated samples was 81 ± 2 and for the dip-coated samples 84 ± 3. Since the ROMP-C60 is a polymer and there were no secondary interactions influencing the structure of the features on the surface both the size and shape are random. The smallest structures seen were ~17 nm in diameter and circular in shape. The largest structures seen were several hundred nm in diameter and had no defined shape (round, triangular, etc). Most structures fell in the category in between the extremes. Dip-coated surfaces produce a more homogeneous size of the features compared to the spin-coated samples. Each of the different types of surface morphologies were then exposed the fluorine plasma for etching.

3.2.6 Etching Using ROMP-C60 as a Molecular Mask

All experiments involving plasma processes were performed in the cleanroom at the Microelectronic Research Center (MIRC) at Georgia Institute of Technology. The Vision- 320 RIE was used as the etch tool. It is important to note that the plasma parameters used successfully here might not be successful with other etch tools since the

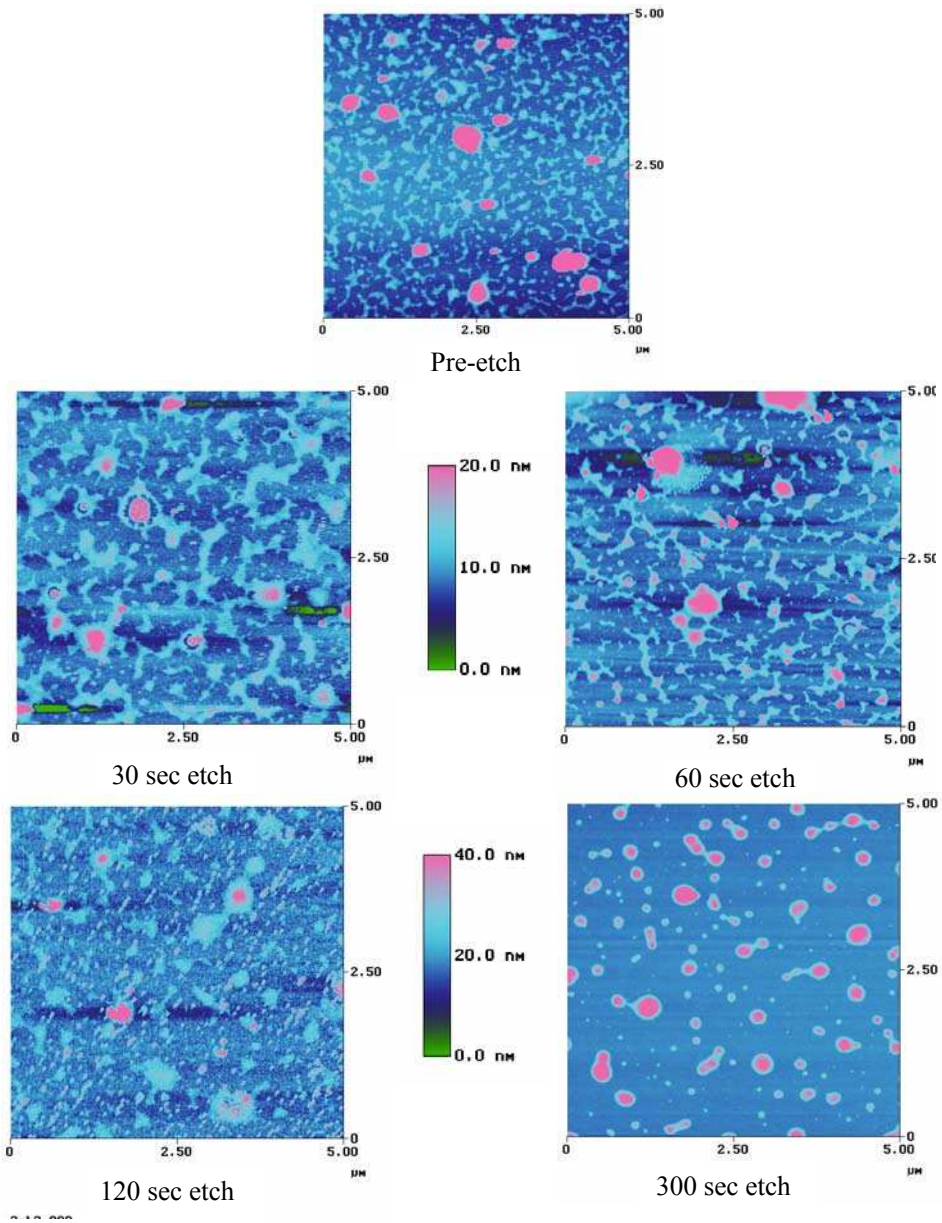

Figure 3.4 AFM of etch results in plasma 3 using ROMP-C60

performance of the plasma also depends on the reactor geometry and other factors that are individual to this tool. Even though the ROMP-C60 was more stable in the fluorine plasma than C96, the same plasma (plasma 3: CF_4 31 sccm, H_2 2 sccm, 50 mTorr, 75 W RF power) proved to be the optimum process for both materials. Both plasma 1 and 2 were too harsh and removed the polymer before it could serve its purpose as an etch

mask. Although the ROMP-C60 layer was thicker than C96 the layer was still only 3-25 nm thick and sensitive towards a harsh environment. The added oxygen in plasma 1 is known to have a high reactivity towards organics and would therefore promote the degradation of the ROMP-C60. The results described below were achieved with plasma 3. The samples were placed in the RIE tool for 30, 60,120, and 300 sec of etching. The feature size and shape stay intact during the etch process. As expected the height of the features increases with increased etch times. The increase in height before and after plasma etching was also consistent with the etch rate of the plasma determined in chapter 2. Since different concentration of ROMP-C60 and different coating techniques gave different polymer densities and morphologies; all plasma etching was done with spin-coated samples from the highest concentration, (10^{-4} M). After the15 sec of etch processing, the height of the features increased 2.8 ± 0.5 nm, see Figure 3.4 for all etch results. A process time of 30 sec gave an increase of 5.7 ± 0.5 nm. After 60 sec the features increased as much as 9.1 ± 0.7 nm. After 120 sec of fluorine plasma etching the structures were still intact and an increased 15.6 ± 1.2. The ROMP-C60 was even stable after 300 sec of etching and the features increased in height 50.9 ± 8.9 nm. This is important since the minimum depth profile for devices produced today is 50 nm. These results showed that an adequate depth profile could be obtained using molecular lithography. However the features start losing their original shape after 300 sec of etching and if the etch time is increased even further the features did not resemble its original shape.

3.2.7 Removal of the Organic Layer Post Etching Using either an Oxygen Plasma or Piranha Solution

As described in chapter 2, it was necessary for the organic etch-resist to be stripped off the surface, leaving the SiO_2 behind. In device fabrication it is vital that each step is built onto the correct feature and material and therefore, the complets removal of the resist is critical. The structures created in SiO_2 using the ROMP-C60 were both taller and wider in diameter, compared to the structures created using C96 as the molecular mask. As a result the larger structures were more robust and could withstand more physical stress, allowing for the use of an oxygen plasma to remove the organic resist, without destroying the features. The plasma recipe used for the stripping consisted of: O_2 50 sccm, 200 W RF power, 30 mTorr. The process time used for the stripping experiments was 10 min unless specified otherwise. The surface was monitored by

Table 3.1 Contact angle results for ROMP-BHHDFPF

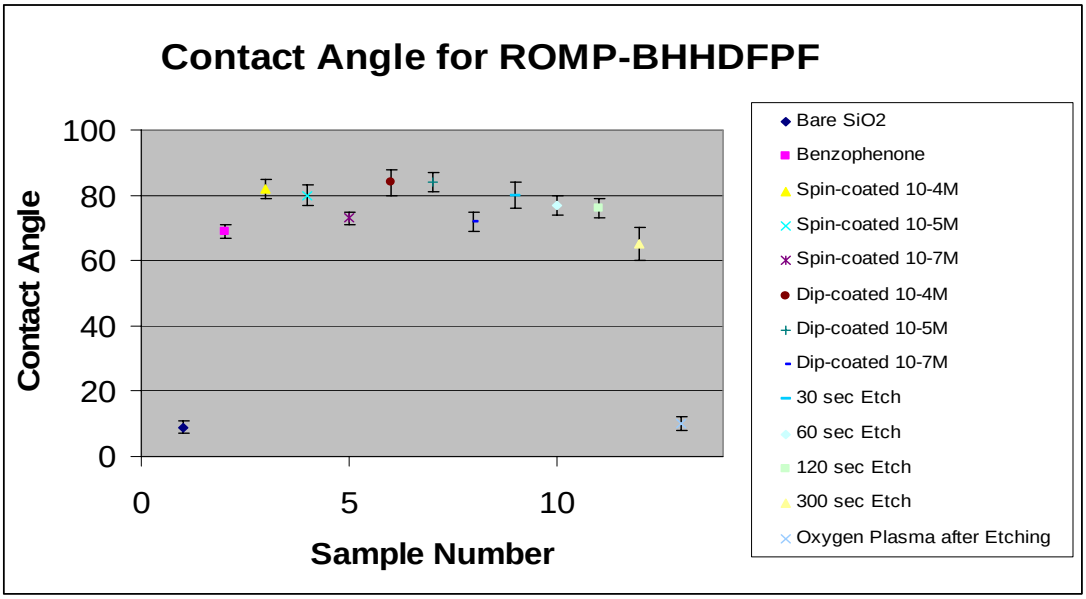

contact angle and EDS throughout the process. The water contact angle after the fluorine etched samples was 75 ± 3. See Table 3.1 for a summary of all contact angle results involving ROMP-C60. After 10 min of treatment in the oxygen plasma, the contact angle

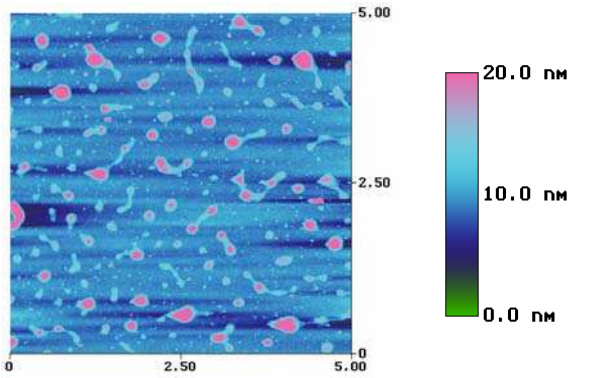

30 sec etch followed by oxygen plasma

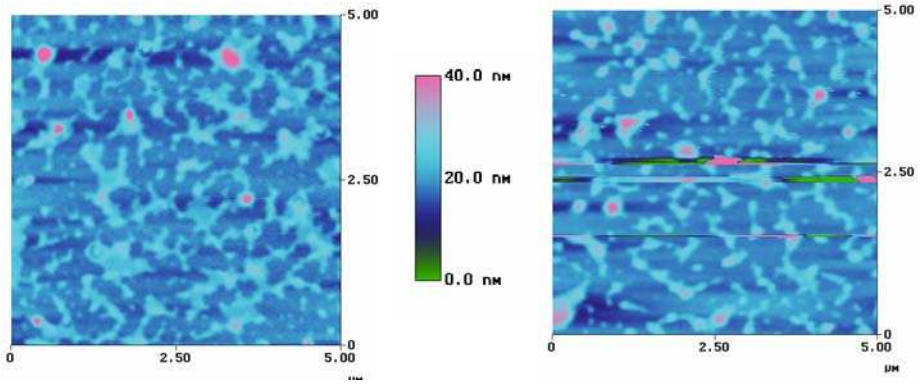

60 sec etch followed by oxygen plasma

120 sec etch followed by oxygen plasma

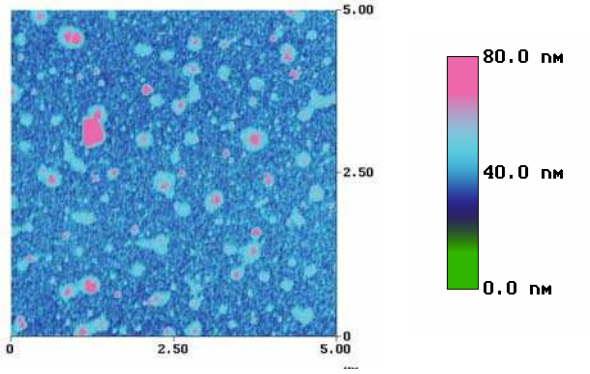

300 sec etch followed by oxygen plasma

Figure 3.5 Etching followed by oxygen plasma treatment to remove ROMP-BHHDFPF from the surface

decreased to 9 ± 2. The features seen before and after the oxygen plasma process were identical in shape, but the height of the features had decreased. The decrease in height was consistent with the initial height of the polymer monolayer. After 15 sec of fluorine

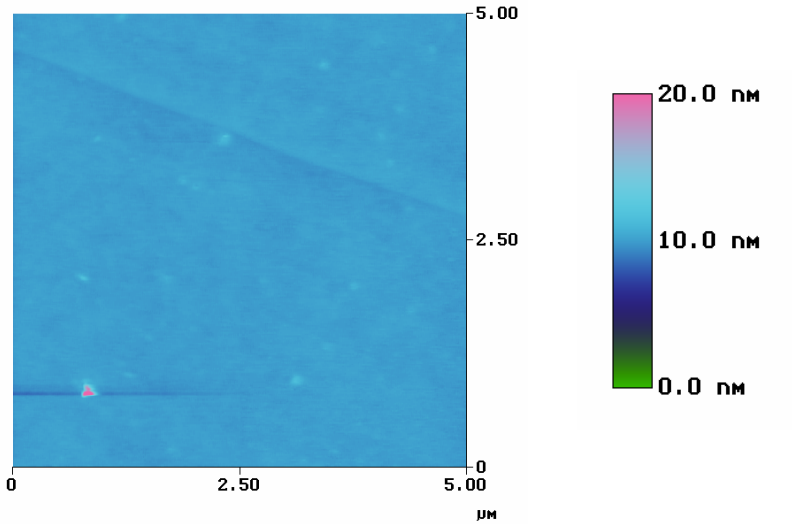

Figure 3.6 Control experiment

etch, followed by oxygen plasma processing, the height of the features were 2.3 ± 0.5 nm. See Figure 3.5 for all results of etching followed by oxygen plasma treatment. 30 sec of fluorine etch followed by oxygen plasma processing gave the features a height of 5.1 ± 0.5 nm. After 60 sec of fluorine etch followed by oxygen plasma processing, the features were 8.4 ± 0.7 nm tall. After 120 sec of fluorine etch followed by oxygen plasma processing the structures remained intact and 14.5 ± 1.2 nm of height is observed. Using 180 sec of fluorine etch followed by oxygen plasma processing results in a height of 18.5 ± 2.3 nm. The ROMP-C60 was even stable after 300 sec of fluorine etch followed by oxygen plasma processing 42.9 ± 8.9 nm. All results were consistent with the etch rate for fluorine plasma 3. In the control experiment sample with covalently attached ROMP-C60 was placed on the surface directly in the oxygen plasma without first exposing it to the etching fluorine plasma. As seen in Figure 3.6 there were no features on the control sample indicating complete removal of the organic layer. The water contact angle for the control sample was 9 ± 2. Placing the samples in a piranha solution (70 % H_2SO_4, 30 %

H_2O_2) for 1.5 hrs also removed the organic etch barrier. The only advantage using piranha rather then an oxygen plasma was that the smaller structures possible were less damaged in the process. Since molecular lithography is geared towards industry it is important to create methods that are attractive for and can be used in the commercial production of ICs. Therefore using the oxygen plasma successfully for the stripping process is an important accomplishment for the development of molecular lithography.

3.3 Summary and Conclusion

In this chapter it has been shown that a polymer can be used as an etch mask in molecular lithography. The polymer, ROMP-C60, had an excellent etch resistance towards a fluorine plasma due to its molecular structure. The fullerene part of the polymer provides stability because of its aromatic moiety. Also, the many covalent bonds in the polymer gave more stability than the secondary interactions which is the case for C96. Features as tall as 50 nm can be produced which is important since, today, industry currently have a minimum depth profile of 50 nm for commercial devices. Also the features produced were much larger then the features made using C96 as the etch mask which can make for a great platform if larger sized features are required. The larger features also allowed for oxygen plasma to be used in the removal process of the organic resist after the fluorine etch. Although the piranha treatment also will remove the resist it is more attractive for industry to use a dry etch process to strip the resist than using the highly reactive piranha. Organization of ROMP-C60 into organized pillars is probably the most direct application. An alternative alignment method is dip-pen lithography which is discussed in Chapter 5. Molecular lithography could also be used in conjunction

with patterns created by block-copolymer chemistry to enhance the and improve the etch resistance of the polymer.

3.4 REFERENCES

[1] Hillmyer, M.; Grubbs, R. *Macromolecules,* **1993,** 26, 872

[2] Dyer, D. *Final Post-doctorial Report,* **2004.**

[3] Meyers, A.; Weck, M. *Macromolecules* **2003**, *36,* 1766-1768.

[4] Maggini, M.; Scorrano, G.; Prato, M. *J. Am. Chem. Soc.* **1993,** 9798.

[5] Gokan, H.; Esho, S.; Ohnishi, Y *J. Electrochem. Soc.* **1983,** *130(1),* 143.

[6] Kunz, R.; Palmateer , S.; Forte, A.; Allen, R.; Wallraff, G.; DiPetro, A.; Hofer, D. *SPIE*, **Vol. 2724,** 365.

CHAPTER 4

INDIVIDUAL FULLERENE MOLECULES IN A MONOLAYER AS MOLECULAR RESISTS

4.1 Introduction

For a process to truly defined as molecular lithography, an individual molecule would act as the etch resist. In this chapter, individual fullerene molecules were attached to the SiO_2 surface through the silane benzophenone derivative, described earlier in Chapter 2. Success with a single fullerene molecule as an etch resist would prove that molecular lithography is possible for the creation of any feature size is SiO_2 or Si. The size range of molecular lithography would be from one molecule (0.3-1 nm depending on the molecule) to several hundreds of nm with a polymer as the etch mask. Molecular design, synthesis, and self-assembly of the material would be the limiting factors of what type and size features could be created and transferred into the substrate. Fullerene molecules are ideal for use as etch resists due to their molecular structure and properties, described in the Ohnishi parameter. Since its discovery and later production in large quantities, the fullerene molecule (C_{60}), has attracted much attention from the research community[1,2]. Thin films of C_{60} have shown to have potential applications in organic circuits and devices which take advantage of its interesting electrical and optical properties. Fullerenes have been covalently attached in self-assembled monolayers (SAMs) to a variety of surfaces such as Si/SiO_2, Au, and $In\text{-}SnO_2$ (ITO) using different attachment methodologies[3,4,5,6,7]. Since SAMs of C_{60} are highly attractive to the research community, new methodologies for making such films are desired. Here, we have

presented new ways to attach a SAM of C_{60} to a Si surface using photochemical reaction with benzophenone as the link to the surface. It is known that the electron transfer capabilities through the interface decreases with increasing length in the linker of the alkyl[8,9,10]. This was not a concern for this work since the electrical properties are not important for etch resistance. However, the alkyl chains and the native oxide on the Si make it more difficult to tunnel electrons from the tip to the Si in STM analysis. Therefore, some of the STM images reported here are not 100 % perfect. Instead the chemical and mechanical stability of C_{60} was utilized and individual molecules were used as molecular masks for plasma etching. The individual C_{60} molecule has the best etch resistance towards dry fluorine plasma etching as a molecule with the particular molecular weight of C_{60} can have; this is discussed in more detail in the Ohnishi and Ring parameter in section 4.2.1. Since the benzophenone photochemistry requires a point of attachment through an alkyl chain, it was designed to meet this criterion. The alkyl chain also improved the solubility of the molecules which made it easier to fabricate the thin films used in later experiments. The molecule of choice is 1-methyl-2-nonyl-[60]fulleropyrrolidine (MNFP), see Figure 4.1 for synthesis and molecular structure.

4.2 Experimental

The methodology used to create the fullerene monolayer is the same as for C96 and ROMP-C60, described in Chapter 2 and 3. Therefore, all data concerning the synthesis and immobilization of 4-(3'chlorodimethylpropyloxysilane) benzophenone into a monolayer are reported in chapter 2. The surface used in this chapter is silicon (Si) rather then SiO_2. The reason for this is so that the monolayer of MNFP can be analyzed with STM to get a better understanding in the film morphology. Si is a better conductor

then SiO_2 which is a requirement for STM analysis. The order of the experiments here were identical to C96: (1) creation of benzophenone monolayer, (2) thin film fabrication of MNFP on the surface, (3) covalent attachment of MNFP to the benzophenone derivative through photoirradiation, (4) extraction of unattached molecules in a Soxhlet extraction apparatus, (5) plasma etching, (6) removal of the remaining organic layer through piranha solution. The samples were appropriately analyzed after each step of the process. All chemicals used were purchased and used as received from Fisher unless specified otherwise.

4.2.1 The Ohnishi and Ring Parameter for 1-methyl-2-nonyl-[60]fulleropyrrolidine (MNFP)

Described in the first chapter, the Ohnishi[11] and Ring[12] parameter are indicators on how resistant a material is towards a fluorine or oxygen plasma process. Here we present the parameter values for MNFP. The Ohnishi parameter was calculated to be 1.43 and the Ring parameter was 0.82. The unique, soccer-ball like, molecular structure of the C_{60} moiety in MNFP will provide most of the etch resistance in the molecule and therefore it would be important to calculate the different parameter values for only C_{60} as well. Both the Ohnishi and Ring parameter for a fullerene molecule are 1, which is the best value possible for a molecule regarding plasma resistance. However, it is important to understand that both of these parameters do not take into account the molecular weight of a molecule or a polymer. The molecular weight, hence size, of the molecule would be most relevant in the case of molecular lithography since a monolayer is used as the etch resist. The larger the molecule, the more etch resistant is would be since it would take a longer time for the fluorine plasma to break it down. The same might not be true for

common photoresists since they are in multilayers on the surface. Both parameters indicate that MNFP should have excellent etch resistance towards a fluorine plasma which were also the case and the results are reported below.

4.2.2 Preparation and Synthesis of the Silane Benzophenone Monolayer

The preparation of the silane benzophenone monolayer was prepared as described previously. The only difference here was that the benzophenone monolayer was attached to a native oxide on the Si surface rather than to a thermally grown SiO_2 surface. The allowed for a dense MNFP monolayer similar in terms of coverage to previously reported C_{60} monolayers in literature[19]. Since the formation of a dense monolayer is critical for the process to perform satisfactorily, special care was taken to exclude moisture from all chlorosilane molecules. Therefore, all reactions involving a chlorosilane derivative were done under inert atmosphere using standard Schlenk glassware and technique. All specific reactions and results involving the monolayer were previously reported in Chapter 2.

4.2.3 Synthesis of 1-methyl-2-nonyl-[60]fulleropyrrolidine (MNFP)

This molecule was synthesized by Dr. Simon Jones in the Seth Marder group at the Georgia Institute of Technology. The Marder group has much experience with the synthesis of fullerene derivatives and successfully helped making the molecules of choice. See Figure 4.1 for the synthesis and structure of MNFP. The C_{60} derivative included an alkyl chain and could easily be obtained using chemistry based on the 1,3-dipolar cycloaddition of azomethine ylides to fullerenes, developed by Prato[13]. Sarcosine (*N*-methyl glycine) (0.116 g, 1.3 mmol), decanal (0.438 g, 2.8 mmol), and C_{60} (0.216 g,

0.3 mmol) were refluxed in dry toluene (200 ml) under N_2 for 16 hrs to give 1-methyl-2-nonyl-[60]fulleropyrrolidine (MNFP) (0.05 g, 0.06 mmol, 18 %) after chromatography on SiO_2 with 1:1 hexanes/toluene elution, see Scheme 1. The ^1H NMR spectrum was consistent with that reported in the literature[14]. ^1H NMR (CDCl3): δ 4.81 (d, 1H, pyrrolidine, *J*= 9.23 Hz), 4.15 (d, 1H, pyrrolidine, *J*= 9.26 Hz), 3.89 (t, 1H, pyrrolidine), 2.98 (s, 3H),1.90 (m, 2H, -CH2R), 1.25 (s, 14H), 0.87(m, 3H,-RCH3).

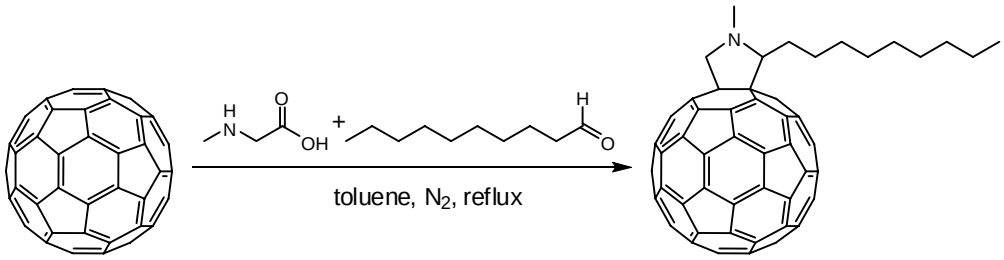

Figure 4.1 Synthesis of MNFP

4.2.4 Morphology of MNFP Monolayer on Si

The surface morphology differed from the other surfaces discussed in previous chapters. The MNFP was monodisperse which was not the case with the ROMP-C60, which resulted in various sized features. C96 on the other hand was also monodisperse, but the discotic molecules self assembled into one dimensional columnar supramolecular structures due to the π-π interaction between the aromatic regions in the core of the molecules[15,16,17,18]. Even though molecular resolution was obtained in both the X (one molecule in width) and Y (monolayer of molecules) axes, "true" molecular resolution is not achieved due to the secondary π-π interaction which align the molecules in the Z axis. A 10^{-5} M solution of MNFP was prepared in chloroform in which this molecule is highly soluble. A thin film of MNFP was created either via spin-coating the solution onto a

benzophenone modified surface at 1000 rpm for 1 min, dip-coating MNFP onto the substrate, or drop-casting and letting the solvent evaporate. The samples were then placed onto a hotplate at 100º C for 30 sec to remove any solvent residue. The samples were placed in a Stratalinker 2400 for 120 min which gave rise to the $n \rightarrow \pi^*$ transition in the benzophenone, which allows for a reaction with the alkyl chain at MNFP. The static water contact angle for these films was 93 ± 1 before extraction of unattached molecules in the Soxhlet apparatus. Upon Soxhlet extraction and removal of non-bonded MNFP molecules, the water contact angle was 80 ± 1. These results were somewhat higher from previous recorded SAMs of C_{60} on Si[19]; the contact angle previously reported was 70. This indicated that the fullerene monolayer produced here was more closely packed than the surfaces reported in literature. This was confirmed by AFM and STM analysis. Also, the surface analysis previously reported was not complete, poor imaging gave a bad insight of the morphology of the surface since the only imaging tool used was AFM. Here STM images support the AFM analysis which gave a better understanding of the surface coverage and molecular arrangements. The morphology of the surface was not dependent on either the concentration of the solution or method of coating. This is because the molecules are monodisperse and also does not interact with each other, through secondary forces, to create fibers seen with C96. The MNFP surface would also be interesting to study for its electrical properties for other possible applications, such as charge mobility etc. This new method of attaching fullerenes to Si showed to have a high density of fullerene molecules on the surface. A tightly packed fullerene surface would allow for better mobility than a surface with low fullerene density. However, this was not in the scope of the research and such studies could be carried out further down the road.

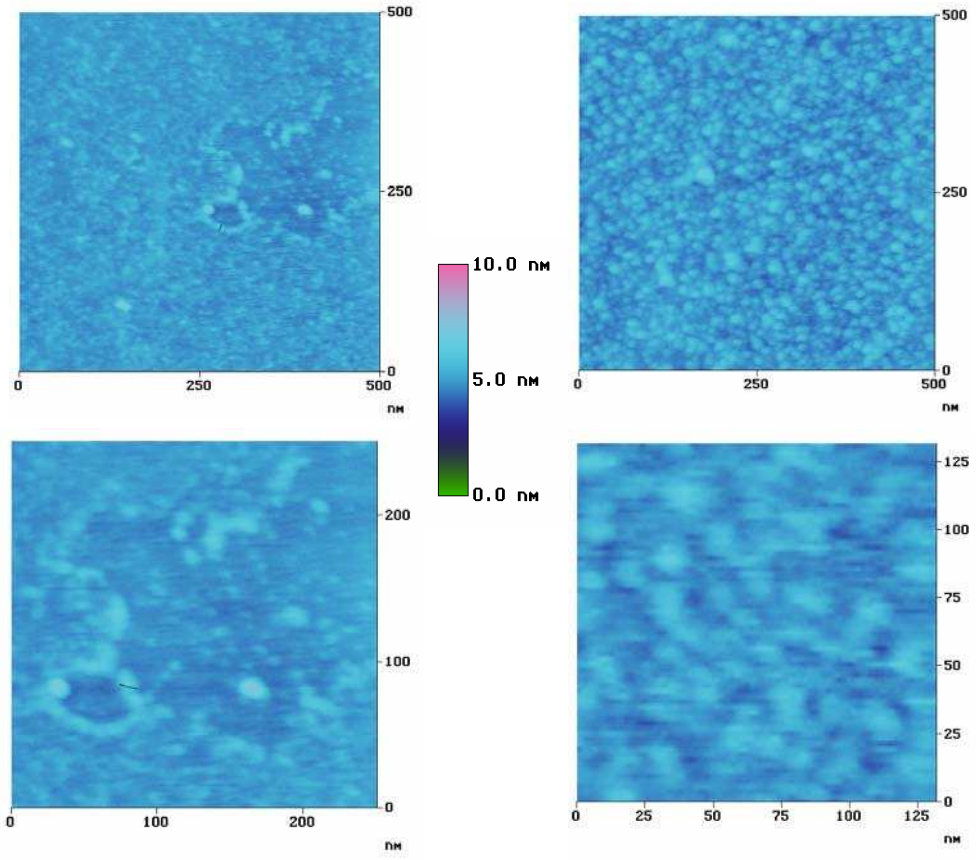

Figure 4.2 AFM of MNFP monolayer.

Also, there has been only been a few reports of SAMs of fullerenes on Si in the literature and those surfaces were not very well characterized and understood. Here STM images gave a better understanding of the surface morphology. AFM analysis on the final MNFP monolayer surface revealed a flat surface with some structures 1.1 ± 0.2 nm tall which corresponds well to the diameter of an individual fullerene molecule, see Figure 4.2. The high contact angle of the sample indicated a high density of MNFP which would be difficult to resolve with AFM. The individual C_{60} molecules are too small to image using the AFM since the tip radius is about 10 times the size of the molecule, and also because the maximum number of data points taken in the AFM were 512. This meant that in a 1

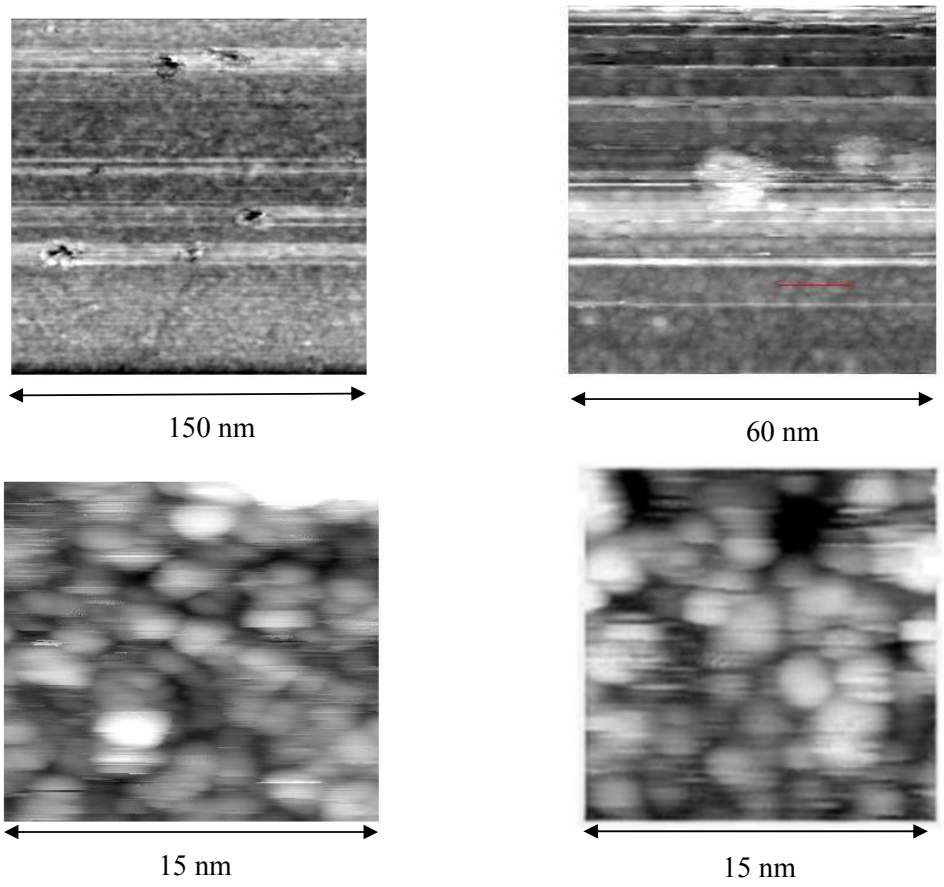

Figure 4.3 STM of MNFP monolayer.

μm scan size has 512 data points resulted in the that each data point were 1.95 nm apart which is about 3 times the size of each MNFP molecule. When trying to decrease the scan size so that reaching molecular resolution would be possible the instrument became difficult to operate and no good images could be taken. The structures seen in the AFM could be explained from molecules that have not been removed in the Soxhlet extraction which forms multilayers of molecules. However, STM analysis revealed a better understanding to the structures observed in the AFM. STM has the ability to achieve a much higher resolution than AFM since STM operates by tunneling electrons rather then physically touching the surface like the AFM. The STM images showed a highly dense

monolayer of MNFP with both individual molecules and clusters of MNFP. The diameter of the MNFP molecules and clusters ranged from 0.7 nm to 3 nm, this corresponds well with the diameter of an individual fullerene molecule (0.7 nm) and also the size of clusters one could expect from MNFP, see Figure 4.3. The surface also had the occasional cluster of MNFP that are on top of and higher then the rest of the surface, which could be linked to the structures observed in the AFM. The fuzziness in the STM images was due to the native oxide on the Si, which was an insulating layer. The insulating layer makes it difficult for the electrons to tunnel from the tip to the surface. Even though the monolayer was dense, there were still some uncovered areas which will later serve as the spots where the fluorine plasma could etch into the exposed Si. XPS data showed a 23% increase of carbon on the surface from the blank Si wafer to the MNFP monolayer; this is consistent with earlier reports[6].

4.2.5 Etching Using MNFP as a Molecular Mask

All experiments involving plasma processes was been performed in the cleanroom at the Microelectronic Research Center (MIRC) at the Georgia Institute of Technology. The Vision- 320 RIE was used as the etch tool. It is important to understand that the plasma recipes used successfully here may not be successful in other etch tool since the performance of the plasma not only depends on the recipe but also depends on the reactor geometry and other factors that are individual to this tool. The MNFP monolayer used here was the most fragile etch mask when compared to the other materials. The height of the monolayer was ~1 nm, which was less then the other monolayers used and also MNFP does not gain stability from secondary interactions characteristic of like C96, or the stability gained through covalent bonds as for ROMP-C60. Also, MNFP only has one

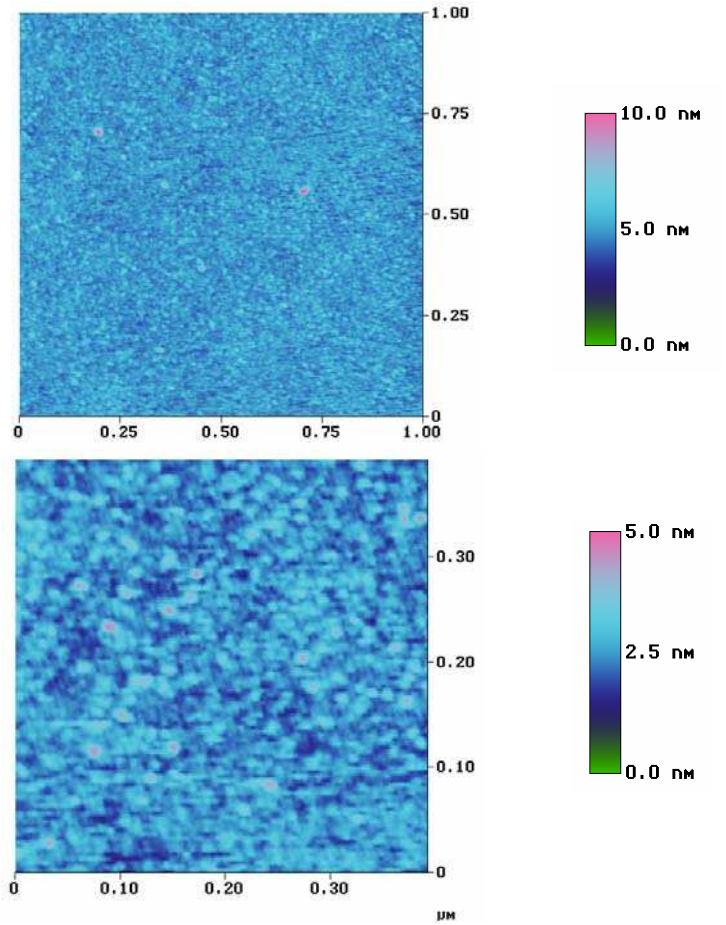

Figure 4.4 AFM after 15 sec of etch in plasma 3

alkyl chain for covalent attachment to the surface; both ROMP-C60 and C96 have several alkyl chains that could possibly be attached to the benzophenone. Multiple attachments would improve the stability of the molecules in a plasma process. The MNFP etch mask was very sensitive to the fluorine plasma and, naturally, plasmas 1 and 2 were too harsh toward the monolayer. In plasma 3, the monolayer was stable and functioned successfully as an etch mask. However, the monolayer was not stable for very long and after 30 sec of etching the monolayer was gone and the features were destroyed. However, after 15 sec of plasma etching, the monolayer was still stable and acted as the etch barrier. The structures seen after etching resembled the structure of the monolayer in the AFM, See

Figure 4.4.For this surface, it was difficult to clearly see how well MNFP act as an etch mask since there are no easily distinguished edges or features, which was the case in for both C96 and ROMP-C60 experiments discussed previously. The dense MNFP monolayer would only allow the plasma to reach the surface in few places which made it impossible to predict the features of the surface after the etch. The features seen on the surface had a height of 1.9 ± 0.3 nm, determined via AFM and STM, which was consistent with the etch rate for plasma 3. STM analysis of the surface after 15 sec of etching showed intact NMFP molecules on the surface, See Figure 4.5. Although it was difficult to clearly resolve the structures etched into the substrate this data provided valuable information. The monolayer was stable in an etching plasma with a etch rate of

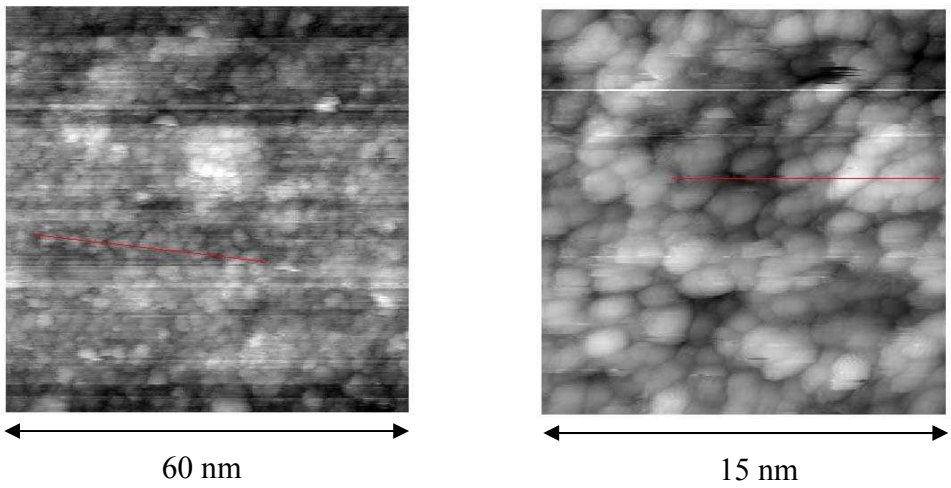

Figure 4.5 STM of 15 sec etch MNFP monolayer in plasma 3.

91 ± 5 Å/min which meant that individual molecules could independently act as etch resists. However, the size of the features makes them extremely fragile and difficult to analyze. The surface was also monitored by contact angle pre and post etching. The contact angle decreased from 80 ± 1 to 56 ± 6 after 15 sec of etching. After 30 sec of

etching the contact angle is 32 ± 4 which also indicated that the MNFP layer was destroyed in the plasma process. See Table 4.1 for summary of all contact angle results. These types of surfaces had very small features both in the X and Y direction can be difficult to analyze, However, the control experiment showed that when a benzophenone covered sample without MNFP was placed in the plasma 3, for 15 sec, the surface is flat and no features are seen indicating that the features seen after the process arose from the MNFP etch mask. Also the contact angle for the control experiment was significantly lower than the MNFP covered surface after the plasma process. The benzophenone monolayer layer had been removed from the surface leaving behind a flat Si surface.

Table 4.1 Contact angle for MNFP covered surfaces

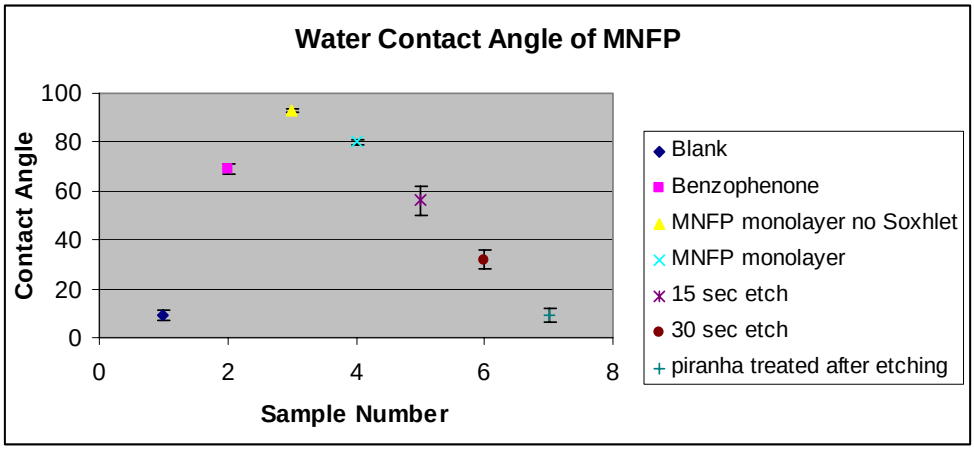

4.2.6 Removal of MNFP Post Etching Using a Piranha Solution

Removal of the MNFP etch barrier was necessary for potentially incorporating this methodology into device fabrication, and this must be done without damaging the Si structures. As described in chapter 2 and 3 removal of the resist can be done with either a piranha solution or with an oxygen plasma. Here, the oxygen plasma created an

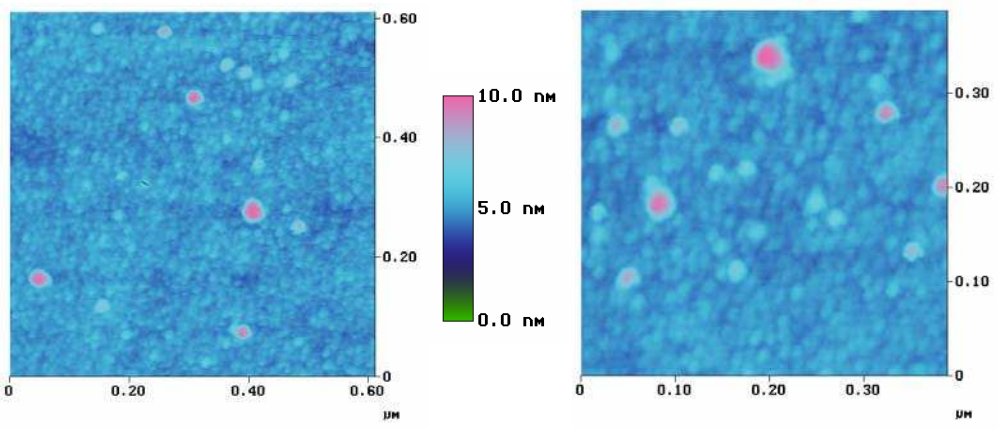

Figure 4.6 AFM of etch surface followed by MNFP stripping by piranha treatment.

environment too violent the small structures and they were destroyed in the process. Instead, the samples were placed in a piranha solution (70 % H_2SO_4, 30 % H_2O_2) for 1 hr followed by a thorough rinse with DI water and dried with N_2 gas. For the 15 sec plasma etched samples, the contact angle decreased from 56 ± 6 before the piranha treatment to 9 ± 3 after the treatment, indicating a pure Si surface. EDS confirmed the contact angle results, which indicated, that all organic molecules were stripped leaving the remaining Si structures undamaged. As described in the previous paragraph it was difficult to predict a pattern in the substrate after etching and consequently also after stripping of the resist. STM analysis shows a rough surface which could be expected from using the dense MNFP monolayer as the resist. It is clear that all MNFP molecules have been removed in the stripping process and no circular fullrenene like structures are observed, see Figure 4.6 and 4.7. The height of the structures after being processed in plasma 3 for 15 sec and then stripped with piranha is 1.5 ± 0.6 nm which was consistent with the etch rate of the plasma. In the control experiment, a MNFP monolayer was directly placed in the piranha solution without any fluorine etching. AFM analysis revealed a flat surface and the

contact angle was 9 ± 2. The STM images revealed that all fullerenes, circular features in previous STM images, have been removed by the piranha treatment, See Figure 4.7.

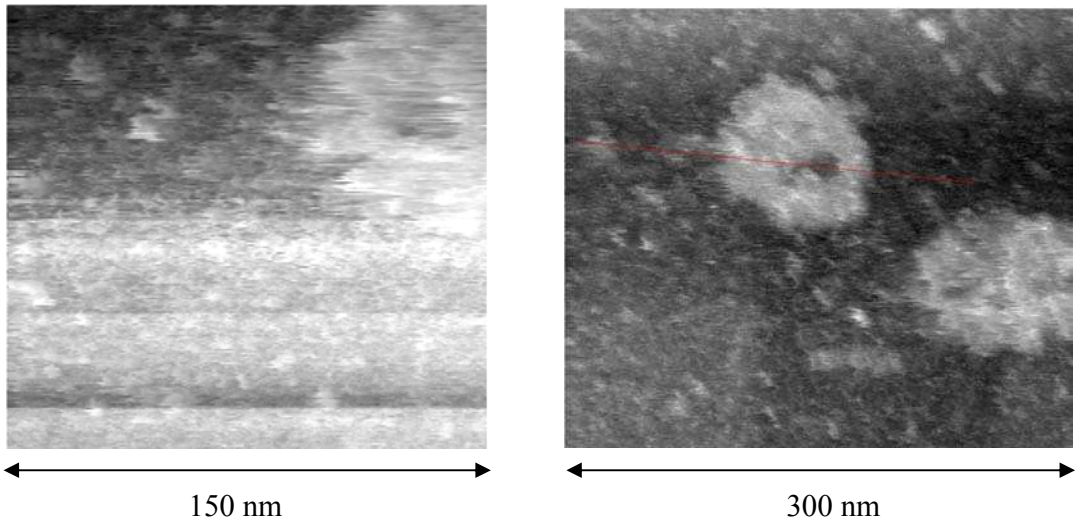

Figure 4.7 STM of Si surface after piranha treatment

4.3 Summary and Conclusion

Here, a new methodology was used to create a monolayer of fullerene molecules (MNFP). MNFP was covalently attached to the surface through a photochemical reaction with a silane benzophenone derivative. All non-attached molecules were extracted from the surface in a Soxhlet apparatus. STM analysis showed a tightly packed monolayer which and had a higher contact angle than previously reported monolayers of fullerenes on Si. The diameter of the features ranged from 0.7 – 3 nm and corresponds well to the diameter of a fullerene molecules (0.7 nm). Both results suggested that this monolayer has a higher density than the others reported. As a result the MNFP monolayer could potentially be used for other applications than molecular lithography, such as in OFETs. The monolayer was placed in plasma 3 and could withstand the plasma process for only a

short period of time, 15 sec. STM results showed that the MNFP molecules were stable in the plasma. The structures created after plasma treatment resembled the initial morphology of the surface. MNFP was stripped off the surface, in a piranha solution, after etching leaving Si structures behind. No fullerenes were seen in the STM analysis after the stripping. The contact angle combined with EDS showed a pure Si surface. The structures created were 1.9 ± 0.3 nm tall which was consistent with the etch rate for plasma 3. Structures this small would be extremely hard to use in the fabrication of a device since they would be extremely fragile, but also it will be difficult to make structures this small tall enough to be useful. The next step for using MNFP molecules as a template is to pattern the molecules on the surface to make distinct features. However this work has demonstrated that it is possible in principle to image molecular size features using single molecules for true molecular lithography. Therefore, features of any size can be created in a silicon surface when using highly aromatic molecules as the template. Organic synthesis, solubility, and self-assembly are the only limitations on what shape or size one could make.

REFERENCES

[1] Kroto, H.; Heath, J.; O'Brian, S.; Curl, R.; Smalley, R. *Nature,* **1985,** 162.

[2] Krätschmer, W.; Lamb, L.; Fostiropoulos, K.; Huffman, D. *Nature,* **1990,** 10039.

[3] Shi, X.; Caldwell, W.; Mirkin, C.; Chen, K *J. Am. Chem. Soc.* **1994,** *116,* 11598.

[4] Chen, K.; Caldwell, W.; Mirkin, C.; *J. Am. Chem. Soc.* **1993,** *115,* 1193.

[5] Chupa, J.; Xu, S.; Fischetti, R.; Strongin, R.; McCauley, J.; Smith, A, III; Blaise. J. *J. Am. Chem. Soc.* **1993,** *115,* 4383.

[6] Tsukruk, V.; Lander, L.; Brittain, W. *Langmuir,* **1994,** *10,* 996.

[7] Feng, W.; Miller, B. *Langmuir,* **1999,** *15,* 3152.

[8] Porter, M.; Bright, T.; Allara, D.; Chidsey, C. *J. Am. Chem. Soc.* **1987,** *109,* 3559

[9] Chidsey. C. *Science,* **1991,** *251,* 919.

[10] Miller, C.; Cuendet, P.; Grätzel, M. *J. Phys. Chem.* **1991,** *95¸* 877.

[11] Gokan, H.; Esho, S.; Ohnishi, Y *J. Electrochem. Soc.* **1983,** *130(1),* 143.

[12] Kunz, R.; Palmateer , S.; Forte, A.; Allen, R.; Wallraff, G.; DiPetro, A.; Hofer, D. *SPIE*, **Vol. 2724,** 365.

[13] Maggini, M.; Scorrano, G.; Prato, M. *J. Am. Chem. Soc.* **1993,** 9798.

[14] Brough, P.; Klumpp, C.; Bianco, A.; Campidelli, S.; Prato, M. *J. Org. Chem.* **2006**, *71*, 2014-2020.

[15] Hatsusaka, K.; Ohta, K.; Yamamoto, I.; Shirai, H. *J. Chem Mater.* **2003,** *11*, 423.

[16] Engelkamp, H.; Middelbeek, S.; Nolte, R. *Science,* **1999,** *284,* 785.

[17] Bushby, R.; Boden, N.; Kilner, C.; Lozman, O.; Lu, Z.; Liu, Q.; Thornton-Pett, M. *J. Mater. Chem.* **2003,** *13,* 470.

[18] Yatabe, T.; Harbison, M.; Brand, J.; Wagner, M.; Müllen, K.; Samori, P.; Rabe, *J. Mater. Chem.* **2000,** *10,* 1519.

[19] Caldwell, W.; Chen, K.; Mirkin, C.; Babinec, S. *Langmuir.* **1993,** 9, 1945.

CHAPTER 5

ORGANIZATION AND ALIGNMENT OF MATERIALS USED FOR MOLECULAR LITHOGRAPHY

5.1 Introduction

As seen in Chapters 2-4 a monolayer of individual molecules and polymers could be used directly as the etch mask to create features in a Si or SiO_2 substrate. This was the first step for potentially incorporating molecular lithography into the fabrication process of a device. However, the structures made thus far have been random in a sense that the organization of the molecules have no particular directionality and rely only on self organization. This is not optimal since the patterns made for devices have to be of a certain shape and size. Naturally the next step in the development of molecular lithography would be to organize the molecular candidates into desired patterns which could be useful and reproducible in device fabrication. The nature of the material would dictate what shape could be achieved. Since C96 self-assembled into fibers via π-π interactions between the molecules[1,2,3], the obvious application would be to organize these fibers into straight lines. For monodisperse ROMP-C60, a potential application could be the fabrication of pillars or possible straight lines created by dip-pen technology. In this chapter various attempts to organize materials in an ordered fashion, some more successful then others will be discussed.

5.2 Experimental

All materials used in this section were purchased from Fisher and used as received without further purification. The single-walled carbon nanotubes (SWNT) were kindly given to me from Dr. Mohan Srinivasarao at Georgia Institute of Technology.

5.2.1 Alignment of C96

Alignment and organization of C96 and other PAHs (mainly HBC) has been studied extensively over the past years for their possible applications in microelectronics, because of their high charge carrier mobility. The charge mobility is an important electronic property in the performance of devices such as FETs. Since structural control and uniaxial directionality is necessary for PAHs to perform with its highest mobility possible in field effect transistors, much work has been designated aligning and controlling the supramolecular organization[4,5,6,7,8,9]. The π-π interaction in PAHs allow for mechanical stimulation for organizing the molecules into straight ribbons on a surface. All alignment done previously has involved multilayers, which would not be useful for molecular lithography, since no boundaries are available. PAHs are known to organize in into highly ordered layers using Langmuir-Blodgett deposition[10], zone-casting[11], zone-crystallization[12], or solution casting onto pre-aligned polytetrafluoroethylene[13]. Here C96 was attempted to be aligned into straight lines or organized to preexisting patterns or structures on the surface.

5.2.2 Alignment of C96 to SWNT

First attempts were made to align C96 to pre-existing molecular patterns; using singled-walled carbon nanotubes (SWNT) on the surface. First, a monolayer of SWNT was attached onto the surface. For the SWNT to adhere onto the surface a monolayer of 3-aminopropyltriethoxysilane (APTES) was prepared. A piranha cleaned SiO_2 surface was placed in a 1 mM solution of APTES in dry CH_2Cl_2 (methylene chloride) for 30 min. Once again it was important for the experiment to take place in inert atmosphere and standard Schlenk glassware and technique was used to eliminate any moisture. The sample was then rinsed with DI water and spun dry at 3000 rpm for 1 min. The surface was monitored by contact angle, which was found to be 65 ± 3. This surface is used directly for the attachment of SWNT. A 1% aqueous Triton X-100 was prepared and 0.1 mg/ml (normally 2 mg of SWNT was added to 20 ml of DI-H_2O and 0.2g of Triton X-100) of SWNT was added to the solution. This solution was sonicated for 24 hrs to fully

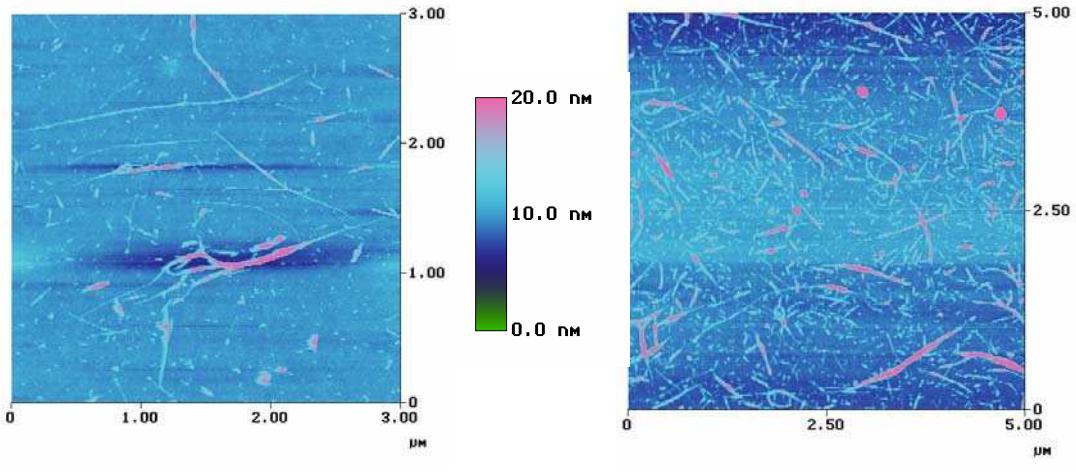

Figure 5.1 SWNT on SiO_2.

suspend the SWNT. The solution was then centrifuged twice and the particulates were removed after each spinning. The APTES covered wafer was then placed in the SWNT solution for 15 min and rinsed thoroughly with H_2O and spun dry at 3000 rpm for 1 min. AFM analysis revealed a moderately dense layer of SWNT on the surface, See Figure 5.1. A 10^{-5} M solution of C96 in chloroform was spin-coated, dip-coated, or drop-casted onto the SWNT surface in hopes that the discotic molecules would align themselves to the nanotubes. Spin-coated and dip-coated surfaces gave no alignment of C96 to the SWNT. Drop-coated samples on the other hand showed some alignment and organization of C96 to the SWNT. C96 required more time to organize using this coating technique which allows for the alignment. However, the alignment was only continued over a few hundred nm in the X axis and also was discontinued at the end on the SWNT, See Figure 5.2. This indicated that C96 could be aligned somewhat to SWNT. Better alignment of C96 to SWNTs could be expected if the SWNT were uniaxial organized on the surface. This would allow for C96 to be influenced only in one direction which could result in highly organized fibers. As seen in the next paragraph C96 will only show some alignment to certain materials, secondary interactions in the most likely force that will make C96 line up with SWNT. SWNT was also an attractive candidate for molecular

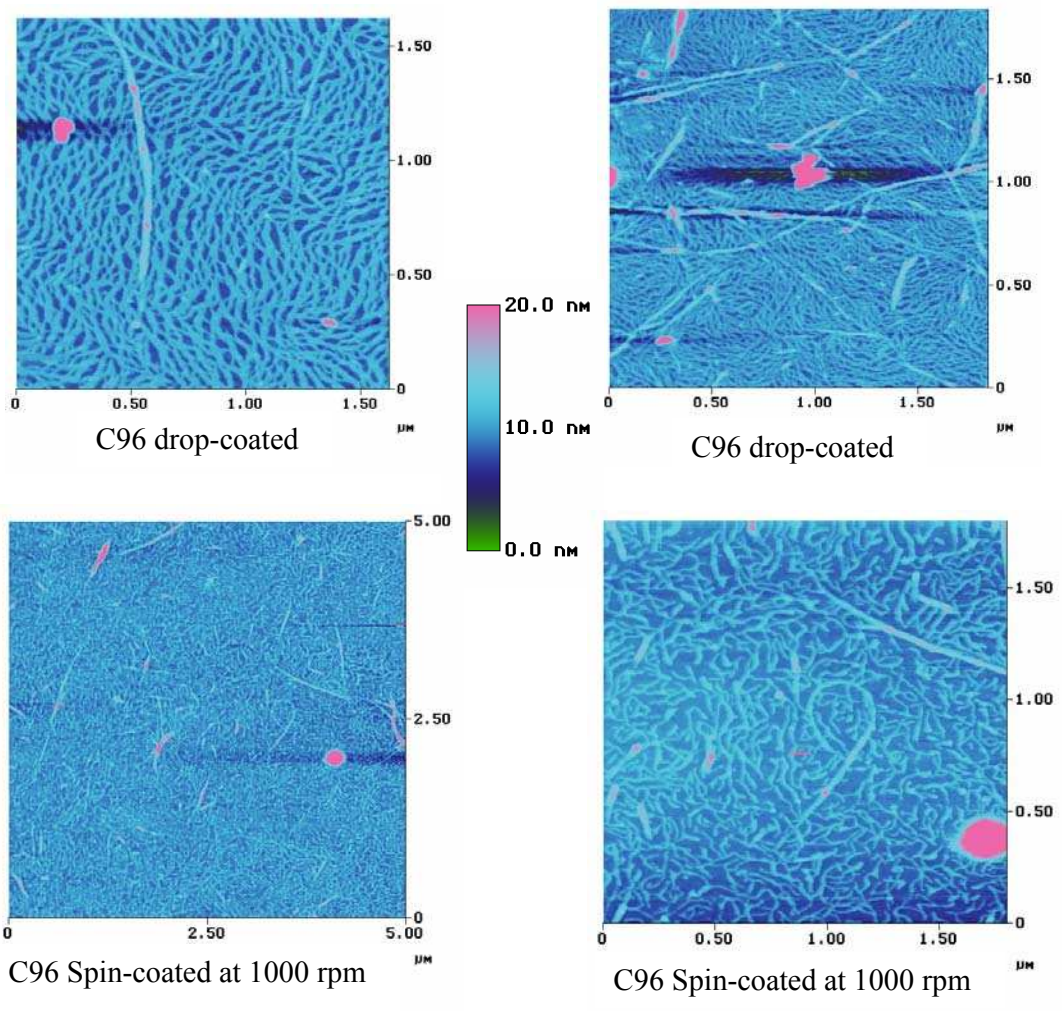

Figure 5.2 Alignment of C96 to SWNT using spin-coating or drop-coating

lithography and the SWNT surface was placed in plasma 3 to see if the SWNT themselves are stable enough to act as etch resists. Since the SWNT were not covalently bound to the surface no structures were seen after the etching process.

5.2.3 Alignment of C96 to ROMP-C60

The same idea as above was investigated using ROPM-C60 as the organizational template. A monolayer of ROMP-C60 was prepared using the benzophenone chlorosilane derivative as the surface linker, described in chapter 3. A 10^{-5} M solution of C96 in chloroform was spin-, dip-, or drop-coated onto the surface. AFM analysis showed that the discotic molecules did not align to the polymeric structures and therefore

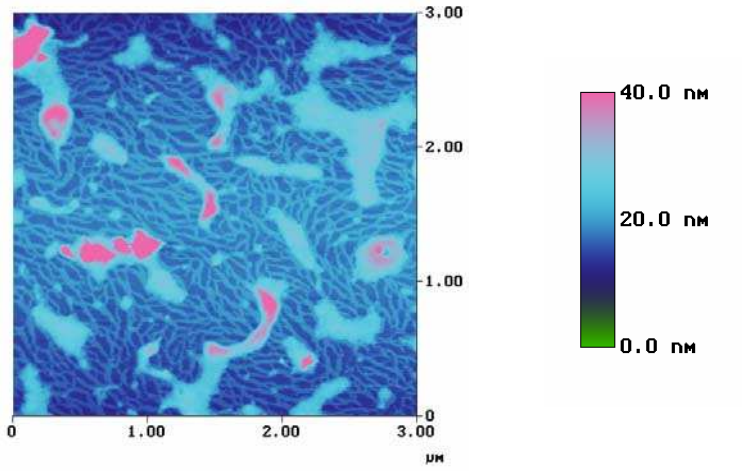

Figure 5.3 AFM of C96 aligned to ROMP-C60

has no mechanical, chemical or secondary interactions with the ROMP-C60, See Figure 5.3. The deposition technique does not, however, influence the outcome of the behavior of C96 to the polymer. This also indicated that C96 would not align itself next to other pre-aligned macroscopic structures.

5.2.4 Alignment of C96 to an Ordered Monolayer of Teflon on SiO_2

Teflon can be ordered into extremely straight and organized lines on a SiO_2 surface. In literature this is normally done by heating a block Teflon to 150º C and then rubbing it in one direction on a surface[14]. The Teflon polymer deposits onto the surface in a ordered fashion. Here we have done the reverse, where a substrate was heated to 200º C and the Teflon was then rubbed on the surface. What this allowed for was to only deposit a few polymer chains on the surface. The surface only heated the outer layer of the Teflon and therefore only the polymer chains that reach high enough temperatures would be transferred to the surface. Regular Teflon tape was wrapped tightly around a glass pipette, care was taken to make sure that the tape was smoothly wrapped on the pipette and no creases were visible. The Teflon covered pipette was rubbed without any force on the heated substrate 3 times in the same direction. AFM analysis showed straight lines on the surface sporadically spread with various distances between each other. The width of

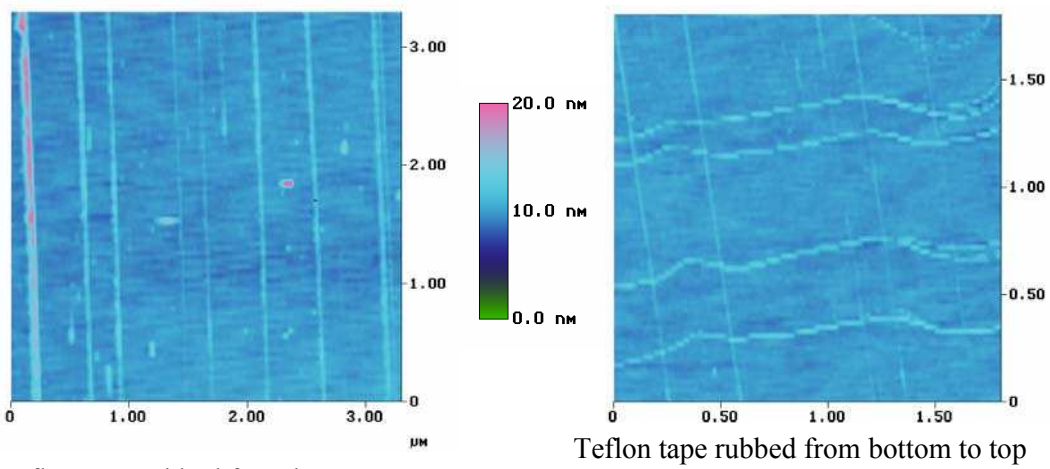

Teflon tape rubbed from bottom to top

Teflon tape rubbed from bottom to top then from left to right

Figure 5.4 Teflon tape rubbed at a 200º C on a SiO_2 surface.

the lines varied from 18 – 80 nm, the height of the features ranged from 2-8 nm. One can also rub the surface in different directions to achieve desired patterns. As seen in Figure 5.4, the surface had been rubbed first in one direction and then perpendicular to the first direction. As a result crosses or boxes were made. Since this material could be organized on the surface it would be an ideal candidate for molecular lithography if it could be used directly as the etch mask. The samples were placed in plasma 3 at was etched for various times. After 30 sec of etching, the features on the surface were intact but there is no significant increase in the height of the features. Even after 45 sec of etching the features were visible but now the height has decreased rather than increased which was desired. The most likely explanation being that the Teflon was not very stable in the plasma and therefore could only act as a molecular resist for very short plasma process times. However, this might be an interesting avenue to investigate fluorocarbon materials as etch barriers due to their organizational capabilities. The control experiment, rubbing with the Teflon tape on to a surface at room temperature, revealed no transferred Teflon. The next idea was to align C96 to the straight Teflon lines. However, when a 10^{-5} M solution of C96 in chloroform was either spun onto the surface at 1000 rpm for 1 min or

dip-coated on no organization of C96 was seen to the Teflon. This further indicates that C96 will not organize it self to aligned structures without any secondary interactions.

5.2.5 Monolayer Alignment transfer of HBC using Zone-Casting Technique with Benzopheone as a Photo Probe

Zone-casting is an alignment technique for discotic materials developed by Dr. Adam Tracz[15]. It works like a reverse vacuum, where a moving substrate is placed underneath a nozzle that deposits a solution of PAHs onto the surface, see Figure 5.5. The PAHs, in this case HBC on SiO_2, align themselves nicely in lines on the surface using this technique. Since there are only three zone-casting instruments in the world the

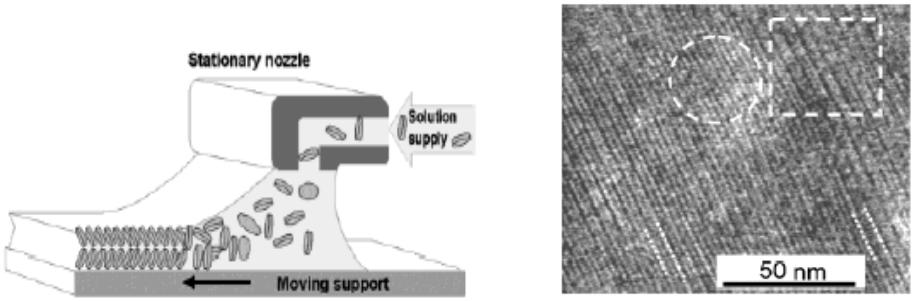

Figure 5.5 Scematic of zone-casting[8].

samples used here were kindly prepared in Prof. Klaus Müllen's laboratories in Mainz, Germany, by Wojtek Pisula. The surface created of the HBCs is of course multilayers of molecules which would not be useful for molecular lithography. Ideally, the zone-casting should be done on a benzophenone terminated surface so that photochemical attachment, followed by Soxhlet extraction of unbound molecules, would allow aligned monolayer to be formed. Since I do not have access to an instrument this experiment would have to be done elsewhere and would be one of the more important experiments to be done for the next person continuing this research. However, these samples were placed in plasma 3 for processing, but as expected not features are seen after the etch process. The idea here was to transfer the top organized HBC layer from one substrate to another. A chlorosilane

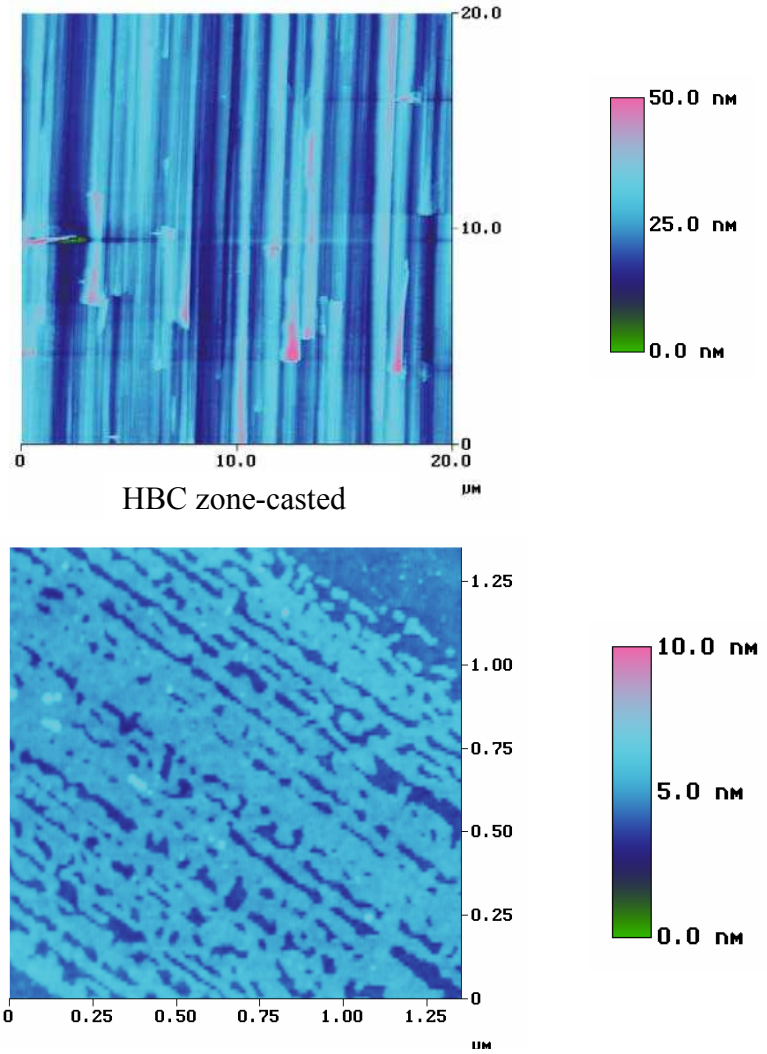

Figure 5.6 AFM of HBC zone-casted and transferred to another substrate.

benzophenone monolayer was prepared and analyzed as described in previous chapters. The benzophenone monolayer substrate was then sandwiched with the zone-casted HBC substrate and held together tightly with regular tape, of course the benzophenone layer and the HBC layer were facing each other. The sample was then places standing on its edge in the Stratalinker 2400 for irradiation. The notion here was to photochmically activate the benzophenone and let it covalently attach to the HBC layer and therefore transfer the organized HBC to the benzophenone substrate. Since the distance required

for the photochemical covalent attachment to work is only a few Å it will be impossible to successfully transfer large areas using this approach, since zone-casting does not produce atomically flat organized layers. However, after 8 hrs of irradiation and AFM analysis a monolayer of ordered HBC molecules were transferred to the surface, see Figure 5.6. The coverage of the HBC on the surface was patchy and found only close to the edge exposed to the irradiating, which was expected not only because of the benzophenone distance issue but also that the light that irradiates the benzophenone cannot penetrate deep into the sample so one around the top edge is where the transferring was taking place. The height, 1.6 ± 0.2 nm, of the transferred features corresponds well to the diameter of HBC (~1.4 nm). However, even if this type of pattern transfer was not ideal in many ways it was proof that one can transfer organized molecules onto a different substrate into a monolayer.

5.2.6 Alignment of C96 using Rubbing Technique with Teflon

The most attractive way to align discotic molecules might be to rub them with various materials such as Teflon, velvet, or flannel. The only requirement for successful alignment is with the surface at which the PAHs are aligned. Generally, the surface needs to be covered with a monolayer of alkyl chains for them the PAHs to align and organize. Here again Teflon tape is used for the rubbing, this was done at room temperature so no Teflon would be deposited on the surface as seen in the previous paragraph. A SiO_2 was cleaned in a piranha solution (70 % H_2SO_4, 30 % H_2O_2) for 1 hr and then rinsed with copious amounts of H_2O. The sample was then placed in a Schenk type beaker due the fact that covalent attachment of the alkyl chain involves a chlorosilane which is moisture sensitive. The same approach of attaching a monolayer of an alkyl chain was taken as previously described when attaching the chlorosilane benzophenone derivative to the SiO_2 surface[16]. Dry toluene was added under inert atmosphere to cover the standing the wafer piece, normally about 50 ml. Chlorodimethyloctadecylsilane (CODS) was added to make a 100 mM solution (about 2

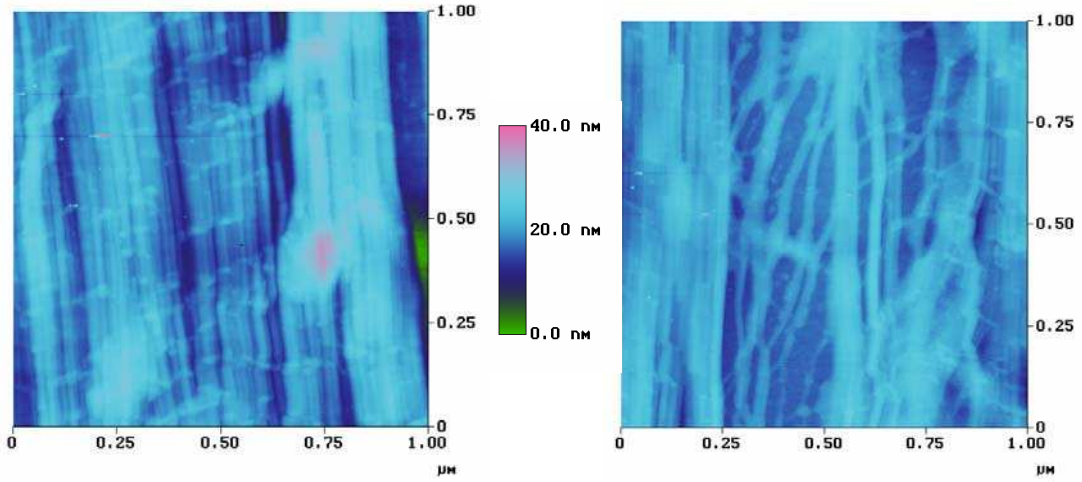

Figure 5.7 AFM of C96 rubbed with Teflon on a CODS surface

ml) and a few drops of Et_3N were added as the acid scavenger and catalyst. The mixture was left standing over night and became cloudy which was a good sign that the covalent attachment to the surface had occurred. The wafer was rinsed extensively with chloroform and dried with N_2. The contact angle after the attachment had increased from 9 ± 2 to 93 ± 1. This surface was then rubbed with the Teflon tape to help with the later alignment of C96. A 10^{-5} M solution of C96 in methylenechloride was spin-coated on the surface at 1000rpm for 1 min. The wafer was again rubbed with Teflon tape in the same direction as the alkyl chains were rubbed. AFM analysis revealed that the C96 molecules are aligned on the surface in the direction of the rubbing. See Figure 5.7 for the complete set of AFM analysis throughout the experiment. However, aligning C96 this way presented a few problems for molecular lithography. The first one being that one could not ensure a monolayer of molecules on the surface. Naturally this would become a problem for using this surface during the plasma process since no SiO_2 would be exposed and therefore no etching in the substrate would occur. Even tough the C96 molecules are aligned very nicely they appear to be in mulitlayers on the surface when looking at the AFM images from this experiment. The second problem is that the molecules are not covalently attached to the surface which decreases their resistance towards the fluorine

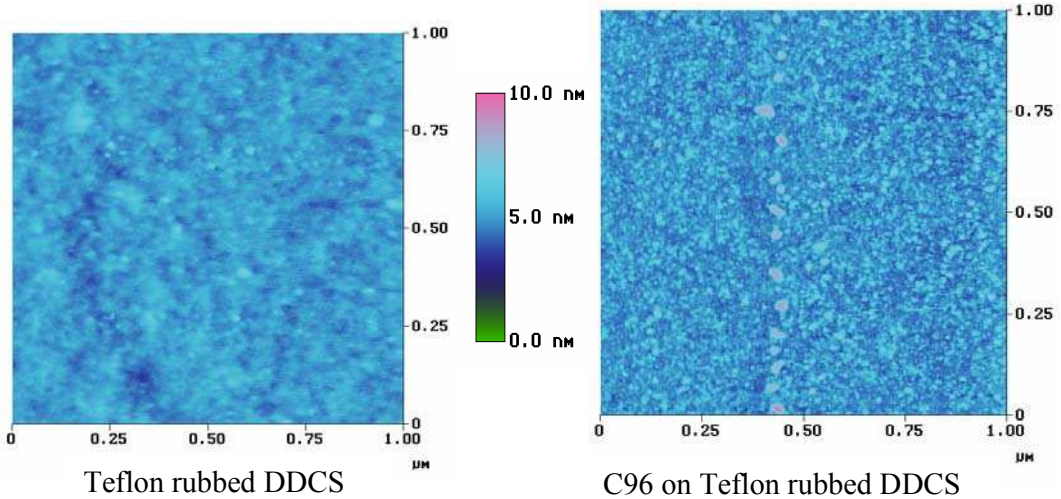

Teflon rubbed DDCS C96 on Teflon rubbed DDCS

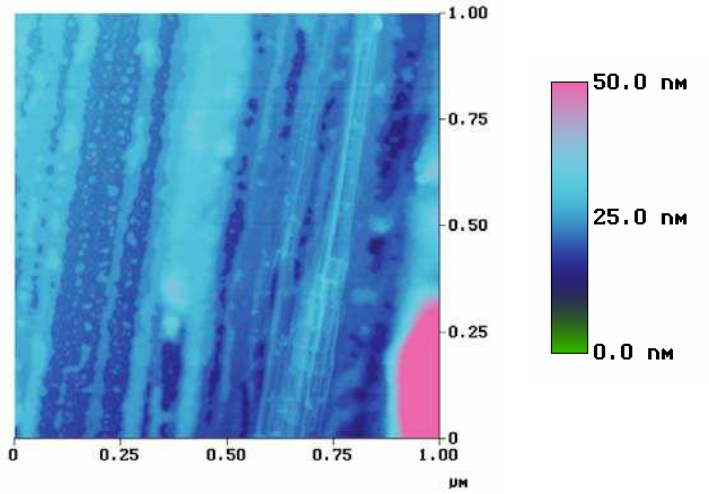

Teflon rubbed C96 on Teflon rubbed DDCS

Figure 5.8 AFM of aligned C96 on DDCS

plasma. This problem is discussed in more detail in chapter 2. When exposing the sample for etching in plasma 3 results for 15 sec, 30 sec, or 45 sec no aligned features are seen on the surface. This was due to one or both of the reasons discussed above. This method proved to be an excellent method of aligning discotic molecules on a surface and can possibly be developed further so features created could be used in device fabrication. The control experiment here was also to rub the C96 molecules in the same fashion but on a benzophenone terminated surface. The C96 molecules did not respond to the rubbing in this experiment and the features seen were identical to the features before rubbing.

Another alkyl terminated surface was also prepared for the same application. A 10 mM solution of dodecyltrichlorosilane (DDCS), normally 30 µl, in hexadecyl 10 ml. DDCS is hydroscopic so care was take to keep moisture out using a Schlenk type beaker. A piranha cleaned wafer piece was placed in the solution and left standing over 3 days. The wafer was rinsed extensively with chloroform and dried under nitrogen gas. The contact angle for this surface increased from 9 ± 2 to 104 ± 2. This could indicate one of two things: the surface coverage was better using this technique then CODS or a network was formed due to the trichlorosilane moiety. AFM analysis of the CODS surface was flat, without any pinholes indicating good coverage. Even if a network was formed it might not influence the outcome of this experiment. The DDCS surface was rubbed with Teflon tape at room temperature and then a 10^{-5} M solution of C96 in methylene chloride was spun-coated onto the surface at 1000 rpm for 1 min. The surface was again rubbed in the same direction as the alkyl chains. AFM analysis before and after rubbing revealed that the C96 molecules do align upon mechanical stimuli on an alkyl terminated surface. The surface morphology before rubbing was covered in small islands (20-40 nm) and after the rubbing the islands come together and form aligned structures on the surface. The long alkyl chains on the surface interfere with the π-π stacking of C96 and therefore do not for the fibers seen on other surfaces such as Si or SiO_2. AFM analysis after rubbing showed that the aligned features probably not were in a monolayer, see Figure 5.8. The height of the Teflon rubbed C96 structures is 7.3 ± 4.5 nm which is an indication of multilayer formation. However, it also showed that there are exposed SiO_2 areas between the features that can be exposed to the fluorine plasma for etching. The multilayer can also stabilize the structure so that the molecules are more stable to the plasma then a monolayer. The molecules are not covalently attached to the surface which will decrease their stability. The control experiment showed that no organization or alignment of C96 occurred. A benzophenone surfaces was first rubbed with Teflon followed by deposition of C96 molecules. The surface was again rubbed in the same direction as the

benzophenone surface. AFM analysis showed a highly disordered surface similar to the ones previously reported in Chapter 2, see Figure 5.9.

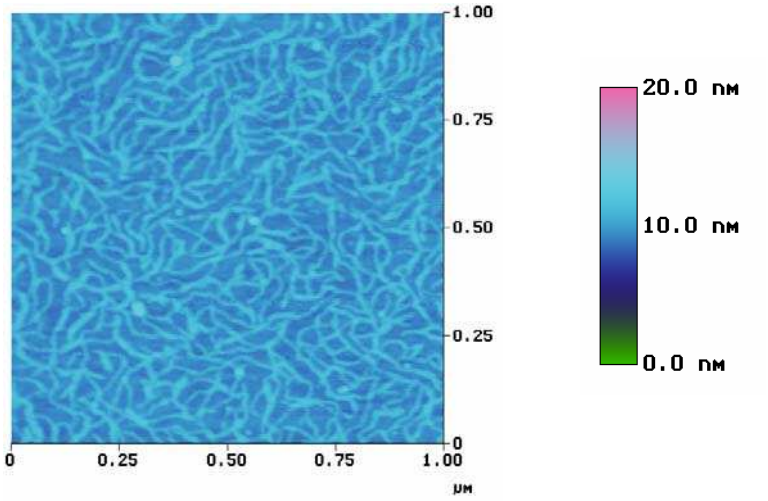

Figure 5.9 AFM of Teflon rubbed C96 on benzophenone

5.2.7 Dip-Pen Lithography with ROMP-C60

One of the more obvious ways to pattern polymers is to use dip-pen technology. This technique would be a great addition for molecular lithography. Dr. Paul Sheehan at the Naval Research Laboratories has explored this technique and was very interested in pattern some materials for molecular lithography applications. Previous material patterned included poly(3-dodecylthiophene), poly(vinylidene fluoride), and poly(n-isopropylacrylamide). The molecule of choice was ROMP-C60 since it was a polymer. The technique they use was that they coat an AFM tip with the material from a solution and then heat the tip to appropriate temperature (melting temperature of the material) and pattern the material when it is flowing. However, ROMP-C60 did not have a melting temperature in reasonable range < 350º C and actually the melting temperature have not been determined. Therefore all attempts to pattern the polymer failed since the material could never be transferred from the tip to the surface. Optimally one would like to pattern the polymer onto a benzophenone terminated surface to covalently attach it to the surface after the dip-pen patterning. This gives more incentive to develop new highly aromatic

materials that have the right properties for both dip-pen lithography and molecular lithography.

5.2.8 Alignment of MNFP and ROMP- C60 by Rubbing with Teflon

Attempts to align and organize MNFP and ROMP-C60 on the surface by rubbing the thin film with Teflon have been done. The main difference between aligning these materials by rubbing and C96 is obvious since the ROMP-C60 is a polymer and MNFP lacks the self-assembly properties of C96 through secondary interactions. Benzophenone and alkyl chain terminated surfaces were prepared as described previously in this chapter and also in Chapter 2. As expected for both materials no organization and directionality is observed after rubbing the surfaces using wither alkyl chain or benzophenone terminated surfaces as the substrate. Experiments were also performed where heated substrates were used to increase the flow of the material but as discussed in the previous paragraph the melting temp was to high and flow of ROMP-C60 was poor.

5.3 Summary and Conclusion

For molecular lithography to become a high impact technology in the semi-conductor industry, control of shape and directionality over the patterns is a must. Here, attempts have been made to pattern materials suitable for molecular lithography. C96 was the easiest of the three materials to pattern since the π-π stacking allowed for self-organization into fibers due to of the aromatic cores. Mechanical sheer of a C96 covered surface gave an organized pattern in the direction of the sheering. For this to be successful, we found that the underlaying substrate must be alkyl terminated. This was not ideal from a molecular lithography point of view since it eliminated the opportunity for the molecules in a monolayer but also lacked the covalent attachment to the surface. However, organization of PAHs was possible via several methods and can be further developed to fit molecular lithography better. Zone-casted C96 molecules on a benzophenone terminated surface were only one of many possible routes to make a patterned monolayer. The control of directionality in zone-casting will be utilized in the

future with molecular lithography as the targeted application. Dip-pen lithography is an attractive approach to pattern materials for molecular lithography since one has total control of the patterns made. As described earlier the properties of ROMP-C60 did not fit the requirement to use thermal dip-pen technology. The next step for the development of molecular lithography is to develop new materials that meet the requirements for both dip-pen and molecular lithography. There are many exciting avenues, materials, and approaches that could possible make molecular lithography a high impact technology.

5.4 REFERENCES

[1] Stein, S.; Brown, R. *J. AM. Schem. Soc.* **1987,** *109,* 3721.

[2] Hatsusaka, K.; Ohta, K.; Yamamoto, I.; Shirai, H. *J. Chem Mater.* **2003,** *11,* 423.

[3] Engelkamp, H.; Middelbeek, S.; Nolte, R. *Science,* **1999,** *284,* 785.

[4] Hatsusaka, K.; Ohta, K.; Yamamoto, I.; Shirai, H. *J. Chem Mater.* **2003,** *11,* 423.

[5] Engelkamp, H.; Middelbeek, S.; Nolte, R. *Science,* **1999,** *284,* 785.

[6] Bushby, R.; Boden, N.; Kilner, C.; Lozman, O.; Lu, Z.; Liu, Q.; Thornton-Pett, M. *J. Mater. Chem.* **2003,** *13,* 470.

[7] Yatabe, T.; Harbison, M.; Brand, J.; Wagner, M.; Müllen, K.; Samori, P.; Rabe, *J. Mater. Chem.* **2000,** *10,* 1519.

[8] Bushby, M.; Nguyen, T.; Nuckolls, C. *J. Am. Chem. Soc.* **2003,** *125,* 8264.

[9] Wu, J.; Watson, M.; Müllen, K. *Angew. Chem. Int. Ed.* **2003,** *42,* 5329

[10] Reizel, N.; Hassenkam, T.; Balashev, K.; Jensen, T. R.; Howes, P. B.; Fechtenkötter, A.; Tchebotareva, N.; Ito, S.; Müllen, K.; Bjornholm, T. *Chem. Eur. J.* **2001,** *7,* 4894.

[11] Tracz, A.; Jeszka, J. K.; Watson, M. D.; Pisula, W.; Müllen, K.; Pakula, T. *J. Am. Chem. Soc.* **2003,** *125,* 1682.

[12] Liu, C. Y.; bard, A. J. *Chem. Mater.* **2000,** *12,* 2353.

[13] Bunk, O.; Nielsen, M. M;. Solling, T. I.; van de Craats A. M.; Stutzmann. *J. Am. Chem. Soc.* **2003,** *125,* 2252.

[14] Fenwick, D.; Pakbz, K.; Smith, P. *J. Mater. Sci,***1996,** *31,* 915

[15] Tracz, A.; Pakula, T.; Jeszka, J. *Mater. Sci-Poland,* **2004,** *22,* 415

[16] Prucker, O.; Naumann, C.A.; Rühe, J.; Knoll, W.; Frank, C.W. *J. Am. Chem. Soc.* **1999,** *121*, 8766.

CHAPTER 6

SUMMARY, CONCLUSIONS, AND FUTURE WORK

6.1 Summary and Conclusion

The developments in photolithography over the past decades have allowed the semiconductor industry to decrease the size of the transistor at rapid pace, according to Moore's Law[1]. The NA and the wavelength used to irradiate the photoresist are the limiting factors of the feature size achievable, described in the Rayleigh equation[2], see Chapter 1. Industry is currently producing devices at the 65 nm node, using immersion lithography technologies. However, the development of photolithography is not only approaching its physical limitations, due to the wavelengths and materials needed, but is also becoming extremely expensive, rendering Moore's Law unsustainable. Therefore, new methodologies, such as block-copolymers[3], for creating patterns on a substrate are highly desired. Here, we have successfully demonstrated that patterns of highly aromatic molecules or polymers, in monolayers, can be used directly as the etch resist and transferred into the underlying substrate. Using monolayers of materials also allows for creation of features with molecular resolution. The fibrous C96 structures, formed via π-π stacking, were used as a template and 3-4 nm wide features were etched into the substrate. Individual fullerene molecules, MNFP, were also used as an etchmask and showed resistance towards the plasma. ROMP-C60 was used to create larger structures, at sizes of 100-200 nm. Using this polymer 50 nm deep structures were created which meets the industrial requirement. A "soft" plasma was developed for these particular substrates to increase the lifetime, i.e. etch resistance, of the materials during the process. Orientation and alignment of the materials are necessary to create features having a size and shape that could be useful in device fabrication. C96 has been aligned into straight lines using rubbing techniques on alkyl terminated surfaces. It would be unrealistic to believe that an entire device could be fabricated using this technology. Many features

required in a device are too sophisticated to accomplish with solely self-assembly or mechanical alignment of materials. However, lines and pillars could be created and used for the creation of the critical dimensions in devices, such as interconnects. Synthetic organic chemistry and the tendency towards self-assembly of a particular material are the limiting factors to the feature sizes created. We have demonstrated that a wide range of the features sizes are achievable using molecular lithography, spanning from molecular size (3-4 nm) to several hundreds of nanometers. Therefore the limitations on feature sizes, which currently plague photolithography, have been bypassed. Using this methodology in conjunction with photolithography could potentially make advanced devices with feature sizes controllable at the molecular level.

6.2 Future Work

Further development of alignment and organization of materials is necessary for molecular lithography to become a high impact technology. Some alignment has already been accomplished, but more development is needed. Among the materials discussed throughout the thesis, C96 has the most potential to be organized into useful patterns. C96 and other discotic materials should be patterned, using zone-casting, on a benzophenone terminated surface for the creation of an organized monolayer. New materials should be synthesized with the objective not only to be utilized as etch resists, but also for alignment purposes. A highly aromatic polymer should be made which meets the requirements for dip-pen technologies. The observations that the molecular weight of a material has significance to it's etch resistance in not described in the Ohnishi and Ring parameter and a new parameter regarding the etch resistance of a material in multi- and mono-layers should also be developed. Molecular lithography can take advantage of the wide variety of materials and alignment techniques available, leading to further development within this field. Therefore, the research over the next few years should be very interesting and hopefully fruitful.

6.3 REFERENCES

[1] Resnick, D.J.; Mancini, D.; Dauksher, W.J.; Nordquist, K.; Bailey, T.C.; Johnson, S.; Sreenivasan, S.V.; Wilson, C.G. *Microelectronic Engineering* **2003**, *69*, 412.

[2] Gil, D.; Brunner, T.; Fonseca, C.; Seong, N.; Streefkerk, B.; Wagner, C.; Stavenga, M. *J. Vac. Sci. Technol. B.: Microelectronics and Nanometer Structures.* **2004**, 3431.

[3] Bendejacq, D.; Ponsinet, V.; Joanicot, M.; Loo, Y.-L.; Register, R. *Macromolecules,* **2002**, *35*, 6645.